การพัฒนาและแสดงลักษณะเฉพาะของอนุภาคนาโนไขมันแข็งที่บรรจุบิสดีเมท็อกซีเคอร์คิวมิน

นางสาวปิญธ์ณิษา ตั้งขจรชัยศักดิ์

วิทยานิพนธ์นี้เป็นส่วนหนึ่งของการศึกษาตามหลักสูตรปริญญาเภสัชศาสตรมหาบัณฑิต
สาขาวิชาเภสัชกรรม ภาควิชาวิทยาการเภสัชกรรมและเภสัชอุตสาหกรรม
คณะเภสัชศาสตร์ จุฬาลงกรณ์มหาวิทยาลัย
ปีการศึกษา 2558

DEVELOPMENT AND CHARACTERIZATION OF BISDEMETHOXYCURCUMIN-LOADED SOLID LIPID NANOPARTICLES

Miss Pinnisa Tangkhajornchaisak

A Thesis Submitted in Partial Fulfillment of the Requirements
for the Degree of Master of Science in Pharmacy Program in Pharmaceutics
Department of Pharmaceutics and Industrial Pharmacy
Faculty of Pharmaceutical Sciences
Chulalongkorn University
Academic Year 2015

Thesis Title	DEVELOPMENT AND CHARACTERIZATION OF BISDEMETHOXYCURCUMIN-LOADED SOLID LIPID NANOPARTICLES
By	Miss Pinnisa Tangkhajornchaisak
Field of Study	Pharmaceutics
Thesis Advisor	Phanphen Wattanaarsakit, Ph.D.
Thesis Co-Advisor	Associate ProfessorPornchai Rojsitthisak, Ph.D.

Accepted by the Faculty of Pharmaceutical Sciences, Chulalongkorn University in Partial Fulfillment of the Requirements for the Master's Degree

.....Dean of the Faculty of Pharmaceutical Sciences

(Assistant ProfessorRungpetch Sakulbumrungsil, Ph.D.)

THESIS COMMITTEE

.....Chairman

(Associate ProfessorParkpoom Tengamnuay, Ph.D.)

.....Thesis Advisor

(Phanphen Wattanaarsakit, Ph.D.)

.....Thesis Co-Advisor

(Associate ProfessorPornchai Rojsitthisak, Ph.D.)

.....Examiner

(ProfessorGarnpimol Ritthidej, Ph.D.)

.....External Examiner

(Associate ProfessorWaree Tiyaboonchai, Ph.D.)

ปิญฐ์ณิษา ตั้งขจรชัยศักดิ์ : การพัฒนาและแสดงลักษณะเฉพาะของอนุภาคนาโนไขมันแข็งที่บรรจุบิสดีเมท็อกซีเคอร์คิวมิน (DEVELOPMENT AND CHARACTERIZATION OF BISDEMETHOXYCURCUMIN-LOADED SOLID LIPID NANOPARTICLES) อ.ที่ปรึกษาวิทยานิพนธ์หลัก: อ. ภญ. ดร.พรรณเพ็ญ วัฒนาอาษากิจ, อ.ที่ปรึกษาวิทยานิพนธ์ร่วม: รศ. ภก. ดร.พรชัย โรจน์สิทธิศักดิ์, 106 หน้า.

วัตถุประสงค์ของงานวิจัยนี้เพื่อพัฒนาอนุภาคนาโนไขมันแข็งบรรจุบิสดีเมท็อกซีเคอร์คิวมิน โดยเตรียมจากไขรำข้าว เปรียบเทียบกับ กลีเซอริล บีฮีเนท และซิติล พาลมิเตท สำหรับการนำไปใช้ทางเภสัชกรรม ไขรำข้าวเป็นไขมันแข็งจากธรรมชาติได้จากการผลิตน้ำมันรำข้าว มีสารสำคัญคือแกมม่าออริซานอลซึ่งมีฤทธิ์ต้านอนุมูลอิสระ จึงเป็นสารที่มีประโยชน์และเหมาะในการนำมาพัฒนาทางเภสัชกรรม อนุภาคนาโนไขมันแข็งเตรียมด้วยวิธีปั่นผสมเป็นเนื้อเดียวกันด้วยความดันสูง ประกอบด้วยไขมันแข็งชนิดต่างๆ และทวีน 80 ชนิดและปริมาณของไขมันแข็งที่ใช้ในตำรับส่งผลต่อคุณลักษณะทางกายภาพของอนุภาคนาโนไขมันแข็ง พบว่าอนุภาคนาโนไขมันแข็งที่เตรียมจากไขรำข้าวมีขนาดอนุภาคใหญ่กว่าที่เตรียมจากไขมันชนิดกลีเซอริลบีฮีเนทและซิติลพาลมิเตท และปริมาณไขมันที่เพิ่มขึ้นมีผลทำให้ขนาดอนุภาคใหญ่ขึ้น อนุภาคนาโนไขมันแข็งบรรจุบิสดีเมท็อกซีเคอร์คิวมินที่เตรียมได้มีลักษณะเป็นระบบกระจายตัวเนื้อเดียวกัน มีขนาดอนุภาคในช่วงนาโนเมตรเป็นลักษณะทรงกลม หลังจากบรรจุบิสดีเมท็อกซีเคอร์คิวมิน อนุภาคนาโนไขมันแข็งที่เตรียมจากไขรำข้าวมีขนาดใหญ่สุดและมีการกักเก็บสารสำคัญสูงสุด การปลดปล่อยสารสำคัญแบบภายนอกร่างกายของอนุภาคนาโนไขมันแข็งที่บรรจุบิสดีเมท็อกซีเคอร์คิวมินเป็นแบบชะลอการปลดปล่อย ผลของปริมาณของไขมันที่เพิ่มขึ้นส่งผลให้สารสำคัญถูกปลดปล่อยได้ช้าลง อนุภาคนาโนไขมันแข็งบรรจุบิสดีเมท็อกซีเคอร์คิวมินที่เตรียมจากไขรำข้าวมีคุณลักษณะทางกายภาพที่ดี สามารถกักเก็บสารสำคัญไว้ในอนุภาคได้สูง และมีความคงตัวดี

ภาควิชา	วิทยาการเภสัชกรรมและเภสัชอุตสาหกรรม	ลายมือชื่อนิสิต .....
		ลายมือชื่อ อ.ที่ปรึกษาหลัก .....
สาขาวิชา	เภสัชกรรม	ลายมือชื่อ อ.ที่ปรึกษาร่วม .....
ปีการศึกษา	2558	

5576241333 : MAJOR PHARMACEUTICS

KEYWORDS: BISDEMETHOXYCURCUMIN, HIGH PRESSURE HOMOGENIZATION, RICE BRAN WAX, SOLID LIPID NANOPARTICLES

PINNISA TANGKHAJORNCHAISAK: DEVELOPMENT AND CHARACTERIZATION OF BISDEMETHOXYCURCUMIN-LOADED SOLID LIPID NANOPARTICLES. ADVISOR: PHANPHEN WATTANAARSAKIT, Ph.D., CO-ADVISOR: ASSOC. PROF.PORNCHAI ROJSITTHISAK, Ph.D., 106 pp.

The aim of study was to develop solid lipid nanoparticles containing bisdemethoxycurcumin using rice bran wax compared to glyceryl behenate and cetyl palmitate for pharmaceutical application. Rice bran wax is a by-product from rice bran oil refinery. It contains potent antioxidant of gamma oryzanol utilized in pharmaceuticals. Solid lipid nanoparticles (SLN) were prepared by high pressure homogenization technique using different type and amount concentration of lipid, and stabilized by tween 80. Type and concentration of lipids influenced the physicochemical properties of the SLN. RB-SLN had larger particle size than GB-SLN and CP-SLN. The higher the concentration of lipid, the larger was the particle size. Also, the higher the amount of tween 80 in SLN, the better was physical stability. Bisdemethoxycurcumin-loaded SLN (BDMC-SLN) appeared as a homogeneous dispersion with spherical shape in nanosize range. BDMC-SLN with RB had the largest particle size and the highest entrapment efficiency. *In vitro* release study of the BDMC-SLN exhibited a sustained release pattern. Increasing the lipid concentration resulted in sustaining the BDMC released. BDMC-loaded solid lipid nanoparticles using rice bran wax was successfully prepared. This rice bran lipid carrier provided better physical properties, entrapment efficiency and stability.

Department:	Pharmaceutics and Industrial Pharmacy	Student's Signature .....
		Advisor's Signature .....
Field of Study:	Pharmaceutics	Co-Advisor's Signature .....
Academic Year:	2015	

ACKNOWLEDGEMENTS

This research could not have been accomplished without the dedicated encouragement, as well as invaluable counsel and assistance from a number of persons.

Firstly, I would like to extend most impressive and deepest gratitude to my thesis advisor, Dr. Phanphen Wattanaarsakit and my co-advisor, Assistance Professor Dr. Pornchai Rojsitthisak for their crucial comments, valuable suggestions and helpful advice.

I wish to express my appreciation to all the members of my thesis committee, for their kind and beneficial comments and enlightening discussions. I am gratefully acknowledging the special effort by Department of Pharmaceutics and Industrial Pharmacy for their kindness to facilitate in laboratory.

Special thanks are devoted to Thai agrifoods Co., Ltd., Thailand for their rice bran wax provided. Special acknowledgement is Assistant Professor Dr. Suntharee Watcharadamrongkun for her helpful advice.

My sincere appreciation eventually dedicates to my family. Unless unconditional love, care, support, and warm encouragement provide, this research would not have been successful.

CONTENTS

Page

LIST OF TABLE

LIST OF FIGURE

LIST OF ABBREVIATIONS

% w/v	=	Percent weight by volume
μm	=	Micrometer
A_0	=	Amount at start time
AFM	=	Atomic force microscopy
ANOVA	=	Analysis of variance
AR	=	Analytical reagents
A_t	=	Amount at time
BDMC	=	Bisdemethoxycurcumin
BDMC-SLN	=	Bisdemethoxycurcumin loaded solid lipid nanoparticle
B-SLN	=	Blank solid lipid nanoparticle
CI	=	Crystallinity index
CO_2	=	carbon dioxide
COX-2	=	cyclooxygenase-2
CP	=	Cetyl palmitate
C-SLN	=	Curcuminoid loaded solid lipid nanoparticle
DLS	=	dynamic laser light scattering
DMSO	=	Dimethyl sulfoxide
DSC	=	Differential scanning calorimeter
E.E. %	=	Percentage of entrapment efficiency
e.g.	=	exempli gratia
FESEM	=	Field emission scanning electron microscope
GAMA	=	gas-assisted melting atomization

GB	=	Glyceryl behenate
GF	=	Gel formation
GRAS	=	Generally recognized as safe
HD	=	Homogeneous dispersion
HLB	=	hydrophilic lipophilic balance
HPH	=	High pressure homogenization
ICH	=	International council for harmonization
j/g	=	Joules per gram
MCF-7	=	Human breast adenocarcinoma cells
mg/ml	=	Milligram per milliliter
min	=	Minute
ml	=	Milliliter
mm	=	Millimeter
mmHg	=	Millimeter of mercury
mV	=	Millivolt
MWCO	=	Molecular weight cut off
n	=	Number
nm	=	Nanometer
o/w	=	Oil in water
^{o}C	=	Degree Celsius
PCS	=	Photon correlation spectroscopy
PDI	=	Polydispersity index
PS	=	Phase seperation
RB	=	Rice bran wax

RH	=	Relative humidity
rpm	=	Revolutions per minute
RT	=	Room temperature
SCF	=	Supercritical fluid
SEM	=	Scanning electron microscopy
SFEE	=	Supercritical fluid extraction of emulsions
SKOV 3	=	Human ovarian cancer cells
SLN	=	Solid lipid nanoparticle
SPSS	=	Statistic package of social sciences
TEM	=	Transmission electron microscopy
TW	=	Tween 80
UV-vis	=	Ultraviolet visible
v/v	=	Volume by volume
ZP	=	Zeta potential

CHAPTER I

INTRODUCTION

Bisdemethoxycurcumin (BDMC) is a phenolic compound and demethoxy derivative of curcumin, a natural substance in the turmeric root (*Curcuma longa* L.). Chemical formula $C_{19}H_{16}O_4$ has a Molecular weight 308.3 g/mol, UV/Vis λ_{max} 419 nm. BDMC is supplied as a crystalline solid. BDMC is soluble in organic solvents such as ethanol, DMSO and dimethyl formamide. The solubility of BDMC is approximately 5 µg/mL. BDMC is hydrophobic sparingly soluble in an aqueous solution. (Anand, Kunnumakkara et al. 2007) BDMC has significantly higher soluble and more stable than curcumin in physiological media (Luo, Du et al. 2015) but is still limited therapeutic use due to its instability. The polyphenolic structure of the curcuminoids decomposes rapidly when exposed to the light. Furthermore, curcuminoids are degraded quickly in alkaline aqueous environment (pH 9-10) resulted in poor bioavailability and extensive metabolism. At present, few medicinal researches have been developed to enhance the stability of dissolution and persistence of BDMC. Most researches were focused on dissolution, stability and bioavailability of curcumin. Therefore the problem of BDMC is the same with curcumin. As the qualification curcumin resemble with the qualification of BDMC. However, the low bioavailability of bisdemethoxycurcumin is a main hurdle for the regular application and further examination of this promising substance class. Hence, the development of a suitable pharmaceutical formulation to improve the bioavailability the bisdemethoxycurcumin is needed. Nanoparticle delivery systems could be considered as potential colloidal carriers since they could overcome problems of low solubility and stability, poor bioavailability, rapid breakdown and systemic elimination (Sun, Bi et al. 2013)

Solid lipid nanoparticles (SLN) are selected as lipid particulate delivery system which had more advantages over those of polymeric nanoparticles, fat emulsions and liposomes simultaneously avoid some of their disadvantages. They are biodegradable and non-toxic, stable against coalescence, drug leakage, hydrolysis,

particle growth often observed in lipid emulsions and liposomes. Unlike lipid emulsions, which have a fluid core, they possess a solid matrix which has the potential for allowing drug release over a prolonged period. Other advantages include low cost of ingredients, ease of preparation and scale up, high dispersibility in an aqueous medium, high entrapment of hydrophobic drug, controlled particle size and extended release of entrapped drug after single injection from few hours to several days. The perspectives for the use of SLN for controlled drug delivery were discussed by Üner and Yener (2007). They reported a prolonged in vitro release of up to 6 weeks for prednisolone. A few researchers also reported the use of waxes in the preparation of lipid nanoparticles. Rice bran wax is a natural wax retrieved from rice bran oil refineries. It contains potent antioxidant of gamma oryzanol which might retain stability of active ingredient. There are still less applied for pharmaceutical formulations. Therefore, rice bran wax utilization in pharmaceuticals as a natural lipid composition for SLN delivery systems is worth investigating.

The aim of this study was to develop a solid lipid nanoparticle prepared with rice bran wax for bisdemethoxycurcumin by high pressure homogenization method

General objective of the study:

To formulate and characterize solid lipid nanoparticles loaded bisdemethoxycurcumin

Specific objectives of the study:

1. To study the effect of types and quantities of solid lipids and surfactants on physicochemical properties of blank SLN
2. To prepare bisdemethoxycurcumin loaded SLN
3. To determine the entrapment efficiency and release profile of bisdemethoxycurcumin loaded SLN
4. To study physical stability of bisdemethoxycurcumin loaded SLN during storage

CHAPTER II

LITERATURE REVIEW

1. Bisdemethoxycurcumin

Bisdemethoxycurcumin is a phenolic compound and demethoxy derivative of curcumin. The structure of Bisdemethoxycurcumin was shown in Figure 1. It is a natural substance found in the turmeric root (*Curcuma longa* L.). Chemical formula ($C_{19}H_{16}O_4$) has Molecular weight 308.3 g/mol, and UV/Vis λ_{max} 419 nm. Bisdemethoxycurcumin is supplied as a crystalline solid. It is soluble in organic solvents such as ethanol, DMSO and dimethyl formamide. Bisdemethoxycurcumin is hydrophobic sparingly soluble in aqueous solutions. (Anand, Kunnumakkara et al. 2007) It is significantly higher solubility and more stable than curcumin in physiological media (Luo, Du et al. 2015) but still limited therapeutic application due to its instability. The polyphenolic structure of the curcuminoids decomposes rapidly under the influence of light. Many studies showed that curcuminoids are degraded quickly in alkaline aqueous environment (pH 9-10). They are stable at a pH below 6.5 resulted to poor bioavailability and extensive metabolism.

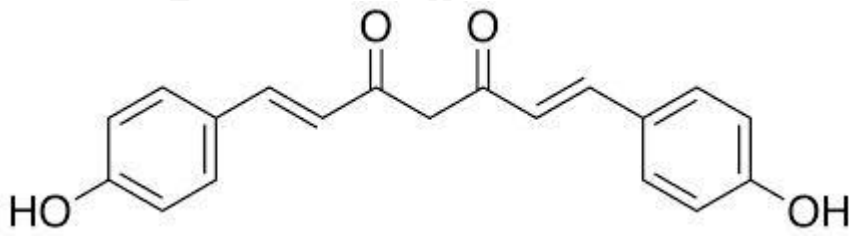

Figure 1. Chemical structure of Bisdemethoxycurcumin
(From: http://www.chemfaces.com/structural/Bisdemethoxycurcumin-CFN99186.jpg)

Curcuminoids are composed of three phenolic compounds: curcumin, demethoxycurcumin, and bisdemethoxycurcumin. They have been used in biomedical researches for many years and numerous articles have been published. An anti-inflammatory effect of curcuminoids was proofed quite a long time, in

traditional medicines. The therapeutic properties were a wound-healing, and an inhibition of transcription factors and enzymes related to inflammation. With regards to anti-inflammatory properties, curcuminoids antioxidants. It induces the transcription of metabolic phase-II enzymes and acts like an anti-oxidant. As known, inflammation and oxidative stress are associated with the carcinogenesis. Bisdemethoxycurcumin claimed to suppress the proliferation and antimetastasis of numerous cancer cells. For examples, MCF-7 breast cancer cell (Li, Gao et al. 2013), SKOV3 human ovarian cancer cells (Hai–xia Duan, Xiang-dong Ma et al. 2011), gastric adenocarcinoma (Luo, Du et al. 2015), Hepatic Stellate Cells (HSCs) (Lee, Woo et al. 2015) and BDMC against colon cancer (Devasena, Rajasekaran et al. 2003). It also has anti-inflammatory properties. Bisdemethoxycurcumin could inhibit inflammatory mediator COX-2 enzyme nitric oxide production (Ramsewak, DeWitt et al. 2000) and Kim, Jeon et al. (2010), Fiala, Liu et al. (2007) said that bisdemethoxycurcumin is a potent activator of macrophage phagocytosis in Alzheimer disease, Antiulcer potency of bisdemethoxycurcumin on gastric ulcer was also founded (Mahattanadul, Nakamura et al. 2009). Curcumin may also be applied topically to animal skin to counteract inflammation and irritated allergies. Topical application of curcumin strongly inhibited TPA-induced inflammation in mouse skin (Huang, Ma et al. 1997), inhibited COX-2 and lipoxygenase activities in TPA-treated mouse epidermis (Huang, Lysz et al. 1991) Anti-inflammatory properties of demethoxycurcumin and bisdemethoxycurcumin inhibited carrageenan-induced paw edema in mice. (Guo, Cai et al. 2008) Until now, there are a lot of curcuminoid formulations. Curcuminoids were formulated in a variety of pharmaceutical formulations especially in different colloidal carriers e.g. emulsion It is a neutral lipophilic oil core surrounded by a monolayer of amphiphilic lipid (Bergonzi, Hamdouch et al. 2014), (Wang, Jiang et al. 2008), (Lin, Lin et al. 2009), The cons of this formulation was the instability of the physical state due to the reduction of zeta potential during storage. The agglomeration and drug expulsion were introduced leading to the breakage of the emulsion. Liposomes contain an outer bilayer of amphipathic molecule such as phospholipid with an aqueous compartment inside. The amount of poorly water-soluble drug that is possible to incorporate is low (Basnet, Hussain et al.), (Swarnlata

Saraf and Jeswani 2014), however limited due to the relatively small volume of the hydrophobic region of the lipid bilayer in comparison to aqueous interior. In addition, other obstacles were physical stability, drug leakage, and instability in the vascular system due to lipid exchange with lipoproteins and rapid removal from circulation following intravenous ad-ministration primarily by Kupffer cells of the liver and fixed macrophages of the spleen, polymeric micelles and polymeric nanoparticles Lack of large scale production methods to yield a product of a quality acceptable for registration, cost of the polymeric material, toxic solvent residues from the production process (e.g. Solvent evaporation method), cytotoxicity of some polymeric particles (e.g. Lactic acid release from polylactic acid particles) and chemical problems with the polymers (e.g. catalyst residues, molecular non-homogeneity) (Tikekar, Pan et al. 2013), (Abbas, Karangwa et al. 2015), self-microemulsifying systems , solid lipid nanoparticles (Zhao, Lu et al. 2013), (Onoue, Takahashi et al. 2010).

2. Solid lipid nanoparticles delivery systems

Solid lipid nanoparticles (SLN) are novel colloidal delivery systems consisted of a biocompatible lipid core and an amphiphilic surfactant as an outer shell. The mean diameter is ranged from 50 to 1,000 nm. These are aqueous colloidal dispersions; the matrix of which is comprised of solid biodegradable lipids. The uses of solid lipids are greater than liquid oils in order to control drug release, and drug mobility in a solid lipid should be considerably lower compared with liquid oil (Martins, Sarmento et al. 2007). SLN can be categorized to 3 Classes (Figure 2). Homogeneous matrix model (Class I) is derived from solid solution of lipid and other active ingredients. Solid solutions obtained when SLN are produced by cold homogenization method. Drug enriched core model (Class II) can be achieved when active ingredient concentration in melted lipid is high, and relatively closed to its saturation solubility. The reason is that the excession of active molecules precipitates and forms drug enriched cores. Drug enriched shell model (Class III) is achieved when SLN are produced by hot homogenization technique and active ingredient

concentration in melted lipid is low. The enrichment of outer area of the particles causes burst release.

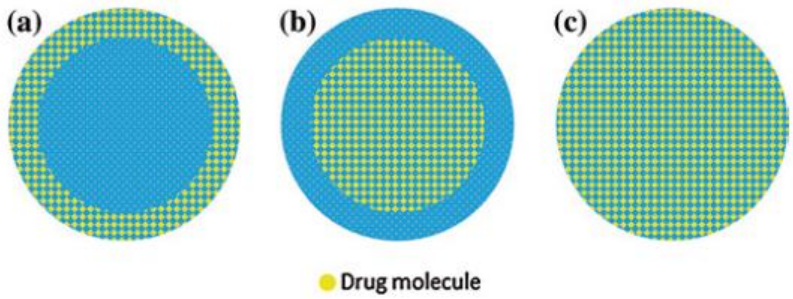

Figure 2. Drug incorporation models of solid lipid nanoparticles. (a) Drug-enriched shell model, (b) Drug-enriched core model, and (c) Homogenous matrix model (Müller, Mäder et al. 2000)

SLN are regularly composed of solid lipid, surfactant, co-surfactant (optional) and active pharmaceutical ingredients. The lipids used in the lipid nanoparticles production are physiological lipids. It was the main ingredient of lipid nanoparticles that influence their drug loading capacity, stability and sustained release behavior of the formulations. Lipids used in the production are broadly categorized based on their structural into fatty acids, fatty esters, fatty alcohols, triglycerides, or partial glycerides (Table 1). Most of these lipids are approved as generally-recognized-as-safe (GRAS) and are physiologically well-tolerated. Lipid polymorphism is another factor that influences the properties of a lipid nanoparticle system. The occurrence of multiple crystalline forms in solid lipids is particularly useful as they provide structural defects in which drug molecules can be accommodated. The perfect crystalline lattice, however, is more thermodynamically stable than the others. For example, the β-forms of triglycerides are more stable than the α-forms and β′-forms.

Table 1. Lipids used in the preparation of lipid nanoparticles

Fatty acids	**Waxes**
Dodecanoic acid Myristic acid Palmitic acid Stearic acid	Cetyl palmitate Carnauba wax Beeswax Rice bran wax
Monoglycerides	**Liquid lipids**
Glyceryl monostearate Glyceryl behenate Glyceryl hydroxystearate	Soya bean oil Oleic acid Medium chain triglycerides (MCT)/caprylic-and capric triglycerides α-tocopherol/Vitamin E Squalene Isopropyl myristate
Diglycerides	
Glyceryl palmitostearate Glyceryl dibehenate	
Triglycerides	**Cationic lipids**
Caprylate triglyceride Caprate triglyceride Glyceryl tristearate/Tristearin Glyceryl trilaurate/Trilaurin Glyceryl trimyristate/Trimyristin Glyceryl tripalmitate/Tripalmitin Glyceryl tribehenate/Tribehenin	Stearylamine (SA) Benzalkonium chloride Cetrimide Cetyl pyridinium chloride Dimethyl dioctadecyl ammonium bromide

Moreover, Glyceryl behenate is a representative of monoglycerides lipid. Glyceryl behenate as recognized in Compritol® ATO 888 is a saturated fatty acid ($C_{25}H_{50}O_4$) based on glycerol esters of behenic acid (C22), where the main fatty acid is behenic acid > 85% but other fatty acids (C16-C20) are also presented. The chemical structure is shown in Figure 3. Melting point is 69-74 °C.

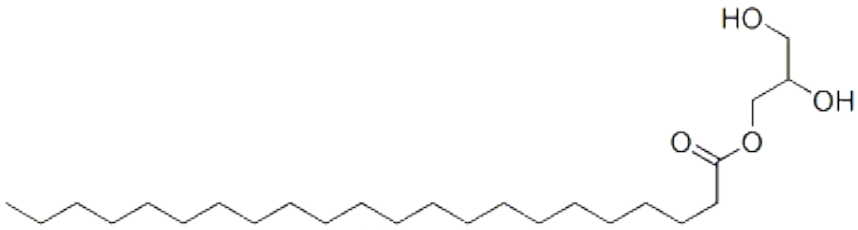

Figure 3. Chemical structure of Glyceryl behenate

(From: https://pubchem.ncbi.nlm.nih.gov/image/imgsrv.fcgi?cid=5362585&t=l)

Cetyl palmitate is a representative of waxes as same as rice bran wax but different physicochemical properties. Cetyl palmitate, called Cutina CP®, is a white waxy solid that achieved from skull of sperm whales. The primary constituent is the esterwax ($C_{32}H_{64}O_2$) derived from palmitic acid (C16) and cetyl alcohol (C16). Melting point is 55-56 °C.The chemical structure as shown in Figure 4.

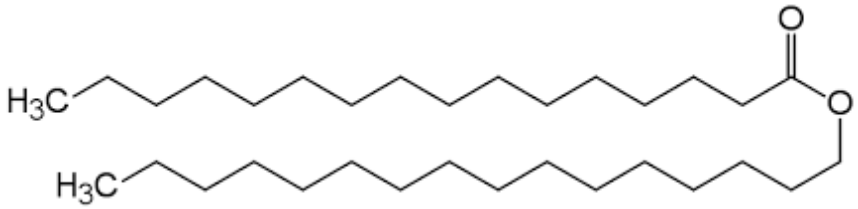

Figure 4. Chemical structure of Cetyl palmitate

(From: https://commons.wikimedia.org/wiki/File:Cetyl_palmitate.svg)

Lipid nanoparticles are stabilized the colloidal system with surfactants. Some may combine with a co-surfactant. Surfactants are amphipathic molecules that possess a hydrophilic moiety (polar) and a lipophilic moiety (non-polar), which together form the typical head and the tail of surfactants. At low concentrations,

surfactants adsorb onto the surface of a system or interface. They reduce the surface or interfacial free energy and consequently reduce the surface or interfacial tension between the two phases. The relative and effective proportions of these two moieties are reflected in their hydrophilic lipophilic balance (HLB) value. Surfactants used in the preparation of lipid nanoparticle preparations play two distinctive important roles. First, they disperse the lipid melt in the aqueous phase during the production process. The other is surfactants stabilize the lipid nanoparticles in dispersions after cooling. Surfactants can be broadly categorized into three classes depended on their charge: ionic, non-ionic and amphoteric. Ionic surfactants are traditionally thought to infer electrostatic stability such as Sodium cholate, Sodium glycocholate, Sodium taurocholate, Sodium taurodeoxycholate, Sodium oleate and Sodium dodecyl sulphate. Non-ionic surfactants are traditionally thought to infer steric repulsion stability. For instance, Tween 20, Tween 80, Span 20, Span 80, Span 85, Tyloxapol, Poloxamer 188, Poloxamer 407, Poloxamine 908, Brij78, Tego care 450, Solutol HS15. As recognized the Tween® families are the most commonly used non-ionic surfactants. Most of surfactants contain a hydrophilic moiety (ethylene oxide) and a hydrophobic moiety (hydrocarbon chain). On the other hand, Phospholipids and phosphatidylcholines are the common amphoteric surfactants employed in lipid nanoparticle preparation. These surfactants have both negatively and positively charged functional groups. They exhibit features of a cationic and an anionic surfactant at low and high pH conditions, respectively. Amphoteric surfactant or Zwitterionic surfactants have both cationic and anionic centers attached to the same molecule. The cationic part is based on quaternary ammonium cations. The ionic part can be more variable. For examples Egg phosphatidylcholine, Egg phospholipid, Hydrogenated egg phosphatidylcholine, Soy phosphatidylcholine, Soy phospholipid and Hydrogenated soy phosphatidylcholine (Pandey and Anushree 2014).

Methods of preparation of SLN:

Various techniques are used to produce SLN. A common step of those techniques is of, the formation of a precursor oil-in-water “nanoemulsion” followed by subsequent solidification of the dispersed lipid phase. SLN production techniques

do not need to employ potentially toxic organic solvents, which may also have deleterious effect on protein drugs. Preparations of SLN were more cost effective and technically simpler alternation, particularly for poorly soluble drugs. This yields a more physically stable product than liposomes; conventional colloidal drug carriers. There are various methods for preparation of SLN: High pressure homogenization technique, Microemulsion-based SLN preparations, Solvent emulsification /evaporation, and Supercritical fluid technology. High pressure homogenization technique prepared the pre-emulsion with hot melt homogenization carried out at temperatures above the melting point of the lipid (Müller, Mäder et al. 2000) A pre-emulsion of the drug loaded lipid melt and the aqueous emulsifier phase (same temperature) is obtained by high-shear mixing device (Ultra-Turrax®). The quality of the pre-emulsion is vital impacted on the quality of the final product. It is desirable to obtain droplets in the size range of a few micrometers. Next, the pre-emulsion is carried out at temperatures above the melting point of the lipid. In general, higher temperatures result in lower particle sizes due to the decreased viscosity of the inner phase. To overcome the polydispersity and larger than desired droplet sizes, researchers often subject the precursor emulsions to large mechanical forces. High pressure homogenizer pushes a liquid with high pressure approximately 100-2000 bar through a narrow gap. The pre-emulsion accelerated on a very short distance to very high velocity. The result from very high shear stress and cavitation forces disrupt the particles down to the submicron range (Figure 5).

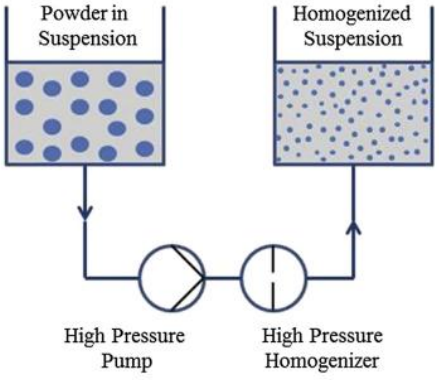

Figure 5. High pressure homogenization techniques

(From: Kluge et al., 2012)

Second, microemulsion-based SLN preparations involve stirring of an optically transparent mixture at 65-70 °C, so as to form microemulsion (de Jesus, Radaic et al. (2013). The microemulsion is typically composed of a low-melting fatty acid, an emulsifier, co-emulsifiers, and water. The hot microemulsion is dispersed in cold water (2–3 °C) under stirring. The dilution process is critically determined by the composition of the microemulsion. In this method, no energy is required to achieve submicron particle sizes as microemulsion is used. The third method is solvent emulsification/ evaporation. The lipophilic material is dissolved in a water-immiscible organic solvent then is emulsified in an aqueous phase Lemos-Senna, Wouessidjewe et al. (1998). Upon evaporation of the solvent, nanoparticle dispersion is formed by precipitation of the lipid in the aqueous medium. The mean particle size depends on the concentration of the lipid in the organic phase. Very small particles could only be obtained with low fat loads (5 % w/v) related to the organic solvent. With increasing lipid content, the efficiency of the homogenization declines due to the higher viscosity of the dispersed phase. The significant advantage of this procedure over the cold homogenization is avoidance of any thermal stress. Lastly, supercritical fluid technology is introduced by Chattopadhyay, Shekunov et al. (2007). Supercritical fluid (SCF) technology is obtained above its critical pressure and temperature. The solubility of a substance in the fluid can be modulated by a relatively small change in pressure if it is above this fluid's critical point. Due to its low critical point at 31 °C and 74 bar with low cost and non-toxicity, carbon dioxide is the most widely used in SCF. Two main SCF- based methods have been developed for SLN production: Supercritical fluid extraction of emulsions (SFEE) and Gas-assisted melting atomization (GAMA). SFEE is based on a simple principle, whereby the lipid nanosuspensions are produced by supercritical fluid extraction of the organic solvent from oil-in-water (O/W) emulsions. One of the advantages of this technique is that the solvent extraction efficiency using supercritical CO_2 is much higher than for the conventional methods, i.e., solvent evaporation, liquid extraction, and dilution. This allows a fast, complete removal of the solvent and a more uniform particle size distribution.

The small size and relatively narrow size distribution provides biological opportunities for site specific drug delivery. lipospheres can behave controlled release of active drug over a long period. It also can be achieved and performed protection chemical degradation of drug. During the preparation process, free from organic solvents and no toxic metabolites residues are produced. The hot dispersion technique provides an easily process for industrial scale production. Moreover, surface modification can easily be accomplished which offer potential for site-specific drug delivery. These benefits were modulated release, improved bioavailability, protection of chemically labile molecules like retinol, peptides from degradation, cost effective excipients, improved drug incorporation, and wide application spectrum. However, it limits drug loading capacity and drug expulsion during storage.

Characterizations of SLN

The parameters are generally used to ensure that a good product is made by the process including particle size, its distribution, particle morphology, and surface charge determined as zeta potential value, drug incorporated capacity, drug release profile, and crystallinity of the lipid particles (Table 2)

Table 2. the characterization methods for SLN

	Parameters	Characterization method
1	Particle size and size distribution	Photon correlation spectroscopy (PCS), Scanning electron microscopy (SEM) Transmission electron microscopy (TEM), Atomic force microscopy (AFM), Laser diffractrometer
2	Charge determination	Laser droplet anemometry, Zeta potentiometer
3	Surface hydrophobicity	Water contact angle measurement, Rose bangle (dye) binding,

		Hydrophobic interaction chromatography, X-ray photoelectron spectroscopy
4	Chemical analysis of surface	Static secondary ion mass spectrometry
5	Carrier drug interaction	Differential scanning calorimetry
6	Release profile	In-vitro release characteristic under physiologic & sink condition
7	Drug stability	Bioassay of drug extracted from nanoparticles, Chemical analysis of drug

Particle size significantly affects the physical stability. The average size and size distribution of solid lipid nanoparticles is also important with respect to the release rate of the loaded drug. So the size of SLN will have to be controlled within reasonable limits. The particle size depends on the matrix constituents as well as on type and amount of emulsifying agent. The increase in the amount of emulsifier generally decreases the mean diameter of the bulk population but not significantly affecting the Polydispersity index (PDI) (Pandey and Anushree 2014). There are a number of methods used to determine the physical attributes, but photon correlation spectroscopy and electron microscopy technique are the most commonly used tools. Photon correlation spectroscopy (PCS) is a dynamic laser based technique. The light scattering (DLS), due to Brownian motion of particles in solution or suspension, is suitable for the measurement of particles ranged from 3 nm to 3 μm. However, polydispersity index (PDI) greater than 0.5 indicates a very broad size distribution. Morphology can be determined by Electron microscopy: These techniques, such as SEM and TEM, are very useful in determining the overall shape and morphology of lipid nanoparticles. SEM uses electrons transmitted from the specimen surface, while TEM uses electrons transmitted through their specimen. SEM has high resolution and the sample preparation is relatively easy. However,

nanoparticles must withstand a strong vacuum, conductive in order to be analyzed. Therefore, the surface of the sample coated with a conductive metal such as gold can modify the original aspect of the particles. Zeta potential measures of the charge on the particles. It imparts colloidal stability due to particle-particle repulsion. A zeta potential measurement also helps in design particles with reducing reticuloendothelial uptake. In order to divert SLN from the lymphatic system, the surface of the particles should be hydrophilic and non-charged (Müller, Mäder et al. 2000) crystallization tendency and polymorphic behavior. Solid lipid nanoparticles are based on physiologically tolerable lipids, predominantly saturated monoacid triglycerides or hard fat that are solid at room temperature as matrix constituents. The solid state of the particles is of prime importance, as it reduces the mobility of incorporated drug and thus prevents drug leakage from the carrier. Moreover, the rigid solid particles are less prone to stability problem called coalescence. As the potential advantages of these novel drug carrier systems essentially rely on the solid state of the lipid particles, the solidification of the particles after the homogenization process must be ensured. It has to be taken into consideration that some lipid particles may not recrystallize in colloid dispersed state and can remain in the supercooled state for a long period time. The melting and crystallization behavior or the kinetics of polymorphic transitions of lipids in the dispersed state as shown in Figure 6 can differ significantly from their bulk material. The presence of emulsifiers, the preparative method and the high dispersity as well as the small particle size of the colloidal drug carrier systems may be behind for changes in the crystallization behavior, the degree of crystallinity, and the crystal modifications of the matrix constituents compared to bulk materials.

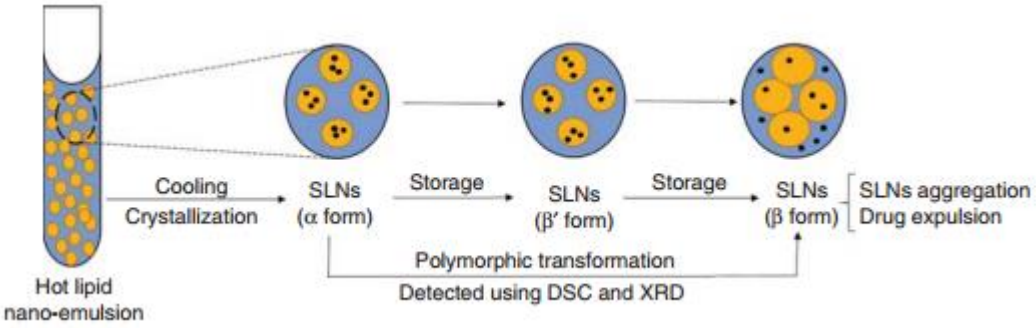

Figure 6. Schematic representations of solid lipid polymorphic transition (Aburahma and Badr-Eldin 2014).

Determination of incorporated drug, it is of prime importance to measure the amount of drug incorporated in SLN. It influences the release characteristics. The amount of drug encapsulated per unit weight of nanoparticles is determined after separation of the free drug and solid lipids from the aqueous medium. This separation can be carried out using ultracentrifugation, centrifugation filtration, or gel permeation chromatography. *In vitro* drug release studies are mainly useful for quality control and the prediction of *In vivo* kinetics. Unfortunately, due to the very small size of the particles, the release rates observed *in vivo* differs greatly from the release obtained in a buffer solution. However, *in vitro* release studies remain very useful for quality control, and evaluation of the influence of process parameters on the release rate of active compounds. In storage stability, the physical stability of the SLN during prolonged storage can be determined by monitoring changes in particle size, drug content, appearance, and viscosity as a function of times.

3. Rice bran wax

Rice bran wax is a vegetable wax extracted from the bran oil of rice (*Oryza sativa*). INCI name: *Oryza Sativa (Rice) Bran Wax* and is abundantly available. Rice bran is the brown layer between the rice and outer husk of the paddy. Rice bran wax is an important by product of rice bran oil industry. The wax deposits at the bottom of the crude oil and can be separated by filtration or centrifugation. The yield varies from 3 to 9% on the total oil basis.

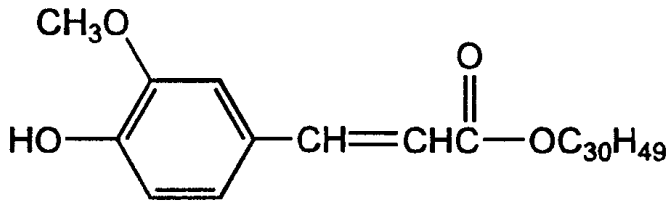

Figure 7. Chemical structure of Rice bran wax main component

(From: http://patentimages.storage.googleapis.com/WO1998019651A1/imgf000006_0001.png)

Main components of rice bran wax are aliphatic acids (wax acids) and higher alcohol esters (Figure 7). The aliphatic acids consist of palmitic acid (C16), behenic acid (C22), lignoceric acid (C24) and other higher wax acids. The higher alcohol esters consist mainly of cetyl alcohol (C26) and melissyl alcohol (C30). Rice bran wax also contains constituents such as free fatty acids (palmitic acid, squalene and phospholipids). Therefore wax was nontoxic and safe to use in pharmaceutical preparations. From the previous study, Rice bran wax is edible and can serve as a substitute for carnauba wax in most applications due to it relatively high melting point (Maru, Surawase et al. 2012) It has chemical constituents and physicochemical properties similar to that of Carnauba wax. In cosmetics, rice bran wax is used as an emollient (UG 2013), and is the basis material for some exfoliation particles. It has been observed that rice bran wax at concentrations as low as 1 % (w/w) in triglycerides can crystallize to form stable gels. The physical properties of rice bran wax has reported Melting point = 77 - 86 °C, Saponification value = 75 – 120, Iodine number = 11.1 - 17.6, Free fatty acids = 2.1 - 7.3%, Phosphorus = 0.01 - 0.15%, Off-white to moderate yellow/brown color, and typical fatty odor. Solubility studies reveal that the wax is soluble in organic solvents like chloroform & petroleum ether showing typical solubility properties of waxes. (U.G. 2013)

CHAPTER III

MATERIALS AND METHODS

1. Materials & Apparatus

1.1. Material

Absolute ethanol, AR grade (Lab Scan Co., Ltd., Thailand)

Bisdemethoxycurcumin

Cetyl palmitate (Cutina CP®) (Thai Sanguanwat Chemical Co., Ltd., Thailand, Lot no. 71490001)

Curcuminoid (Thai china flavours & fragrances industry Co., Ltd., Thailand)

Glyceryl behenate (Compritol® ATO88) (Gattefosse', France, Lot no. 142540)

Methanol, AR grade (Lab Scan Co., Ltd., Thailand, Lot no. 15090100)

Polyoxyethylene 20 sorbitan monooleate (Tween®80) (Thai Sanguanwat Chemical Co., Ltd., Thailand, Lot no. 11043332)

Rice bran wax (Thai agrifoods Co., Ltd., Thailand)

1.2. Apparatus

Analytical balance (Model AX105, Mettler Toledo, Switzerland)

Differential scanning calorimeter (Model DSC 822^e, Mettler Toledo., Germany)

Dry cabinet (Model GH-197, Ampore House, Taiwan)

Field Emission Scanning Electron Microscopy (FESEM) (JSM 7610F, Jeol, Japan)

Freeze dryer (Model FD-6-850MPO, Dura-Dry™, FTS System Inc., USA)

High pressure homogenizer (Model Emulsiflex C5®, Avestin, Canada)

High speed homogenizer (Ultra-Turrax T-25 Basic, IKA-Werk)

High speed refrigerated micro centrifuge (Model Tomy MX-305, Japan)

Magnetic stirrer (CAT, Germany)

Micropipette (Pipetman, Gilson, Inc., France)

Modified Franz Diffusion cells (Crown Glass Company, USA)

Photon correlation spectrometer (Zetasizer Nano ZS, Malvern Instruments, UK)

Stability cabinet (Eurotherm Axyos, Germany)

BMG labtech UV visible spectrophotometer (Model clariostar®, Germany)

Vortex mixer (Vortex Ginies-2, Scientific Industries, USA)

Water bath (Model WB22, Becthai Co., Ltd., Thailand)

1.3. Accessories

96-well plates (Costar® 3912, Corning, Inc., USA)

Aluminium foil (MMP Packaging, Thailand)

Aluminum crucible standard 40 µl (Mettler Toledo., Germany)

Beaker (Pyrex, USA)

Centrifugal Filter Units, MWCO = 100 K (Amicon® Ultra-4, Millipore Ltd., Ireland, Lot no. R2BA90230)

Cylinder (Pyrex, USA)

Disposable pipette tip (Socorex, Switzerland)

Disposable syringe and needle (Terumo, Thailand)

Parafilm (American National Can TM, USA)

Parafilm (American National Can., USA)

Polycarbonate centrifuge tube (Corning, USA)

Polycarbonate Hydrophilic Membrane (Cyclopore® 0.2 µm, Ø 25 mm, Whatman International Ltd., England)

Screwed-cap tube (Pyrex, USA)

Transferring pipette (Witeg, Germany)

Vial type I glass with rubber cap and aluminium ring (Supplied by APPA Industrial Co., Ltd., Thailand)

2. Methods

2.1. Preliminary studies of curcuminoid loaded solid lipid nanoparticles (C-SLN)

2.1.1. Preparation of blank solid lipid nanoparticles

Blank solid lipid nanoparticles (B-SLN) were prepared using different three lipid types and concentrations; rice bran wax, cetyl palmitate and glyceryl behenate at 2.5, 5 and 7.5% w/w by high pressure homogenization technique. Both lipid and aqueous phases were separately melted at temperature of a lipid melting point plus 10 $^{\circ}$C in order to complete pre-emulsification. The hot aqueous phase containing 1, 3 and 5% w/w tween 80 as surfactant, was dispersed in hot lipid phase (Table 3). Pre-emulsion was homogenized using a high speed homogenizer (Ultra-Turrax T-25 Basic, IKA-Werk) at 10,000 rpm for 5 minutes. Then, the emulsion was reduced droplet size to nanorange using a high pressure homogenizer (HPH, EmulsiFlex-C5, Avestin Inc.) at 1,000 bars, 3 cycles and 85 $^{\circ}$C. The nanodispersion was rapidly cooled using an ice bath to solidify the nanoparticles and avoidance of particle fusion during the process. (Sun, Bi et al. 2013)

Table 3. Formulation of blank SLN

Code	Composition			
	Lipid			Surfactant
	RB (% w/w)	GB (% w/w)	CP (% w/w)	Tween 80
RB2.5Tw1	2.5	-	-	1
RB5.0Tw1	5	-	-	1
RB7.5Tw1	7.5	-	-	1
GB2.5Tw1	-	2.5	-	1
GB5.0Tw1	-	5	-	1
GB7.5Tw1	-	7.5	-	1

CP2.5Tw1	-	-	2.5	1
CP5.0Tw1	-	-	5	1
CP7.5Tw1	-	-	7.5	1
RB2.5Tw3	2.5	-	-	3
RB5.0Tw3	5	-	-	3
RB7.5Tw3	7.5	-	-	3
GB2.5Tw3	-	2.5	-	3
GB5.0Tw3	-	5	-	3
GB7.5Tw3	-	7.5	-	3
CP2.5Tw3	-	-	2.5	3
CP5.0Tw3	-	-	5	3
CP7.5Tw3	-	-	7.5	3
RB2.5Tw5	2.5	-	-	5
RB5.0Tw5	5	-	-	5
RB7.5Tw5	7.5	-	-	5
GB2.5Tw5	-	2.5	-	5
GB5.0Tw5	-	5	-	5
GB7.5Tw5	-	7.5	-	5
CP2.5Tw5	-	-	2.5	5
CP5.0Tw5	-	-	5	5
CP7.5Tw5	-	-	7.5	5

2.1.1.1. Particle size analysis of blank SLN

The mean particle size, polydispersity index (PdI) and zeta potential (ZP) of the blank SLN were determined by Malvern Zetasizer Nano ZS (Malvern Instruments, UK). Samples were prepared by diluting the dispersion with distilled

water at ratio of 1:20. Then the mixture sample was vortexed for 30 seconds and subsequently analyzed. Each sample was measured triplicate. (Abdel-Salam, Elkheshen et al. 2015)

2.1.1.2. Physical stability of blank SLN

According to modified ICH guidelines, stability of the developed SLN formulation was evaluated for 3 months. Briefly, samples were stored in the sealed amber colored glass vials at room temperature (RT; 25± 2°C/60± 5% RH) for 3 months. Physical stability of the SLN was assessed in terms of physical appearance, particle size, polydispersity index, zeta Potential and entrapment efficiency at every month. All of the experiments were performed in triplicate. (Vaghasiya, Kumar et al. 2013)

2.1.2. Preparation of curcuminoid loaded solid lipid nanoparticles (C-SLN)

Curcuminoid 0.1% w/w was dispersed in hot aqueous containing tween 80 and ethanol (Table 4). A pre-emulsion of the drug loaded lipid melt and the aqueous phase (at same temperature) was obtained by using a high-shear mixing device (Ultra-Turrax®) followed by a high pressure homogenization which carried out at above the lipid melting temperatures as described in Section 2.1.1.

Table 4. Formulation of curcuminoid loaded SLN

Code	Composition				
	Lipid			Surfactant	Drug
	RB (% w/w)	GB (% w/w)	CP (% w/w)	Tween 80 (% w/w)	BDMC (% w/w)
RB2.5Tw1-C	2.5	-	-	1	0.1
RB5.0Tw1-C	5	-	-	1	0.1
RB7.5Tw1-C	7.5	-	-	1	0.1
GB2.5Tw1-C	-	2.5	-	1	0.1
GB5.0Tw1-C	-	5	-	1	0.1

GB7.5Tw1-C	-	7.5	-	1	0.1
CP2.5Tw1-C	-	-	2.5	1	0.1
CP5.0Tw1-C	-	-	5	1	0.1
CP7.5Tw1-C	-	-	7.5	1	0.1
RB2.5Tw5-C	2.5	-	-	5	0.1
RB5.0Tw5-C	5	-	-	5	0.1
RB7.5Tw5-C	7.5	-	-	5	0.1
GB2.5Tw5-C	-	2.5	-	5	0.1
GB5.0Tw5-C	-	5	-	5	0.1
GB7.5Tw5-C	-	7.5	-	5	0.1
CP2.5Tw5-C	-	-	2.5	5	0.1
CP5.0Tw5-C	-	-	5	5	0.1
CP7.5Tw5-C	-	-	7.5	5	0.1

2.1.2.1. Particle size analysis of C-SLN

The mean particle size, polydispersity index (PdI) and zeta potential (ZP) of the C-SLN were determined as described in 2.1.1.1.

2.1.2.2. Determination of entrapment efficiency

Curcuminoid entrapment efficiency was determined by using ultrafiltration method as previously described with slightly modification (Hsu, Cui et al. 2003). A centrifugal filter device of Amicon® cellulose membrane, MWCO 100K equivalent to 30-90 nm was used. Samples were centrifuged at 12,000 rpm 25°C for 30 minutes. The supernatant was collected for free drug analyzed at 420 nm using UV-vis spectrophotometer (Tiyaboonchai, Tungpradit et al. 2007). Then, the precipitated SLN containing curcuminoid was lyzed by adding methanol and centrifuged. The supernatant of lyzed-lipid matrix was analyzed for amount of drug

entrapment. Triplicate of samples were studied. The percentages of entrapment efficiency was calculated by the following equation.

$$\text{Entrapment efficiency (\%)} = \frac{\text{Amount of entrapped BDMC}}{\text{Amount of initial BDMC added}} \text{x} 100$$

2.1.2.3. Physical stability of C-SLN

Stability of the C-SLN formulation was evaluated for 3 months as described in 2.1.1.2.

2.2. Preparation of Bisdemethoxycurcumin loaded solid lipid nanoparticles (BDMC-SLN)

The system containing 2.5, 5, 7.5% lipid and 5% tween 80 were chosen for bisdemethoxycurcumin loading (Table 5). Bisdemethoxycurcumin 0.1% w/w was dispersed in hot aqueous containing tween 80 and ethanol. BDMC-SLN was prepared similar to the preparation of the C-SLN as described above.

Table 5. Formulation of bisdemethoxycurcumin loaded SLN

Code	Composition				
	Lipid			Surfactant	Drug
	RB (% w/w)	GB (% w/w)	CP (% w/w)	Tween 80 (% w/w)	BDMC (% w/w)
RB2.5Tw5-BDMC	2.5	-	-	5	0.1
RB5.0Tw5-BDMC	5	-	-	5	0.1
RB7.5Tw5-BDMC	7.5	-	-	5	0.1
GB2.5Tw5-BDMC	-	2.5	-	5	0.1
GB5.0Tw5-BDMC	-	5	-	5	0.1
GB7.5Tw5-BDMC	-	7.5	-	5	0.1
CP2.5Tw5-BDMC	-	-	2.5	5	0.1
CP5.0Tw5-BDMC	-	-	5	5	0.1
CP7.5Tw5-BDMC	-	-	7.5	5	0.1

2.2.1. Particle size analysis of BDMC-SLN

Particle size analysis of the BDMC-SLN was carried out as described in Section 2.1.1.1.

2.2.2. Scanning electron microscopy (SEM)

Shape and surface morphology of the BDMC-SLN were examined by field emission scanning electron Microscopy (FESEM). Samples were analyzed in the form of aqueous dispersion using JSM 7610F (JEOL, Japan) Analysis was performed at 25 ± 2 $^{\circ}$C.

2.2.3. Differential Scanning Calorimetry (DSC)

The BDMC-SLN formulations were lyophilized using Dura-Dry^{TM} lyophilizer. Five milliliters of each sample was rapidly precooled at -40°C, lyophilized for 24 hours at a temperature range -10°C to 20°C with 500 mmHg vacuum. Water in the SLN sample was eliminated by freeze-dryer. Melting and recrystallization behavior of crystalline material was assessed using Mettler DSC 822^{e} (Mettler Toledo, Germany). DSC scans of the bulk lipids and SLN formulations were carried out. An empty aluminum pan served as reference. All of the samples were kept in desiccators for 24 hours before thermal analysis. DSC studies on bisdemethoxycurcumin, RB, GB, CP, tween 80, physical mixture (BDMC, lipid and tween 80 at the same ratio as used in the formulation) and BDMC-SLN were performed. Dry nitrogen gas was used as the purge gas through a DSC cell at a flow rate of 40 ml/min and heated at a rate of 20 $^{\circ}$C/min from 25 to 200°C. Crystallinity index (CI) was calculated from the heat of fusion to determine the degree of crystallinity of the SLN according to the following equation (Vaghasiya, Kumar et al. 2013).

$$\text{Crystallization Index (\%)} = \frac{\text{Enthalpy}_{\text{SLNs}}(J/g)}{\text{Enthalpy}_{\text{Bulk lipid}}(J/g)\text{x}\text{Concentration}_{\text{Lipid}}}\text{x}100$$

2.2.4. Determination of entrapment efficiency

Bisdemethoxycurcumin entrapment efficiency was determined by ultrafiltration method as described in Section 2.1.2.2.

2.2.5. *In vitro* release study

The release was studied using vertical Franz diffusion cells (Model No. 57-951-061, Meditron,Volklingen, Germany) at 37± 0.5°C. Polycarbonate hydrophilic membrane (Cyclopore™ Membrane 0.22 µm,25 mm) was fitted between donor and receptor compartment. The receptor chamber volume was 14 ml. The receptor medium consisting of 50% (v/v) ethanol and 2%v/v tween 80 was continuously stirred (Tiyaboonchai, Tungpradit et al. 2007). The vertical Franz diffusion cell was allowed to equilibrate for 15 min before applying the sample. One milliliter of the SLN formulation was dropped into the donor chamber then covered with parafilm to prevent evaporation. One milliliter of a solution with 1 mg/mL of the bisdemethoxycurcumin in Tween 80 5%w/v, ethanol 15%w/v, and water 80% w/v was used as control. Two milliliters of the receptor medium was taken at predetermined time intervals of 30 minutes, 1, 2, 3, 4, 5, 6, 10, 12, 18, 20 and 24 hours. The receptor compartment was replaced with the same volume of receptor solution to keep the constant volume during the experiment and to maintain sink condition. The receptor fluid was diluted at appropriated concentration and measured amount of bisdemethoxycurcumin by UV-vis spectrophotometry method as in section 2.1.2.2. The triplicate observations were measured. The cumulative amount of bisdemethoxycurcumin release was calculated by the following equation:

$$\text{Cumulative amount of free BDMC release } (\%) = \frac{A_t}{A_0} \text{x} 100$$

2.2.6. Physical and chemical stability

According to modified ICH guidelines, the stability of the developed SLN formulation was evaluated for 3 months. Briefly, samples were stored in the sealed amber colored glass vials at room temperature (RT; 25± 2°C/60± 5% RH) for 3 months; as described in Section 2.1.1.2. The stability of BDMC-SLN was assessed in terms of physical appearance, particle size, polydispersity index, zeta potential, differential scanning calorimetry and entrapment efficiency.

2.3. Statistical analysis

The data were statistically analyzed by using student's t-test, one-way analysis of variance (ANOVA). When a significant difference ($p<0.05$) was indicated, the data were subjected to multiple comparison by Tukey or Dunnett test to compare the difference. The licensed statistical package for social sciences (SPSS) software for windows version 17.0 was used in this study.

CHAPTER IV
RESULTS AND DISCUSSION

1. Preparation of blank solid lipid nanoparticles by high pressure homogenization method

Blank-SLN dispersions were composed of Rice bran wax, Glyceryl behenate or Cetyl palmitate as core matrices used in different concentrations 2.5, 5 and 7.5 % (w/w). These lipid based carrier systems were stabilized by 1, 3 and 5 % (w/w) Tween 80.

1.1. Physical characterization

1.1.1. Physical appearance

Appearance of different lipid type of blank-SLN dispersions was observed after freshly prepared. All of these SLN were homogeneous dispersion. The SLN containing rice bran wax (RB) had light-brown color, while glyceryl behenate (GB) and cetyl palmitate (CP) had off-white color. At higher amount of lipid, their appearance showed more turbidity. On the other hand, these dispersions showed clearer when increased tween 80 concentration (Figure 8 to 10).

Figure 8. Appearances of freshly prepared blank-SLN: lipid 2.5, 5.0 and 7.5 (% w/w); tween 80 at 1 (% w/w) (RB = Rice bran wax, GB = Glyceryl behenate, CP = Cetyl palmitate, Tw = Tween 80)

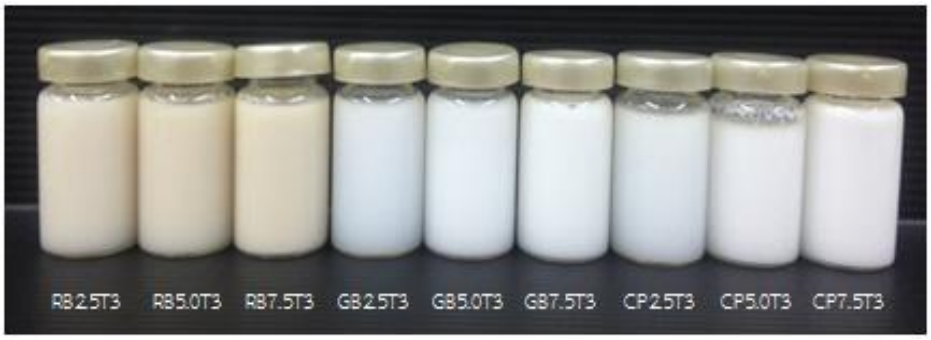

Figure 9. Appearances of freshly prepared blank-SLN: lipid 2.5, 5.0 and 7.5 (% w/w); tween 80 at 3 (% w/w) (RB = Rice bran wax, GB = Glyceryl behenate, CP = Cetyl palmitate, Tw = Tween 80)

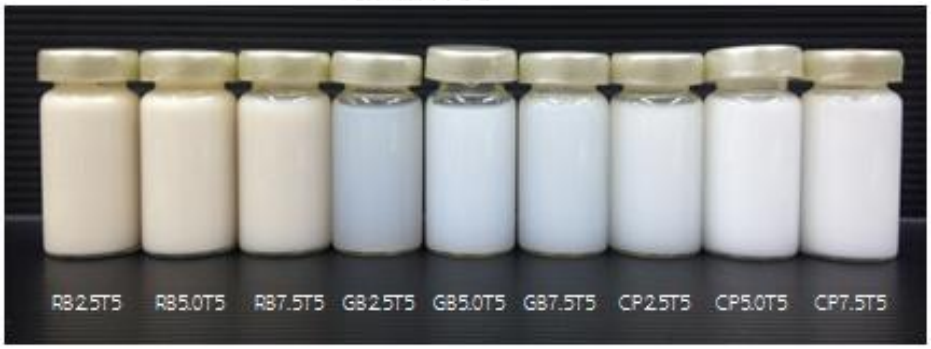

Figure 10. Appearances of freshly prepared blank-SLN: lipid 2.5, 5.0 and 7.5 (% w/w); tween 80 at 5 (% w/w) (RB = Rice bran wax, GB = Glyceryl behenate, CP = Cetyl palmitate, Tw = Tween 80)

1.1.2. Particle size analysis

All of SLN dispersion had nanosize range (106-410 nm). The dispersion characteristics were influenced by lipid types, amount of lipid and concentration of surfactant in formulation. Different lipid type of SLN (RB, GB and CP) dispersions, most of their particle size was increased when their lipid concentration increased from 2.5 to 7.5% w/w. At 1% tween 80, these three lipid types had less influence on their particle size. From Table 6 the SLN containing RB had smallest size compared to GB and CP at lower tween 80 concentrations. While tween 80 concentrations were increased from 3 to 5% w/w, their particle size were larger than those of GB and CP. On the other hand, the GB-SLN particle size was decreased when increased tween 80

concentration. In case of SLN containing CP, there had no effect of increasing tween 80 concentrations on their particle size. The CP-SLN and GB-SLN had narrow of size distributions while RB-SLN had board size distributions. Zeta potential measured for blank-SLN shows all formulations were negatively charged, the zeta potential varied from -15.2 to -32.4 mV. This zeta potential result indicated that the SLN of three type lipids had high charge on their particles and repulses each other which resulted in good long term stability (Pragna Shelat, Vinod K. Mandowara et al. 2015). Considering the effect of lipid type and concentration on the zeta potential of the SLN formulations, the results showed no direct relationship between the type of lipid used and the measured zeta potential values. On the contrary, as the lipid concentration increased the zeta potential was found to be more negative. Rawia M. Khalila, Ahmed Abd El-Baryb et al. (2013) reported the same observation when studying the effect of increasing glyceryl behenate amount in formulation. Tween® 80 being non-ionic surfactant succeeded in the production of relatively stable dispersions. Non-ionic surfactant could not ionize into charging group like ionic ones, but still showed its zeta potential. The reason might be due to molecular polarization and the adsorption of emulsifier molecule on the charge in aqueous; it was absorbed to the emulsifier layer of particle/water interface and electric double layer similar to ionic was formed.

Table 6. Size, polydispersity index (PDI), zeta potential and physical appearance of freshly prepared blank SLN formulations

SLN Formulation	Freshly prepared SLN (week 0)			
	Size (nm)	PDI	Zeta potential (mV)	Appearance
RB2.5Tw1	168.2 ± 0.6	0.40 ± 0.01	-25.9 ± 0.7	HD
RB5.0Tw1	178.3 ± 1.9	0.29 ± 0.01	-32.4 ± 0.4	HD
RB7.5Tw1	208.6 ± 2.7	0.29 ± 0.01	-27.9 ± 0.5	HD
GB2.5Tw1	177.6 ± 0.8	0.32 ± 0.01	-26.3 ± 1.1	HD

GB5.0Tw1	246.8 ± 2.5	0.30 ± 0.04	-24.0 ± 0.4	HD
GB7.5Tw1	410.5 ± 1.4	0.63 ± 0.04	-31.9 ± 0.7	HD
CP2.5Tw1	186.0 ± 1.5	0.21 ± 0.01	-23.0 ± 0.5	HD
CP5.0Tw1	216.6 ± 3.6	0.22 ± 0.02	-34.7 ± 1.4	HD
CP7.5Tw1	216.5 ± 3.9	0.21 ± 0.01	-33.6 ± 0.1	HD
RB2.5Tw3	199.2 ± 5.5	0.34 ± 0.04	-23.2 ± 0.8	HD
RB5.0Tw3	210.7 ± 6.8	0.50 ± 0.04	-24.2 ± 2.0	HD
RB7.5Tw3	232.3 ± 2.9	0.27 ± 0.01	-23.7 ± 0.5	HD
GB2.5Tw3	111.4 ± 0.8	0.40 ± 0.02	-22.3 ± 0.2	HD
GB5.0Tw3	240.6 ± 5.4	0.43 ± 0.01	-15.2 ± 0.9	HD
GB7.5Tw3	295.5 ± 3.4	0.45 ± 0.02	-19.9 ± 0.4	HD
CP2.5Tw3	186.3 ± 4.8	0.25 ± 0.01	-20.6 ± 2.6	HD
CP5.0Tw3	219.2 ± 2.0	0.21 ± 0.01	-28.5 ± 0.4	HD
CP7.5Tw3	198.5 ± 3.0	0.21 ± 0.01	-24.5 ± 0.8	HD
RB2.5Tw5	197.9 ± 2.5	0.33 ± 0.03	-22.4 ± 1.1	HD
RB5.0Tw5	137.3 ±2.4	0.25 ± 0.01	-27.5 ± 1.5	HD
RB7.5Tw5	220.1 ± 4.3	0.29 ± 0.01	-19.2 ± 0.6	HD
GB2.5Tw5	106.5 ± 1.9	0.52 ± 0.01	-21.3 ± 0.8	HD
GB5.0Tw5	121.1 ± 0.7	0.25 ± 0.01	-16.6 ± 3.8	HD
GB7.5Tw5	266.0 ± 3.4	0.53 ± 0.01	-16.6 ± 0.4	HD
CP2.5Tw5	183.1 ± 2.1	0.26 ± 0.01	-18.6 ± 1.2	HD
CP5.0Tw5	194.9 ± 1.9	0.23 ± 0.01	-21.3 ± 0.7	HD
CP7.5Tw5	168.5 ± 0.8	0.18 ± 0.02	-19.5 ± 0.7	HD

Note: RB = Rice bran wax, GB = Glyceryl behenate, CP = Cetyl palmitate, TW80 = Tween 80, HD = Homogeneous dispersion, PS = Phase separation, GF = Gel formation

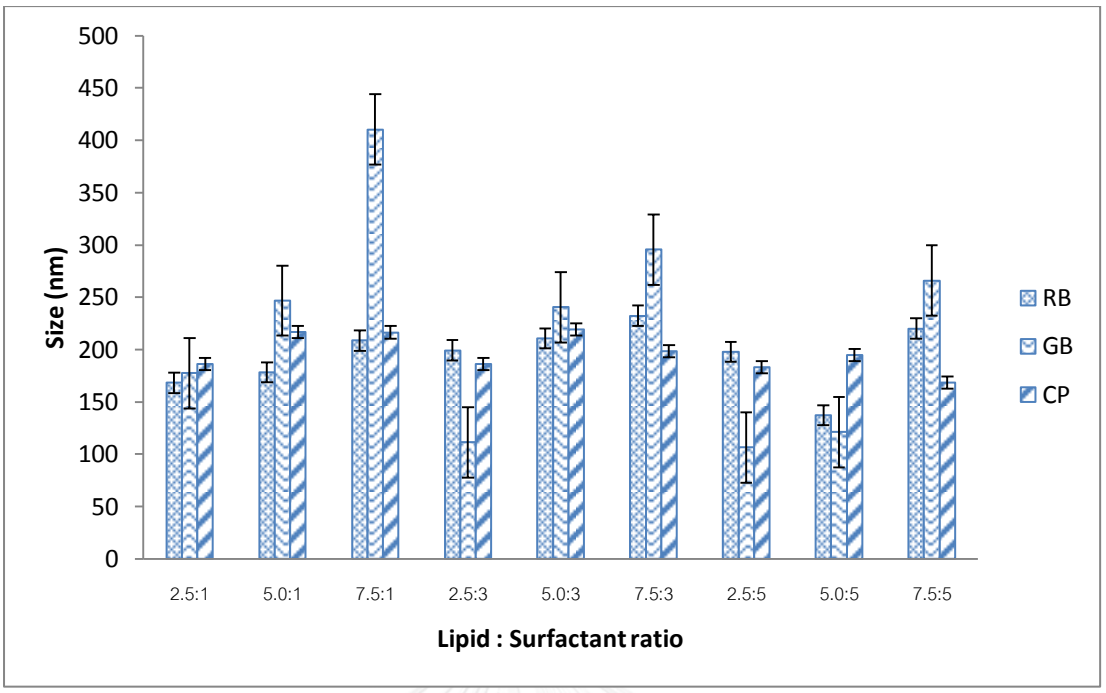

Figure 11. Comparison of particle size of freshly prepared blank-SLN formulations (RB = Rice bran wax, GB = Glyceryl behenate, CP = Cetyl palmitate)

The lipid types and their amount had impacted on physical properties of the SLN agreed with Ahlin Grabnar, Kristl et al. (1998). A possible explanation for the differences in sizes may be due to differences in chain lengths and lipid content used. Rice bran wax is a long chain (C36) lipid wax. It has similar chemical composition to cetyl palmitate (C32). RB also has a mixture of fatty acid of both palmitic acid and behenic acid, while cetyl palmitate has most of palmitic acid. On the other hand, main chemical composition of glyceryl behenate (C25) is glyceride lipid consisted of mainly behenic acid. From structure of long chain lipid wax and fatty acid, mixture of RB may be resulted to yield a larger of SLN particle size and boarder size distribution. Some of the SLN formulation had similar particle size may be resulted from same type of wax lipid.

The surfactant concentrations demonstrated the influence on particle size. From Figure 11, It was noticeable that particle size decreased with increasing concentration of tween 80 from 1 to 3 and 5% (w/w). This observation might be due to higher of surfactant for stabilizing the smaller lipid droplets. Similar observations were also reported by other researchers (De Pintu Kumar, Dinda Subas C et al. 2012).

When the amount of lipid was increased, the systems might require more concentration of surfactant to stabilize those of small droplets. This result can be seen from most of the SLN which the particle size increased as lipid content was increased. Tween 80 had significant influence on particle size of the SLN containing GB more than the CP and RB. At high lipid content of 7.5% w/w GB, the concentration of tween 80 at 1% w/w was not enough to stabilize their lipid droplets, ultimately and gel formation was occurred. This result may be due to the hydrophilic lipophilic balance of GB (HLB=2) is far different from those of RB (HLB=10) and CP (HLB=10).

1.2 Physical stability of the blank SLN

Physical stability of the blank SLN during 3 months storage at 25 $^{\circ}$C was determined by monitoring changes in appearance, particle size and zeta potential (Table 7). All of SLN formulations at 1 month study showed stable homogeneous appearance. After 3 months, the systems of RB7.5Tw1, GB5.0Tw1, RB5.0Tw1, GB5.0Tw3, RB5.0Tw3, CP5.0Tw3, and CP7.5Tw5 showed unstable appearance with visible aggregation, phase separation and increasing of particle size. GB7.5Tw3 and GB7.5Tw1 were found gel formation. The result was due to lower of surfactant concentration (1 -3 % w/w) and high amount of lipid content. While the systems with high surfactant concentration (5% w/w) showed more stable dispersion with slightly changed of particle size during studied.

Table 7. Size, polydispersity index (PDI), zeta potential and physical stability during 3 months storage at ambient room temperature of various blank-SLN formulations

	SLN (1 Month)			
Code	Size (nm)	PDI	Zeta potential (mV)	Appearance
RB2.5Tw1	172.2 ± 1.3	0.42 ± 0.01	-29.2 ± 0.7	HD
RB5.0Tw1	179.8 ± 1.6	0.31 ± 0.04	-33.2 ± 1.2	HD
RB7.5Tw1	211.3 ± 4.9	0.26 ± 0.02	-22.5 ± 0.3	HD
GB2.5Tw1	180.2 ± 2.5	0.33 ± 0.04	-28.2 ± 1.6	HD
GB5.0Tw1	250.6 ± 0.4	0.27 ± 0.02	-27.5 ± 0.5	HD

GB7.5Tw1	433.9 ± 1.4	0.59 ± 0.09	-32.0 ± 0.7	HD
CP2.5Tw1	188.0 ± 1.8	0.21 ± 0.02	-32.9 ± 0.2	HD
CP5.0Tw1	219.4 ± 3.4	0.22 ± 0.01	-36.1 ± 0.7	HD
CP7.5Tw1	225.7 ± 2.8	0.21 ± 0.01	-25.4 ± 0.8	HD
RB2.5Tw3	210.4 ± 5.4	0.32 ± 0.04	-21.1 ± 0.5	HD
RB5.0Tw3	203.6 ± 1.8	0.34 ± 0.05	-26.6 ± 1.2	HD
RB7.5Tw3	235.0 ± 4.0	0.29 ± 0.03	-22.5 ± 0.8	HD
GB2.5Tw3	111.6 ± 0.7	0.41 ± 0.01	-21.5 ± 0.8	HD
GB5.0Tw3	266.7 ± 4.7	0.68 ± 0.01	-24.3 ± 0.5	HD
GB7.5Tw3	309.1 ± 8.3	0.44 ± 0.05	-21.5 ± 1.0	HD
CP2.5Tw3	191.2 ± 1.4	0.24 ± 0.01	-25.9 ± 0.2	HD
CP5.0Tw3	239.8 ± 2.8	0.30 ± 0.02	-24.3 ± 0.4	HD
CP7.5Tw3	200.1 ± 1.7	0.24 ± 0.01	-21.8 ± 0.3	HD
RB2.5Tw5	201.0 ± 2.9	0.35 ± 0.01	-22.9 ± 1.1	HD
RB5.0Tw5	138.6 ± 0.7	0.24 ± 0.04	-26.7 ± 1.1	HD
RB7.5Tw5	223.9 ± 3.2	0.30 ± 0.02	-24.8 ± 0.5	HD
GB2.5Tw5	108.1 ± 1.0	0.50 ± 0.03	-20.1 ± 0.2	HD
GB5.0Tw5	123.6 ± 1.5	0.27 ± 0.02	-22.4 ± 0.9	HD
GB7.5Tw5	292.5 ± 1.7	0.53 ± 0.12	-24.9 ± 0.7	HD
CP2.5Tw5	185.4 ± 2.5	0.27 ± 0.01	-15.8 ± 0.8	HD
CP5.0Tw5	198.4 ± 2.2	0.26 ± 0.02	-19.9 ± 0.3	HD
CP7.5Tw5	169.8 ± 2.7	0.20 ± 0.02	-18.1 ± 0.7	HD
		SLN (3 Months)		
RB2.5Tw1	172.9 ± 5.7	0.40 ± 0.01	-30.1 ± 0.8	HD
RB5.0Tw1	-	-	-	PS
RB7.5Tw1	-	-	-	PS
GB2.5Tw1	445.1 ± 4.2	0.51 ± 0.06	-23.8 ± 0.8	HD
GB5.0Tw1	-	-	-	PS
GB7.5Tw1	-	-	-	GF
CP2.5Tw1	194.1 ± 4.9	0.25 ± 0.01	-26.1 ± 0.3	HD
CP5.0Tw1	225.6 ± 1.7	0.21 ± 0.01	-32.5 ± 0.6	HD
CP7.5Tw1	230.2 ± 4.6	0.22 ± 0.01	-25.1 ± 0.3	HD
RB2.5Tw3	288.6 ± 9.4	0.57 ± 0.03	-25.2 ± 1.7	HD
RB5.0Tw3	-	-	-	PS
RB7.5Tw3	241.5 ± 2.9	0.32 ± 0.04	-23.6 ± 0.5	HD

GB2.5Tw3	116.2 ± 0.6	0.40 ± 0.06	-20.4 ± 1.6	HD
GB5.0Tw3	-	-	-	PS
GB7.5Tw3	-	-	-	GF
CP2.5Tw3	239.8 ± 2.8	0.30 ± 0.02	-24.3 ± 0.4	HD
CP5.0Tw3	-	-	-	PS
CP7.5Tw3	200.2 ± 1.9	0.18 ± 0.01	-26.1 ± 1.1	HD
RB2.5Tw5	219.6 ± 4.7	0.38 ± 0.01	-24.2 ± 0.7	HD
RB5.0Tw5	144.8 ± 0.7	0.25 ± 0.01	-30.3 ± 1.4	HD
RB7.5Tw5	224.3 ± 1.1	0.31 ± 0.04	-26.8 ± 0.9	HD
GB2.5Tw5	116.0 ± 2.3	0.54 ± 0.02	-21.6 ± 0.3	HD
GB5.0Tw5	127.1 ± 2.5	0.29 ± 0.03	-19.5 ± 1.0	HD
GB7.5Tw5	299.2 ± 4.3	0.44 ± 0.02	-26.5 ± 0.5	HD
CP2.5Tw5	185.0 ± 3.7	0.25 ± 0.01	-17.2 ± 1.2	HD
CP5.0Tw5	201.5 ± 1.9	0.28 ± 0.01	-21.1 ± 0.6	HD
CP7.5Tw5	-	-	-	PS

Note: HD = Homogeneous dispersion, PS = Phase separation, GF = Gel formation

The result was perhaps due to increase in particle size which may partially be related to the viscosity of the samples. The use of a low viscous lipid phase improved size reduction and promoted stability in SLN production (Manjunath, Reddy et al. 2005). A similar finding was previously reported upon at higher lipid contents, the efficiency of homogenization decreased due to a higher viscosity of the sample, resulted in larger particles. Also, a high particle concentration at high lipid contents increased the probability of particle contact and subsequent aggregation (Freitas and Mullera 1998).

The higher amounts of lipid added the systems need more surfactant concentration enough to stabilize the systems also leading to nanoparticles aggregation. For GB-SLN, at high amount of GB the SLN was unstable and occur gel formation may be due to physical property of GB was viscosity-inducing agent that resulted to increase viscosity of dispersion (Aburahma and Badr-Eldin 2014). Also the stable systems might require strong repulsion by steric stabilization of the surfactants (Freitas and Mullera 1998), emphasizing the importance of surfactant concentration for SLN stabilization.

2. Preliminary study of curcuminoid loaded solid lipid nanoparticles (C-SLN)

From the results of Blank-SLN, 18 formulations of Rice bran wax, glyceryl behenate and cetyl palmitate at 2.5, 5.0 and 7.5 % (w/w) and 1, 5 % (w/w) tween 80 were selected as a suitable SLN lipid for curcuminoid loading.

2.1 Physical characterization

2.1.1 Physical appearance

Curcuminoid loaded SLN systems were observed appearance after freshly prepared. The SLN prepared by rice bran wax (RB) had yellowish color. The SLN with glyceryl behenate (GB) and cetyl palmitate (CP) had pale yellow color. All formulations were homogeneous dispersion. At higher amount of lipid, their appearance showed more turbidity. On the other hand, their appearance showed less turbidity when increased surfactant concentration (Figure 12 and 13).

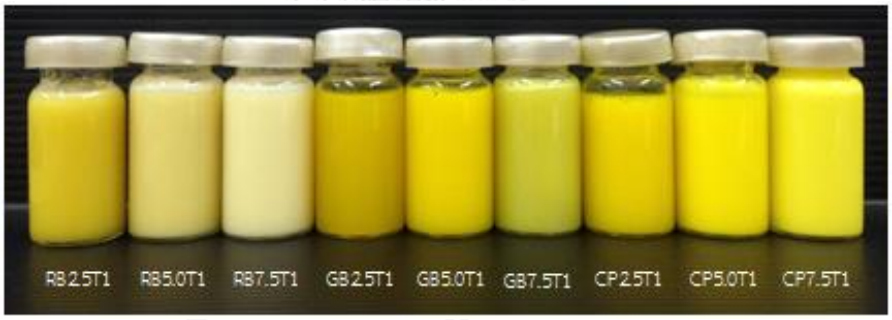

Figure 12. Appearances of freshly prepared C-SLN: lipid 2.5, 5.0 and 7.5 (% w/w); tween 80 at 1 (% w/w) (RB = Rice bran wax, GB = Glyceryl behenate, CP = Cetyl palmitate, Tw = Tween 80)

Figure 13. Appearances of freshly prepared C-SLN: lipid 2.5, 5.0 and 7.5 (% w/w); tween 80 at 5 (% w/w) (RB = Rice bran wax, GB = Glyceryl behenate, CP = Cetyl palmitate, Tw = Tween 80)

2.1.2 Particle size analysis

Table 8 showed particle size, polydispersity index (PDI), zeta potential of the SLN containing curcuminoid. The particle size of curcuminoid loaded SLN had larger size than the blank SLN. The C-SLN containing RB had largest particle size and boarder of polydispersity index than those of system containing GB and CP after curcuminoid loading. Increase of lipid concentrations led to larger of SLN particle size. Excluding the 7.5% w/w RB, particle size was decreased might resulted from the system had boarder of polydispersity index. After curcuminoid loading, the systems had high PDI value indicated boarding size distribution systems. All of SLN, zeta potential were less than -13.5 to -30.8 mV (Figure 14).

Table 8. Size, polydispersity index (PDI), zeta potential and physical appearance of freshly prepared curcuminoid loaded SLN (C-SLN) formulations

	Freshly prepared C-SLN (week 0)					
C-SLN formulation	Size (nm)	PDI	Zeta potential (mV)	Appearance	Entrapment Efficiency (%)	Recovery (%)
RB2.5Tw1-C	304.1 ± 5.8	0.43 ± 0.02	-28.2 ± 0.8	HD	62.18 ± 0.3	85.66 ± 0.3
RB5.0Tw1-C	342.7 ± 4.8	0.57 ± 0.02	-26.5 ± 0.4	HD	65.27 ± 0.1	74.82 ± 0.1
RB7.5Tw1-C	302.2 ± 3.7	0.41 ± 0.03	-26.1 ± 0.8	HD	71.62 ± 0.1	86.07 ± 0.4
GB2.5Tw1-C	223.5 ± 6.2	0.31 ± 0.02	-23.6 ± 0.6	HD	47.51 ± 0.4	61.08 ± 0.6
GB5.0Tw1-C	330.6 ± 4.1	0.36 ± 0.05	-24.1 ± 1.5	HD	59.73 ± 0.1	73.08 ± 0.2
GB7.5Tw1-C	380.2 ± 4.7	0.62 ± 0.10	-23.2 ± 1.3	HD	53.37 ± 0.1	70.55 ± 0.1
CP2.5Tw1-C	205.4 ± 2.3	0.16 ± 0.02	-30.8 ± 0.6	HD	34.30 ± 0.3	46.68 ± 0.7
CP5.0Tw1-C	207.3 ± 1.9	0.15 ± 0.02	-28.7 ± 0.4	HD	48.70 ± 0.4	60.38 ± 0.1
CP7.5Tw1-C	209.9 ± 1.6	0.16 ± 0.01	-26.2 ± 0.4	HD	38.27 ± 0.1	73.02 ± 0.2
RB2.5Tw5-C	575.3 ± 2.4	0.72 ± 0.04	-19.6 ± 0.8	HD	36.19 ± 0.1	59.67 ± 0.2
RB5.0Tw5-C	571.8 ± 4.3	0.56 ± 0.01	-16.7 ± 0.4	HD	46.57 ± 0.1	56.12 ± 0.5
RB7.5Tw5-C	378.2 ± 9.8	0.63 ± 0.01	-16.2 ± 1.1	HD	71.04 ± 0.3	85.49 ± 0.2

GB2.5Tw5-C	161.7 ± 3.6	0.41 ± 0.02	-20.4 ± 0.1	HD	37.89 ± 0.2	51.46 ± 0.1
GB5.0Tw5-C	232.7 ± 3.7	0.35 ± 0.01	-19.7 ± 0.3	HD	50.41 ± 0.1	63.77 ± 0.3
GB7.5Tw5-C	363.9 ± 3.0	0.79 ± 0.01	-17.1 ± 0.5	HD	43.59 ± 0.1	60.80 ± 0.2
CP2.5Tw5-C	278.3 ± 7.0	0.22 ± 0.06	-13.5 ± 0.2	HD	43.49 ± 0.1	55.87 ± 0.4
CP5.0Tw5-C	300.9 ± 4.7	0.24 ± 0.01	-15.5 ± 0.3	HD	44.60 ± 0.3	56.27 ± 0.1
CP7.5Tw5-C	309.8 ± 0.3	0.25 ± 0.01	-17.4 ± 0.9	HD	60.61 ± 0.2	73.02 ± 0.1

Note: RB = Rice bran wax, GB = Glyceryl behenate, CP = Cetyl palmitate, TW80 = Tween 80, HD = Homogeneous dispersion, PS = Phase separation, GF = Gel formation

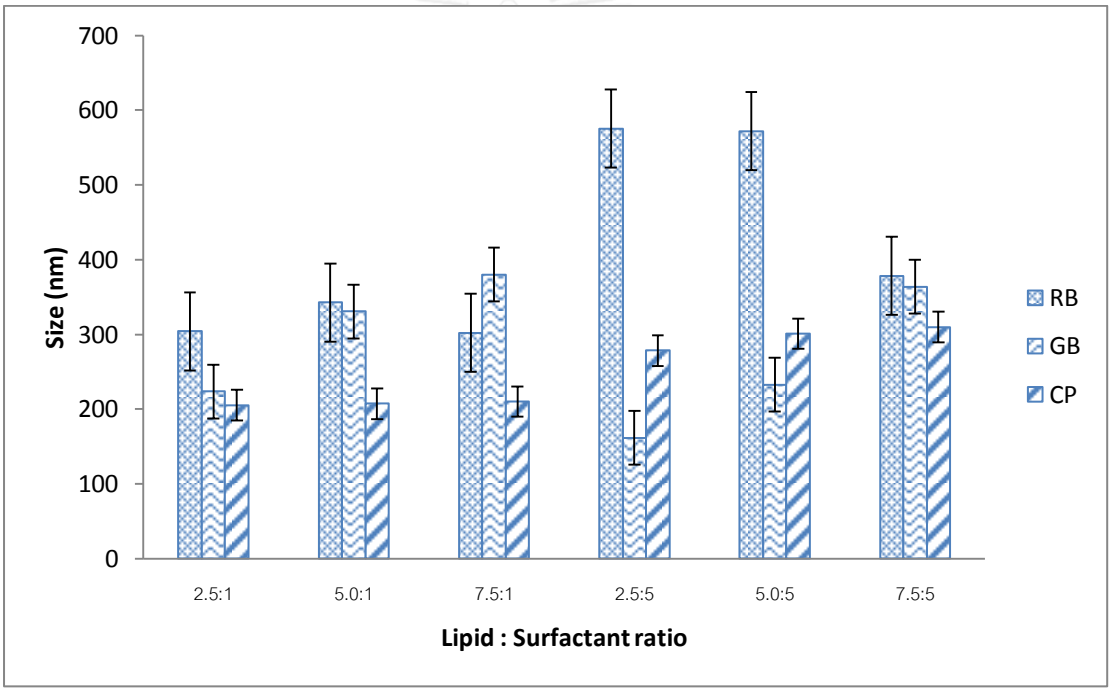

Figure 14. Particle size of freshly prepared C-SLN formulations (RB = Rice bran wax, GB = Glyceryl behenate, CP = Cetyl palmitate)

2.2 Entrapment efficiency

The entrapment efficiencies of all C-SLN formulations are shown in Table 8. The data clearly shows that formulations possessed entrapment efficiency (E.E. %)

ranged from 34.30 to 71.62 %. RB-SLN showed highest of entrapment efficiency following by Glyceryl behenate and Cetyl palmitate (Figure 15).

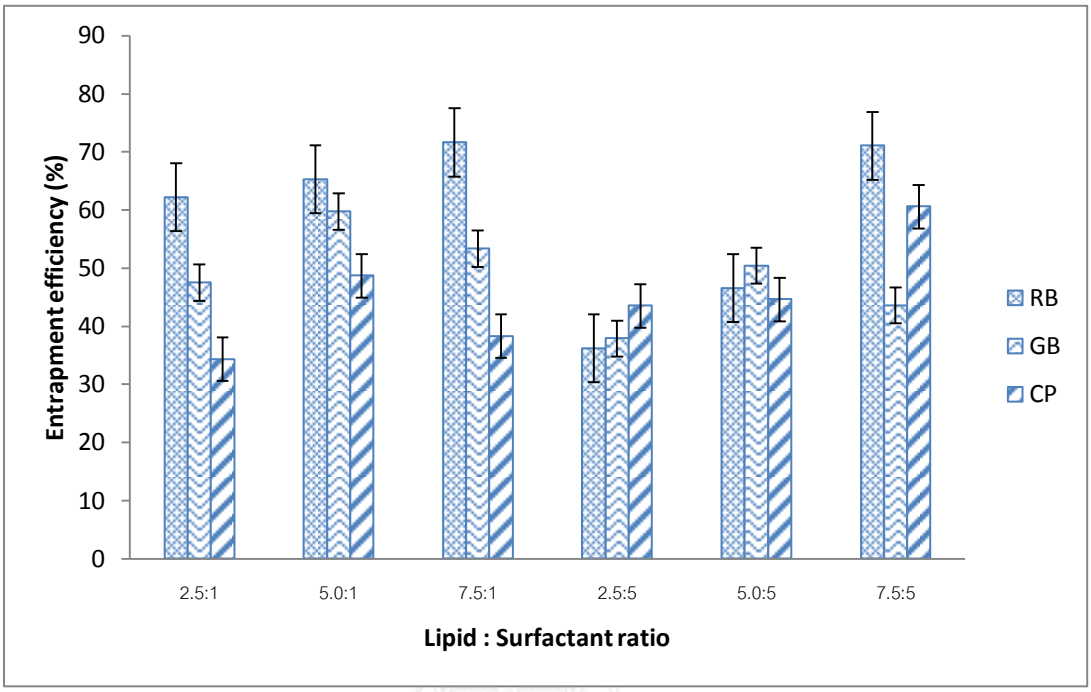

Figure 15. Diagram of percentage entrapment efficiency of freshly prepared C-SLN formulations (RB = Rice bran wax, GB = Glyceryl behenate, CP = Cetyl palmitate)

Glyceryl behenate was a glyceride lipid exhibited orthorhombic subcell arrangements (β' polymorph) which promotes the drug to be entrapped comparing to a wax lipid of cetyl palmitate (Jenning, Schäfer-Korting et al. 2000). Rice bran wax SLN showed better entrapment efficiency. This result may be due to lipid structure of its long chain fatty acids consisted of mixture of palmitic acid and behenic acid. Also long chain fatty acids of rice bran wax led to higher lipophilicity resulted in increased loaded of lipophillic drugs.

Moreover, high entrapment efficiency might be related to an amount of lipid in SLN. It was noticeable that entrapment efficiency significantly increased with increasing lipid content as revealed in Figure 16. For RB-SLN, the lipid increased from 2.5 % (w/w) to 7.5% (w/w) enhanced drug entrapment from 36.19 to 71.62 %.

Enhancing drug entrapment when lipid content was increased also can be seen in GB-SLN and CP-SLN.

At 1% w/w tween 80, RB showed highest drug entrapment. Increasing tween 80 at 5%, resulted to lower entrapment efficiency. This could be attributed to the increase in the solubility of curcuminoids in the aqueous phase as the percentage of surfactant increased, due to the solubilization effect of the emulsifier. (Abdelbary and Fahmy 2009).

2.3 Stability of C-SLN

The physical stability of the C-SLN during long term storage (25^0C) was determined by monitoring changes in particle size, zeta potential, and appearance.

Table 9. Size, polydispersity index (PDI), zeta potential and physical appearance of C-SLN formulations during storage at ambient room temperature for 3 months

	SLN (1 Month)			
C-SLN Formulation	Size (nm)	PDI	Zeta potential (mV)	Appearance
RB2.5Tw1-C	306.7 ± 7.8	0.44 ± 0.07	-27.6 ± 0.7	HD
RB5.0Tw1-C	412.6 ± 9.6	0.49 ± 0.03	-23.2 ± 0.8	HD
RB7.5Tw1-C	330.4 ± 8.7	0.40 ± 0.05	-23.4 ± 0.9	HD
GB2.5Tw1-C	304.1 ± 5.8	0.43 ± 0.04	-28.2 ± 0.9	HD
GB5.0Tw1-C	330.4 ± 8.7	0.40 ± 0.02	-23.4 ± 0.9	HD
GB7.5Tw1-C	330.6 ± 7.8	0.55 ± 0.02	-23.9 ± 0.5	HD
CP2.5Tw1-C	204.9 ± 2.7	0.17 ± 0.02	-30.2 ± 1.6	HD
CP5.0Tw1-C	213.3 ± 3.6	0.18 ± 0.01	-26.4 ± 8.4	HD
CP7.5Tw1-C	207.0 ± 1.9	0.15 ± 0.02	-28.7 ± 0.4	HD
RB2.5Tw5-C	583.6 ± 2.6	0.52 ± 0.01	-13.4 ± 0.5	HD
RB5.0Tw5-C	528.4 ± 1.7	0.46 ± 0.01	-12.2 ± 0.4	HD
RB7.5Tw5-C	422.1 ± 7.5	0.53 ± 0.01	-11.0 ± 0.5	HD
GB2.5Tw5-C	151.0 ± 2.7	0.44 ± 0.01	-14.7 ± 0.3	HD
GB5.0Tw5-C	254.6 ± 7.2	0.31 ± 0.01	-12.5 ± 0.4	HD
GB7.5Tw5-C	360.3 ± 1.6	0.42 ± 0.01	-11.0 ± 0.7	HD
CP2.5Tw5-C	278.6 ± 9.9	0.21 ± 0.01	-10.6 ± 0.4	HD

CP5.0Tw5-C	332.7 ± 3.8	0.28 ± 0.01	-10.3 ± 0.5	HD
CP7.5Tw5-C	274.3 ± 4.8	0.23 ± 0.01	-10.4 ± 0.2	HD
		SLN (3 Months)		
RB2.5Tw1-C	391.6 ± 9.0	0.64 ± 0.02	-26.8 ± 0.8	HD
RB5.0Tw1-C	-	-	-	PS
RB7.5Tw1-C	-	-	-	PS
GB2.5Tw1-C	330.6 ± 4.1	0.36 ± 0.04	-24.1 ± 1.5	HD
GB5.0Tw1-C	-	-	-	PS
GB7.5Tw1-C	-	-	-	GF
CP2.5Tw1-C	208.8 ± 0.8	0.15 ± 0.02	-30.9 ± 2.7	HD
CP5.0Tw1-C	228.3 ± 2.3	0.22 ± 0.01	-20.9 ± 0.7	HD
CP7.5Tw1-C	224.6 ± 4.6	0.22 ± 0.01	-24.9 ± 0.4	HD
RB2.5Tw5-C	603.3 ± 6.9	0.53 ± 0.01	-12.6 ± 0.6	HD
RB5.0Tw5-C	559.5 ± 2.3	0.47 ±0.01	-11.5 ± 0.2	HD
RB7.5Tw5-C	481.7 ± 9.1	0.51 ± 0.01	-11.1 ± 0.8	HD
GB2.5Tw5-C	349.1 ± 5.9	0.42 ± 0.01	-13.7 ± 0.5	HD
GB5.0Tw5-C	344.7 ± 7.8	0.39 ± 0.01	-12.1 ± 0.3	HD
GB7.5Tw5-C	470.2 ± 3.6	0.44 ± 0.01	-11.6 ± 0.3	HD
CP2.5Tw5-C	389.1 ± 4.3	0.39 ± 0.10	-10.3 ± 0.3	HD
CP5.0Tw5-C	480.0 ± 5.3	0.34 ± 0.10	-9.7 ± 0.7	HD
CP7.5Tw5-C	-	-	-	PS

Note: HD = Homogeneous dispersion, PS = Phase separation, GF = Gel formation

Most Formulation showed suitable stability during the 3 months period of the study show in Table 9. No obvious aggregation or phase separation was observed. Physical properties of particles showed no significant changes after 3 months. Except RB7.5Tw1, CP7.5Tw5, RB5.0Tw1, GB5.0Tw1 were found phase separation, and GB7.5Tw1 was found gel formation.

3 Development of Bisdemethoxycurcumin loaded solid lipid nanoparticles (BDMC-SLN)

From the preliminary study of C-SLN, The formulation which was stable for 3 months was chosen. The SLN selected contained 2.5, 5.0 or 7.5% (w/w) rice bran wax, glyceryl behenate or cetyl palmitate as a lipid with 5% Tween® 80 as a surfactant. While the C-SLN formulation with 1% tween 80 was found unstable.

3.1 Physical characterization

3.1.1 Physical appearance

BDMC-SLN was observed appearance after freshly prepared. The formulations that contained rice bran wax (RB) had yellowish color. Glyceryl behenate (GB) and cetyl palmitate (CP) had yellow color similar to the appearance of C-SLN. All of formulations were homogeneous dispersion (Figure 16).

Figure 16. Appearances of freshly prepared BDMC-SLN: lipid 2.5, 5.0 and 7.5 (% w/w); tween 80 at 5 (% w/w) (RB = Rice bran wax, GB = Glyceryl behenate, CP = Cetyl palmitate, Tw = Tween 80)

3.1.2 Particle size analysis of freshly prepare BDMC-SLN

Table 10 showed particle size, polydispersity index (PDI), zeta potential of the SLN containing bisdemethoxycurcumin. The result of particle size analysis was related to those of C-SLN system. Their mean particle size was between 275.5 and 773.3 nm. Mean particle size of BDMC loaded SLN had larger size than the blank SLN.

Increase of lipid concentrations from 2.5 to 5 % w/w leading to larger of SLN particle size. Except at 7.5% w/w of lipid, the particle size slightly decreased (Figure 17). The BDMC-SLN containing RB had largest particle size and boarder of polydispersity index than those of system containing GB and CP. After BDMC loading, the systems had high PDI value of 0.14 to 0.75 indicated boarding size distribution systems. All of SLN, zeta potential were less than -13.0 to -16.9 mV.

Table 10. Size, polydispersity index (PDI), zeta potential and physical appearance of freshly prepared BDMC-SLN formulations

	Freshly prepared BDMC-SLN (week 0)					
BDMC-SLN formulation	Size (nm)	PDI	Zeta potential (mV)	Appearance	Entrapment Efficiency (%)	Recovery (%)
RB2.5Tw5-BDMC	684.2 ± 6.9	0.65 ± 0.05	-16.4 ± 0.4	HD	66.46 ± 12.44	78.69 ± 0.6
RB5.0Tw5-BDMC	773.3 ± 11.6	0.75 ± 0.07	-15.7 ± 0.3	HD	76.44 ± 11.92	87.64 ± 0.1
RB7.5Tw5-BDMC	541.9 ± 33.5	0.48 ± 0.02	-16.8 ± 1.0	HD	73.41 ± 4.27	72.93 ± 0.4
GB2.5Tw5-BDMC	356.5 ± 13.7	0.53 ± 0.03	-16.9 ± 1.2	HD	56.70 ± 0.59	59.89 ± 0.1
GB5.0Tw5-BDMC	275.5 ± 5.6	0.26 ± 0.01	-14.9 ± 1.0	HD	65.31 ± 15.03	78.85 ± 0.3
GB7.5Tw5-BDMC	275.8 ± 6.5	0.25 ± 0.02	-14.9 ± 0.6	HD	45.14 ± 0.55	52.78 ± 0.1
CP2.5Tw5-BDMC	324.6 ± 0.4	0.22 ± 0.01	-13.0 ± 0.4	HD	65.94 ± 6.33	66.01 ± 0.1
CP5.0Tw5-BDMC	541.9 ± 33.5	0.48 ± 0.02	-16.8 ± 1.0	HD	70.41 ± 1.19	73.32 ± 0.3
CP7.5Tw5-BDMC	280.8 ± 2.2	0.14 ± 0.02	-13.1 ± 0.5	HD	62.75 ± 2.10	69.58 ± 0.4

Note: RB = Rice bran wax, GB = Glyceryl behenate, CP = Cetyl palmitate, TW80 = Tween 80, HD = Homogeneous dispersion, PS = Phase separation, GF = Gel formation

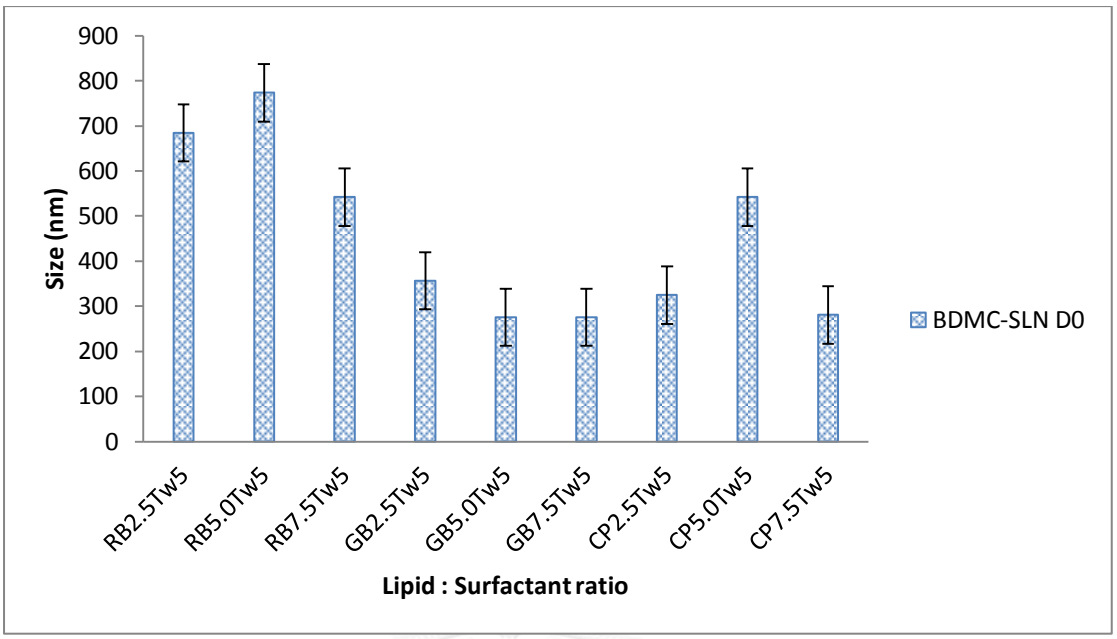

Figure 17. Comparison of particle size for each lipid content of freshly prepared BDMC-SLN formulations

3.1.3 Particle morphology

The FE-SEM image of BDMC-SLN was shown in Figure 18. Shape and surface morphology of the nanoparticles was observed by FE-SEM which obtaining more detail of information. The image revealed that the BDMC-SLN was spherical shape in nanosize range with broad size distribution. The BDMC-SLN particle size observed by FE-SEM was conforming to the result of particle size data determined by PCS. All of the BDMC-SLN systems had smooth surface and spherical shape, except the SLN containing 7.5% w/w GB. The BDMC-SLN with GB, their particle was found to be agglomerated and at 7.5% w/w of lipid amount its look like lipid fragment. This result may be due to the stickiness nature of the lipid carrier.

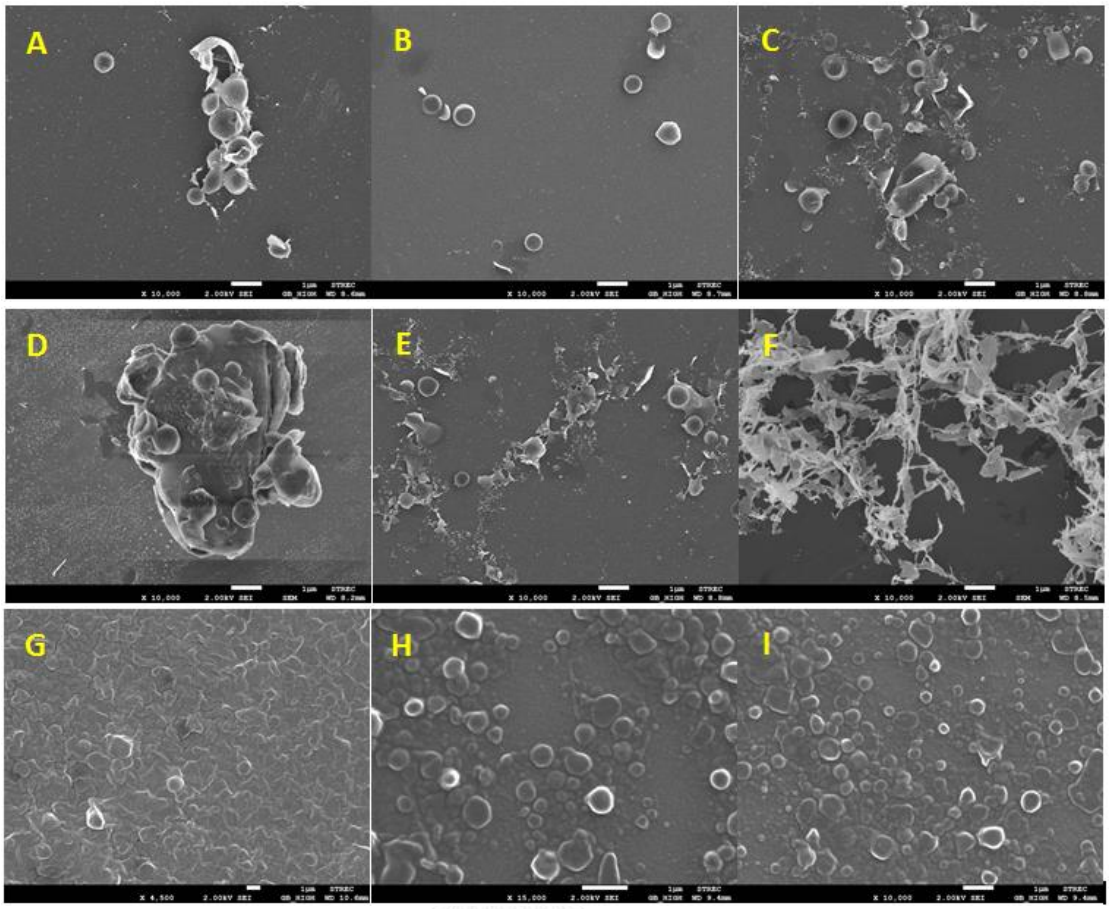

Figure 18. Scanning electron micrographs of BDMC-SLN from various formulations RB2.5Tw5 (A), RB5.0Tw5 (B), RB7.5Tw5 (C), GB2.5Tw5 (D), GB5.0Tw5 (E), GB7.5Tw5 (F), CP2.5Tw5 (G), CP5.0Tw5 (H) and CP7.5Tw5 (I) (RB = Rice bran wax, GB = Glyceryl behenate, CP = Cetyl palmitate Tw = Tween 80)

3.2 Thermal analysis by differential scanning calorimetry (DSC)

DSC is an effective tool to find out drug and excipient incompatibilities as well as melting and recrystallization behavior of crystalline materials like SLN. All the lipid, surfactant and active pharmaceutical ingredient were investigated by DSC to find a corresponding to its melting point, indicating its characteristic crystalline nature or polymorphic transitions of the lipid matrix, because of its loading capacity, and to evaluate the crystalline quality of included active substance. (Souto, Anselmi et al. 2005)

The bulk lipids, physical mixture of BDMC and each type of lipid, and BDMC-SLN formulations were examined by DSC.

For pure compositions, as revealed in Table 9, DSC results of bulk lipid (A) Rice bran wax, (B) Glyceryl behenate, (C) Cetyl palmitate and (D) BDMC exhibits a sharp endothermic peak at 80.72, 73.75, 54.42, 175.69 ^{O}C, respectively. The enthalpy of rice bran wax, glyceryl behenate, cetyl palmitate and bisdemethoxycurcumin are -79.98, -108.15, -213.43 and -97.37, respectively.

The crystallinity index (CI) of the bulk lipid and BDMC-SLN was estimated by comparison of the melting enthalpy of the bulk material with the melting enthalpy of the BDMC-SLN formulation. From the CI calculation, the CI of BDMC-SLN was less than those of the bulk lipid. The result found that the CI of BDMC-SLN for all lipid types was decreased when increasing of lipid content. BDMC-SLN prepared by RB had higher CI than the GB and CP respectively. Generally, crystallization in lipids with longer chains of fatty acids was slower than those with shorter fatty acid chains. Wax-based lipid nanoparticles are physically more stable.

Table 11. DSC results of composition of solid lipid nanoparticles and BDMC-SLN (RB = Rice bran wax, GB = Glyceryl behenate, CP = Cetyl palmitate, Tw = Tween 80, BDMC = Bisdemethoxycurcumin)

Name	Onset (^{O}C)	Peak(^{O}C)	Endset(^{O}C)	Crystallinity index (%)
Rice Bran wax	76.41	80.94	83.93	100
Glyceryl Behenate	70.75	73.75	76.95	100
Cetyl Palmitate	50.43	54.42	56.94	100
BDMC	171.66	175.69	178.44	100
RB2.5Tw5-BDMC	72.26	78.84	83.78	86.11
RB5.0Tw5-BDMC	73.05	79.40	84.46	60.12
RB7.5Tw5-BDMC	70.47	78.11	83.12	33.05
GB2.5Tw5-BDMC	68.53	73.22	75.54	34.31
GB5.0Tw5-BDMC	65.21	70.87	73.65	19.30

GB7.5Tw5-BDMC	66.48	70.82	73.65	9.41
CP2.5Tw5-BDMC	49.43	52.84	55.38	15.26
CP5.0Tw5-BDMC	47.69	51.89	53.66	3.23
CP7.5Tw5-BDMC	47.62	51.77	53.56	3.69

The DSC curve illustrated in Figure 19 showed DSC thermogram of physical mixture of lipid (RBW, GB, and CP) and BDMC showed the presence of endothermic peak both peak of lipid and drug.

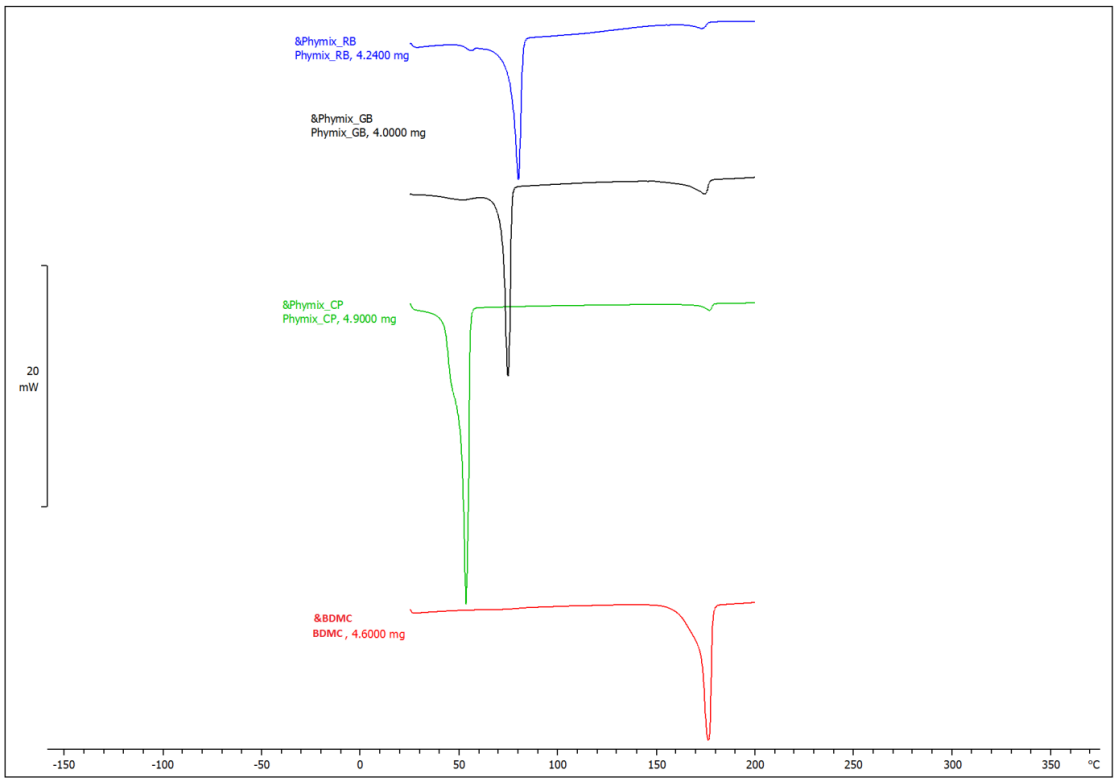

Figure 19. DSC thermogram of the Physical mixture (RB = Rice bran wax, GB = Glyceryl behenate, CP = Cetyl palmitate, BDMC = Bisdemethoxycurcumin)

The BDMC-SLN thermograms, as shown in Figure 20 to 22 displayed complete disappearance of characteristic peak BDMC. The characteristic peaks of lipid was showed (A) RB2.5Tw5 at 78.84°C, (B) RB5.0Tw5 at 79.40 °C, (C) RB7.5Tw5 at 78.11°C, (D) GB2.5Tw5 at 73.22 °C, (E) GB5.0Tw5 at 70.87 °C, (F) GB7.5Tw5 at 70.82, (G)

CP2.5Tw5 at 52.84 °C, (H) CP5.0Tw5 at 51.89 °C and (I) CP7.5Tw5 at 51.77 °C with minimum shifting.

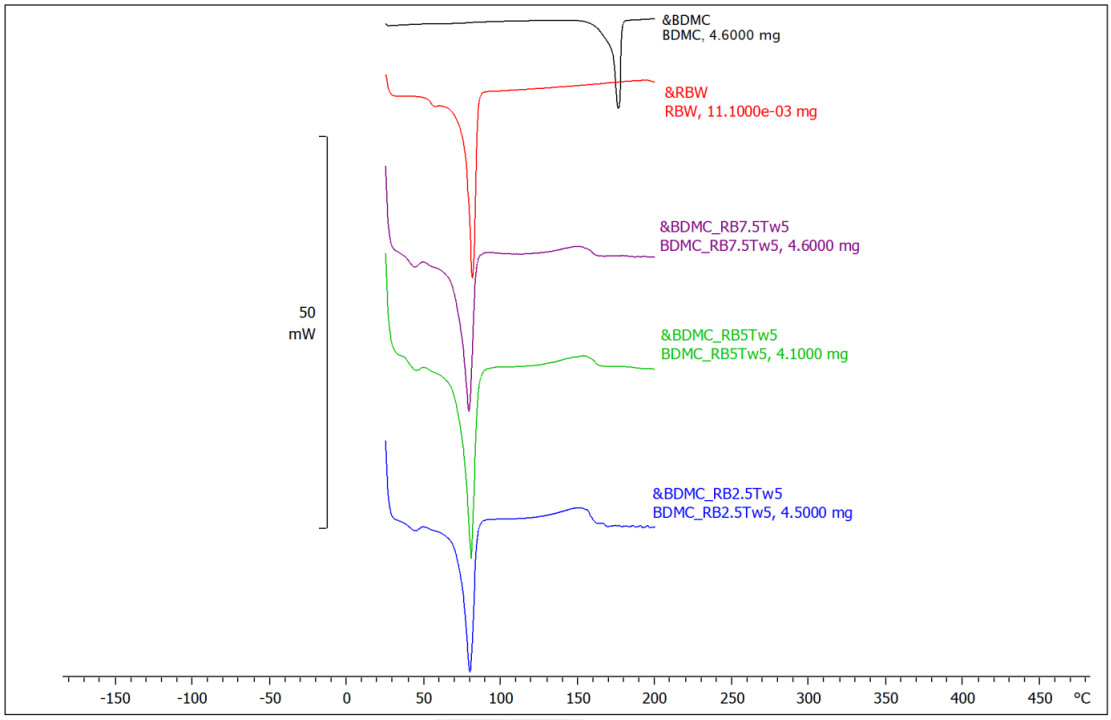

Figure 20. DSC thermograms of the BDMC-SLN prepared with rice bran wax (RB = Rice bran wax, BDMC = Bisdemethoxycurcumin)

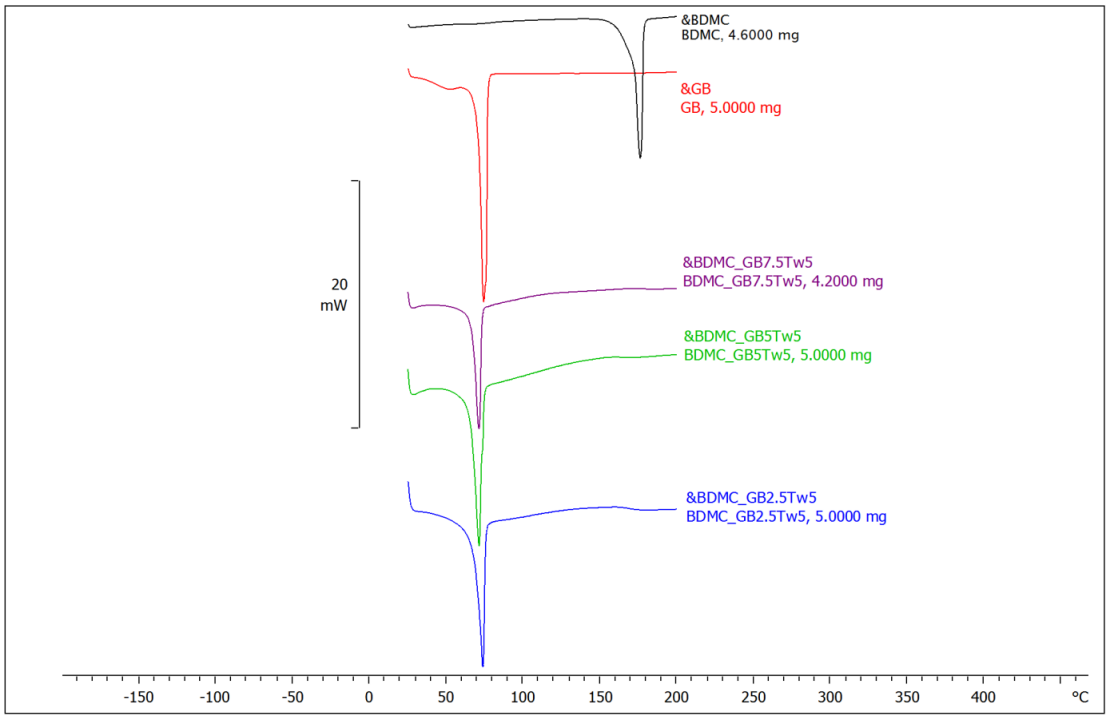

Figure 21. DSC thermograms of the BDMC-SLN prepared with glyceryl behenate (GB = Glyceryl behenate, BDMC = Bisdemethoxycurcumin)

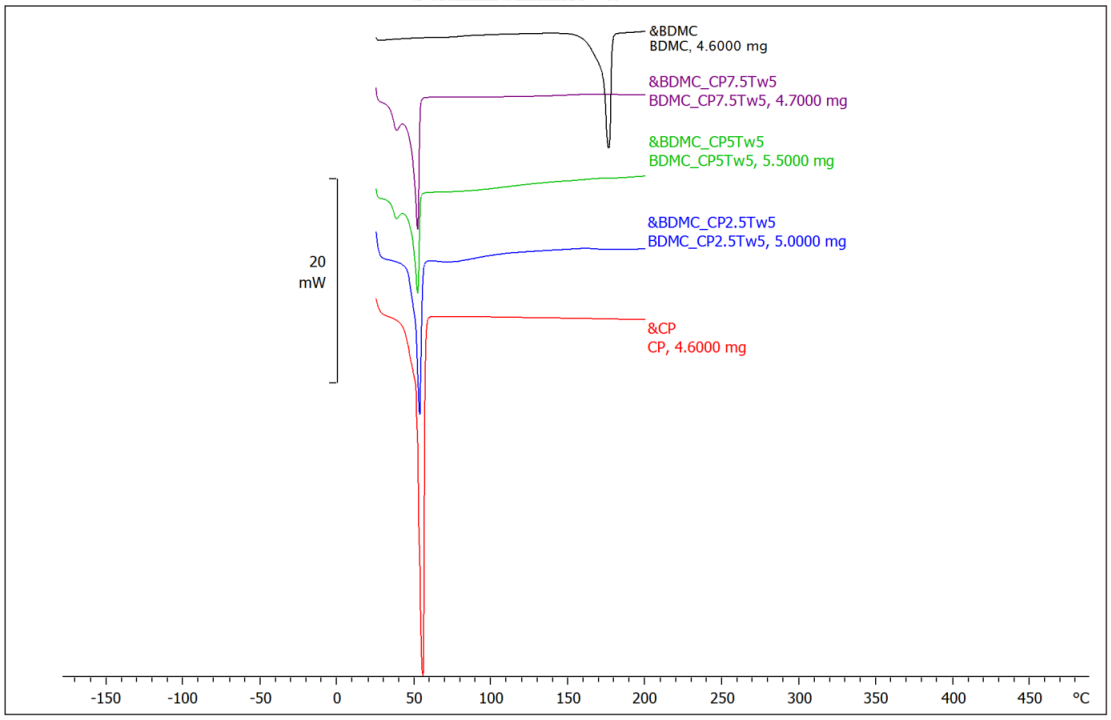

Figure 22. DSC thermograms of the BDMC-SLN prepared with cetyl palmitate (CP = Cetyl palmitate, BDMC = Bisdemethoxycurcumin)

The absence of the characteristic peak of drug as shown in Figure 20 to 22 was due to the fact that the drug was molecularly dispersed within the lipid matrix and indicated the conversion of crystalline BDMC to the amorphous form. This could be attributed to complete dissolution of the drug in the molten lipid matrix as found for ibuprofen by De Pintu Kumar, Dinda Subas C et al. (2012)

The height of the endothermic peak in the thermogram of SLN containing BDMC was less than that in the lipid without BDMC. This finding was in agreement with Das, Ng et al. (2011) who reported that the loss of crystallinity of the lipids and drug after incorporation into SLN. The results indicate that drug incorporated in SLN was not in a crystalline state but in an amorphous form. When the materials were formulated as SLN, the endothermic temperature was slightly shifted.

3.3 The percentage of entrapment efficiency

The data clearly shows that all formulations achieved high entrapment efficiency (E.E. %) ranged from 45.14 to 73.41 %. At a constant amount of Tween® 80 (5% w/w), the BDMC-SLN containing RB achieved highest entrapment efficiency followed by CP and GB similar to the result of C-SLN entrapment efficiency. Increasing the lipid concentration from 2.5 to 5 % (w/w) resulted in a consequent increase in E.E. %, while decreased upon further lipid increased to 7.5% (w/w) (Figure 23). This finding was in agreement with Abdelbary and Fahmy (2009) who reported the study on diazepam-loaded SLN, in which they found that increasing the GB concentration to 10% (w/w), consequently resulted in a decrease in the amount of diazepam entrapped. A possible explanation was that during the crystallization of the lipid phase a partial expulsion of the drug on the particle surface may occur. Furthermore, the higher viscosity at the interface produced by higher lipid amount may lead to a decrease in diffusion, hence fewer lipid molecules will be carried into the aqueous phase. Therefore, the formation and stabilization of lipid aggregated at these higher concentrations are reduced.

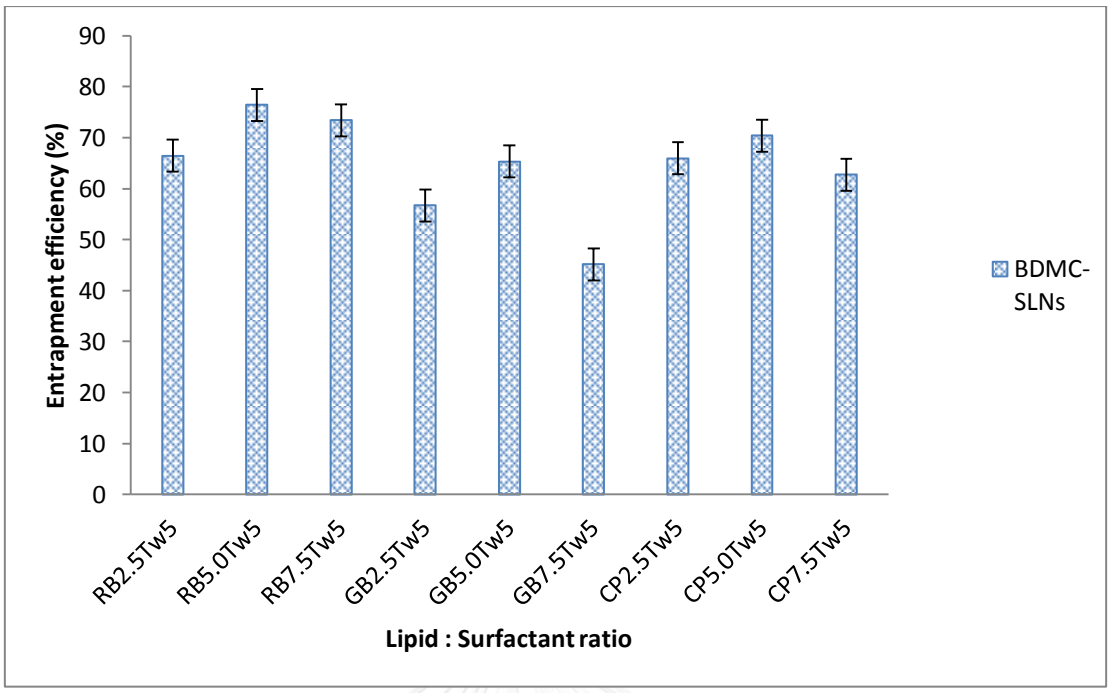

Figure 23. Diagram of percentage entrapment efficiency of freshly prepared BDMC-SLN formulations

3.4 Evaluation of *In vitro* release of BDMC-SLN

Comparative *In vitro* release studied was carried out for BDMC solution (control) and BDMC-SLN formulations. As aqueous solubility of BDMC was very low, 2% (w/v) Tween®80 was added to the release media to maintain sink condition. Hence, drug released from the SLN were measured by determining drug concentration in the release medium. Percent cumulative drug release versus time was plotted to demonstrate the drug release pattern shown in Figure 24. *In vitro* release studies of BDMC-SLN was observed over a period of 24 hours. The BDMC-SLN exhibited a sustained release pattern. The percentage of drug release gradually higher until 24 hours. At 5% w/w lipid content, the release profile of BDMC-SLN with CP had highest amount of drug release followed by GB and RB. BDMC-SLN with RB. The release profile showed at higher lipid amount led to lower percent of drug release.

The cumulative percentage of free BDMC release versus time at 24 hours were respectively from high to low: CP5Tw5 (64.72%), GB5Tw5 (40.72%), RB2.5Tw5 (13.84), RB5.0Tw5 (18.77), RB7.5Tw5 (20.75%) and control BDMC solution (13.84%).

The initial release within 1 hour and followed by a sustained release possibly explained by the release of BDMC which absorbed on the matrix surface. While the sustained release over a period of 24 hours may be resulted from BDMC dispersed into lipid matrix. This finding was in agreement with Pragna Shelat, Vinod K. Mandowara et al. (2015) who reported that sustained release was observed over a period of 7 days.

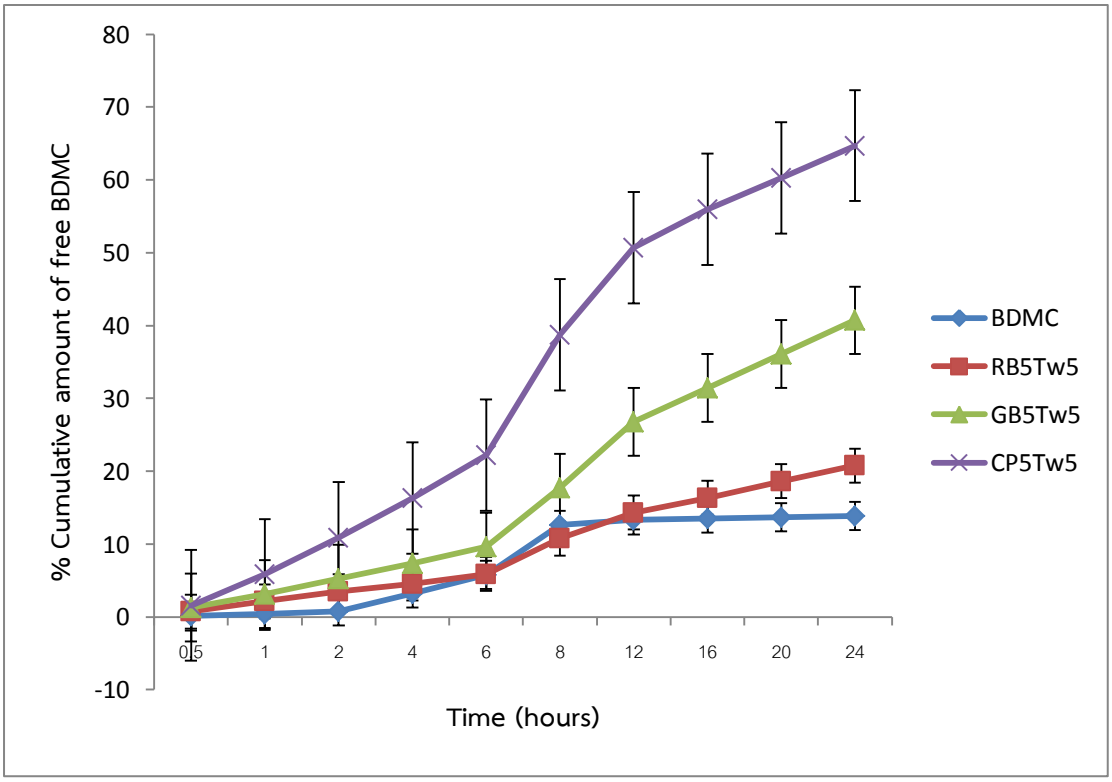

Figure 24. Release profiles of BDMC from SLN prepare with different types of lipid

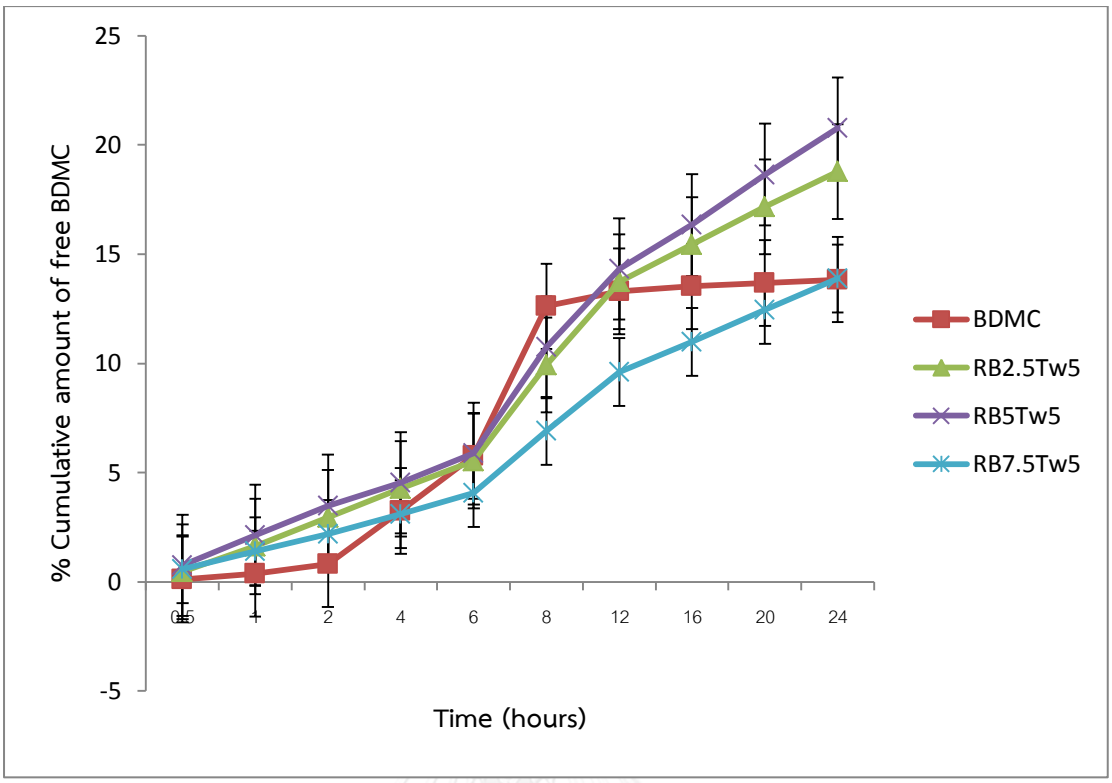

Figure 25. Release profiles of BDMC from SLN prepare with different concentration of lipid

Concerning the type of lipid matrix, the results clearly showed that among the wax and glycerides used, the highest release was achieved with Cetyl palmitate compared to Glyceryl behenate and Rice bran wax. Cetyl palmitate had shown the highest release efficiency because of cetyl palmitate containing of higher alcohol esters content (C26). While in case of Rice bran wax and Glyceryl behenate, the relatively slow release can be attributed to the hydrophobic long chain fatty acids of the triglycerides that retained the hydrophobic drug resulted in more sustained release effect This finding was in agreement with (Manjunath, Reddy et al. 2005). Furthermore, the lower melting point of Cetyl palmitate (55-56 $^{\circ}$C) may be resulted in a higher mobility at the temperature used in the release experiment. As known, the melting point of colloidal structures may be lower than that of the bulk due to the influence of surface energy as same as result of Bhalekar, Pokharkar et al. (2009).

The results also pointed to the effect of lipid concentration on SLN release profile. Similar observations were also reported by Wissing, Kayser et al. (2004)

Increasing the lipid concentration from 2.5, 5.0 to 7.5 % (w/w) resulted in a corresponding to decrease in percentage of drug released; this decreased in release profile observed can be attributed to the higher lipid content encapsulating the drug, thus reducing drug partition in the outer phase and consequently its release in the receiver medium. The release profiles of these SLN look like the drug enriched core model. In such a model, the drug enriched core was enclosed by a practically drug-free lipid shell. Due to the increased diffusional distance and obstruct effects by the surrounding solid lipid shell, the drug has a sustained release profile.

During particle production by the hot homogenization technique, drug partitions from the liquid oil phase to the aqueous water phase increased with higher temperature of the aqueous phase and increased surfactant concentration. The higher temperature and surfactant concentration led to more saturated solubility of the drug in the water phase. During the cooling of the produced o/w nanoemulsion, the solubility of the drug in the water phase decreased continuously, while decreased temperature of the water phase. That means a re-partitioning of the drug into the lipid phase occurred. When reaching the recrystallization temperature of the lipid, a solid lipid core started forming including the drug presented in this lipid phase. Reducing the temperature of the dispersion reduced solubility in water to further re-partition into the lipid phase. The already crystallized core was not accessible anymore for the drug; consequently the drug concentrated in the still liquid outer shell of the SLN or on the surface of the particles. The amount of drug in the outer shell and on the particle surface was released in the form of a burst; the drug incorporated into the particle core was released in a prolonged way (Müller, Mäder et al. 2000).

3.5 Physical stability of BDMC-SLN

3.5.1 Physical appearance

BDMC-SLN was observed appearance at 1 and 3 month. Most of the formulations were homogeneous; no obvious aggregation or phase separation was

observed. Physical properties of particles showed no significant changes after 3 months, except CP2.5Tw5 and CP7.5Tw5 were found phase separation.

3.5.2 Particle size analysis

In order to evaluate the stability of lipid nanoparticles, the physical stability of the BDMC-SLN during 3 months storage (25^0C) was determined by changing in particle size, zeta potential, and appearance. As illustrated in Table 12, BDMC-SLN prepared from different lipids showed suitable stability and achieved non-significant change in particle size indicating good stability during the period of study. The zeta potential of BDMC-SLN had less difference also supporting their stability.

Table 12. Size, polydispersity index (PDI), zeta potential and physical appearance of BDMC-SLN formulations during storage at ambient room temperature for 3 months

	SLN (1 Month)			
BDMC-SLN Formulation	Size (nm)	PDI	Zeta potential (mV)	Appearance
RB2.5Tw5-BDMC	672.8 ± 17.9	0.70 ± 0.15	-19.5 ± 0.5	HD
RB5.0Tw5-BDMC	770.7 ± 70.2	0.73 ± 0.14	-19.5 ± 1.1	HD
RB7.5Tw5-BDMC	484.2 ± 12.3	0.43 ± 0.05	-16.7 ± 0.5	HD
GB2.5Tw5-BDMC	305.9 ± 23.6	0.59 ± 0.05	-14.3 ± 0.7	HD
GB5.0Tw5-BDMC	250.4 ± 2.1	0.28 ± 0.01	-13.3 ± 0.5	HD
GB7.5Tw5-BDMC	247.5 ± 1.9	0.23 ± 0.02	-15.3 ± 0.2	HD
CP2.5Tw5-BDMC	317.8 ± 2.2	0.22 ± 0.01	-17.8 ± 0.5	HD
CP5.0Tw5-BDMC	255.6 ± 0.4	0.15 ± 0.01	-15.3 ± 0.2	HD
CP7.5Tw5-BDMC	301.1 ± 1.7	0.17 ± 0.02	-10.1 ± 1.3	HD
	SLN (3 Months)			
RB2.5Tw5-BDMC	667.0 ± 7.9	0.68 ± 0.05	-14.6 ± 0.9	HD
RB5.0Tw5-BDMC	746.7 ± 4.23	0.70 ± 0.17	-14.0 ± 0.3	HD

RB7.5Tw5-BDMC	523.1 ± 10.5	0.6 ± 0.05	-16.0 ± 0.7	HD
GB2.5Tw5-BDMC	239.9 ± 27.6	0.7 ± 0.16	-11.7 ± 0.51	HD
GB5.0Tw5-BDMC	258.8 ± 1.91	0.3 ± 0.01	-12.9 ± 0.15	HD
GB7.5Tw5-BDMC	267.7 ± 2.34	0.2 ± 0.01	-12.7 ± 0.69	HD
CP2.5Tw5-BDMC	-	-	-	PS
CP5.0Tw5-BDMC	264.0 ± 3.12	0.2 ± 0.01	-14.8 ± 0.40	HD
CP7.5Tw5-BDMC	-	-	-	PS

Note: HD = Homogeneous dispersion, PS = Phase separation, GF = Gel formation

3.5.3 Thermal analysis by differential scanning calorimetry (DSC)

As revealed in Table 13 and Figure 25 to 27 DSC thermograms of BDMC-SLN displayed complete disappearance of characteristic peak BDMC, but it showed characteristic peaks of lipid (A) RB2.5Tw5 at 78.42°C, (B) RB5.0Tw5 at 79.40 °C, (C) RB7.5Tw5 at 77.11°C, (D) GB2.5Tw5 at 75.64 °C, (E) GB5.0Tw5 at 74.43 °C, (F) GB7.5Tw5 at 74.46 °C, (G) CP2.5Tw5 at 52.37 °C, (H) CP5.0Tw5 at 52.59 °C and (I) CP7.5Tw5 at 53.44 °C with minimum shifting. The enthalpy of BDMC-SLN was -2.89, -3.24, -3.62, -5.42, -9.66, -10.01, -4.62, -4.07 and -9.14 (RB2.5Tw5, RB5.0Tw5, RB7.5Tw5, GB2.5Tw5, GB5.0Tw5, GB7.5Tw5, CP2.5Tw5, CP5.0Tw5, CP7.5Tw5, respectively).

Table 13. DSC results of BDMC-SLN after 3 months storage
(RB = Rice bran wax, GB = Glyceryl behenate, CP = Cetyl palmitate, BDMC = Bisdemethoxycurcumin)

Name	Onset (°C)	Peak(°C)	Endset(°C)	Crystallinity index (%) 0 month	Crystallinity index (%) 3 months
RB	76.41	80.94	83.93	100	100
GB	70.75	73.75	76.95	100	100
CP	50.43	54.42	56.94	100	100
BDMC	171.66	175.69	178.44	100	100
RB2.5Tw5-BDMC	73.66	78.42	80.22	86.11	1.18

RB5.0Tw5-BDMC	74.91	79.22	80.89	60.12	0.66
RB7.5Tw5-BDMC	74.66	77.11	78.92	33.05	0.49
GB2.5Tw5-BDMC	71.12	74.64	77.19	34.31	2.01
GB5.0Tw5-BDMC	69.96	74.43	76.71	19.30	3.57
GB7.5Tw5-BDMC	71.50	75.99	78.10	9.41	1.24
CP2.5Tw5-BDMC	49.41	52.37	54.02	15.26	0.87
CP5.0Tw5-BDMC	48.02	52.59	54.55	3.23	0.38
CP7.5Tw5-BDMC	50.71	53.44	55.35	3.69	0.57

From the crystallinity index (CI) of various formulations was less than those of the bulk-lipid and freshly prepared BDMC-SLN. The result found that after 3 month storage, BDMC-SLN with CP and RB had low crystallinity form compared to those GB. This lower of CI might affect to their entrapment efficiency and stability.

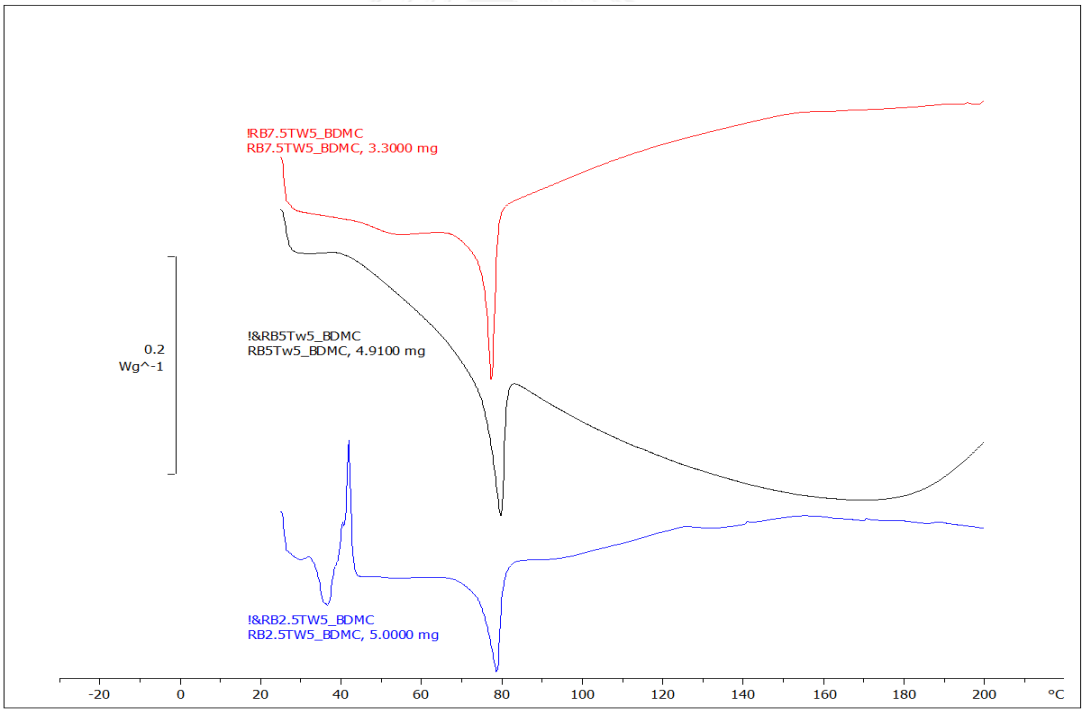

Figure 26. DSC thermograms of the BDMC-SLN prepared with rice bran wax after 3 months storage (RB = Rice bran wax, Tw = Tween 80)

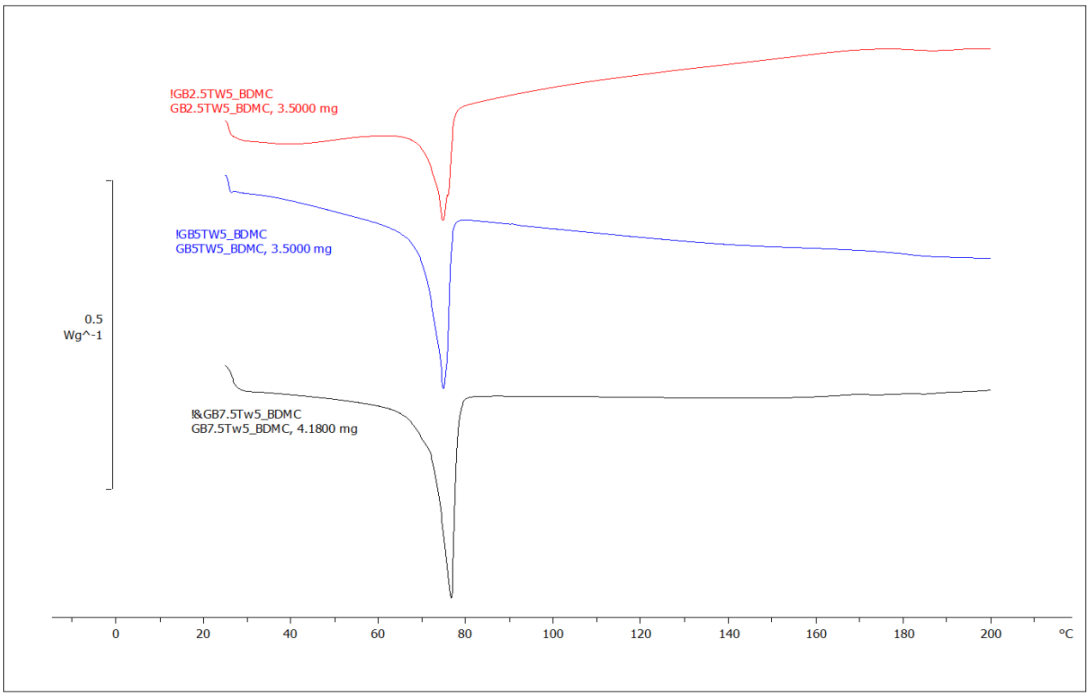

Figure 27. DSC thermograms of the BDMC-SLN prepared with glyceryl behenate after 3 months storage (GB = glyceryl behenate, Tw = Tween 80)

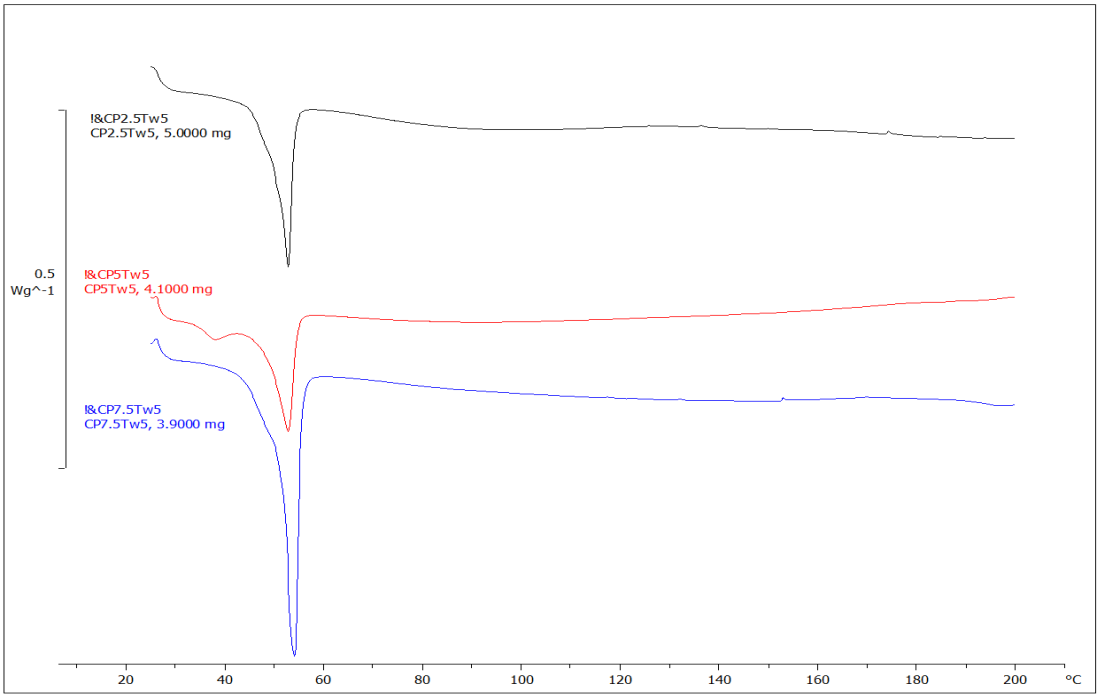

Figure 28. DSC thermograms of the BDMC-SLN prepared with cetyl palmitate after 3 months storage (CP = cetyl palmitate, Tw = Tween 80)

The crystallinity index of the BDMC-SLN might be explained relationship between lattice arrangement and drug incorporation. GB, a glyceride lipid, the BDMC-SLN with GB had highest CI. This result might be related to their lipid structure arrangement. Hou, Xie et al. (2003) realized that these lower melting enthalpy values should produce an effect of less ordered lattice arrangement of the lipid within nanoparticles than the bulk materials. For the less-ordered crystal or amorphous state, the melting of the substance required less energy than the perfect crystalline substance, which needed to overcome lattice force. Lipid nanoparticles seem to loose part of their crystalline state transforming from a mixture of β' and β polymorphs to the most stable β polymorph, permitting drug to fit in the molecular gaps. Therefore, this decreased in the melting point and enthalpy values was associated with numerous lattice defects and the formation of amorphous regions in which the drug was located.

3.5.4 Entrapment efficiency

From the Table 14 at 3 month storage, the BDMC-SLN entrapment efficiency had slightly less than the freshly prepared. The BDMC-SLN, made from CP (70.48%), had highest amount of drug incorporated follow by RB (58.17-70.60%) and GB (50.06-68.51%).

Table 14. Percentage of BDMC-SLN entrapment efficiency at 0 day and 3 months

Code	Entrapment efficiency (%) at 0 day	Entrapment efficiency (%) at 3 months
RB2.5Tw5-BDMC	66.46 ± 12.44	58.17 ± 0.26
RB5.0Tw5-BDMC	76.44 ± 11.92	64.97 ± 0.26
RB7.5Tw5-BDMC	73.41 ± 4.27	70.60 ± 0.36
GB2.5Tw5-BDMC	56.70 ± 0.59	68.51 ± 0.25
GB5.0Tw5-BDMC	65.31 ± 15.03	51.99 ± 0.14

GB7.5Tw5-BDMC	45.14 ± 0.55	50.06 ± 0.11
CP2.5Tw5-BDMC	65.94 ± 6.33	-
CP5.0Tw5-BDMC	70.41 ± 1.19	70.48 ± 0.35
CP7.5Tw5-BDMC	62.75 ± 2.10	-

The comparison of entrapment efficiency from various SLN formulations was demonstrated in figure 28. After long time storage, the SLN carriers contained RB or CP had similar entrapment efficiency to both time intervals. On the contrary, the entrapment efficiency of GB-SLN found slightly decreased accommodation of drug in carrier. A possible explanation was GB had low physical stability may lead to drug repulsion from nanoparticles.

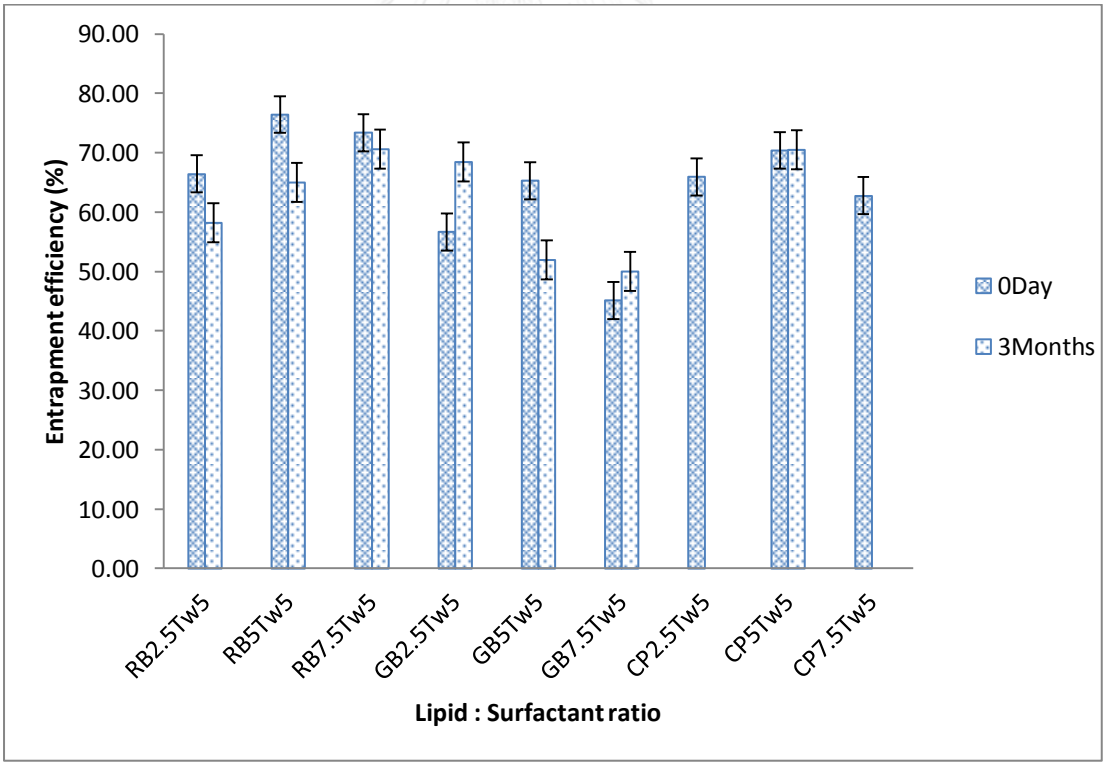

Figure 29. Comparison of percentage entrapment efficiency at day 0 and 3 months of BDMC-SLN formulations

This result might be due to structure of CP that had main fatty acid was palmitic acid more stable than GB (mainly behenic acid), and RB (combined with palmitic acid and behenic acid). The BDMC-SLN with GB had less entrapment efficiency and highest of CI. This result might be related to the structure of GB which was a glyceride lipid, form highly crystalline particles with a perfect lattice led to drug expulsion (Westesen, Bunjes et al. 1997).

CHAPTER V
CONCLUSIONS

The aim of the present study was to find a simple method for fabricating bisdemethoxycurcumin formulation using solid lipid nanoparticles with the rice bran wax as a natural wax. This is to add value to the byproduct received from rice bran oil refineries. It contains potent antioxidant of gamma oryzanol. Rice bran wax utilization in pharmaceuticals is worth investigating. And hope that solid lipid nanoparticles could solve certain pharmaceutical problem of drug. This study tried to examine if this preparation could retain stability of bisdemethoxycurcumin.

In the present work, Bisdemethoxycurcumin loaded SLN were successfully prepared by hot melt homogenization and high pressure homogenization technique. The various physicochemical properties such as particle size and size distribution, zeta potential, particle morphology, recrystallization behavior of lipid, Physical stability at long time storage and the In vitro release behavior of BDMC-SLN were greatly affected and can be controlled by optimizing the compositional variables represented in the concentration of surfactant and lipid as well as the type of lipid used. The sustained release behavior of Bisdemethoxycurcumin loaded SLN with favorable physicochemical characteristics can form a foundation for further clinical studies.

The results of these investigations were summarized as follows:

The influence of lipid types and lipid amount in formulations were investigated that solid lipid nanoparticle which prepared by rice bran wax have larger size than GB and CP which may be due to differences in chain lengths and viscosities of lipids used. The SLN containing RB and CP were more stable at 3 months than the SLN containing GB. At higher amounts of lipid added to these formulations leading to increment in particle size and viscosity which was subsequent to nanoparticles aggregation.

The surfactant concentrations demonstrated influence on particle size and PDI. It was noticeable that particle size greatly decreased with increasing of surfactant concentration at low amount of lipid while lesser effect on higher lipid content. Insufficient surfactant concentration resulted in increased particle which can be observed the SLN at low surfactant concentration (1 -3 % w/w), while at 5% (w/w) surfactant showed the highest stability and particle size was almost unchanged during the course of this investigation.

BDMC-SLN was yellow homogeneous dispersion and spherical shape in nanosize range with broad size distribution. At high amount of lipid and surfactant produce an effect of high loading efficiency. From the DSC thermograms indicated that drug is molecularly dispersed within the lipid matrix and indicating the conversion of crystalline BDMC to the amorphous form which could be attributed to complete dissolution of the drug in the molten lipid matrix. BDMC-SLN containing RB achieves highest entrapment efficiency follow by CP and GB. BDMC-SLN prepared from different lipids showed suitable stability during the 3 months period of the study and achieve non-significant change in particle size indicating good stability during the period of study. No obvious change of clarity or degradation was observed except the cetyl palmitate formulation. In vitro release studies for BDMC-SLN exhibited a sustained release pattern. Initial release within 1 hour and the amount of free BDMC release versus time were CP5Tw5 > GB5Tw5 > RB2.5Tw5 > RB5.0Tw5 > RB7.5Tw5 and control (BDMC solution). Suitable formulation which was stable for 3 months contained 7.5% (w/w) rice bran wax as a lipid and 5% Tween® 80 as a surfactant. Because of RB7.5Tw5 has size approximately 514.9 nm, PDI 0.43, zeta potential value -16.8 that point to good physicochemical characteristic and also has high drug entrapment in lipid carrier.

REFERENCES

Abbas, S., E. Karangwa, M. Bashari, K. Hayat, X. Hong, H. R. Sharif and X. Zhang (2015). "Fabrication of polymeric nanocapsules from curcumin-loaded nanoemulsion templates by self-assembly." Ultrason Sonochem **23**: 81-92.

Abdel-Salam, F. S., S. A. Elkheshen, A. A. Mahmoud and H. O. Ammar (2015). "Diflucortolone valerate loaded solid lipid nanoparticles as a semisolid topical delivery system." Bulletin of Faculty of Pharmacy, Cairo University.

Abdelbary, G. and R. H. Fahmy (2009). "Diazepam-loaded solid lipid nanoparticles: design and characterization." American Association of Pharmaceutical Scientists PharmSciTech **10**(1): 211-219.

Aburahma, M. H. and S. M. Badr-Eldin (2014). "Compritol 888 ATO: a multifunctional lipid excipient in drug delivery systems and nanopharmaceuticals." Expert Opinion on Drug Delivery. **11**(12): 1865-1883.

Ahlin Grabnar, P., J. Kristl and J. Smid-Korbar (1998). "Optimization of procedure parameters and physical stability of solid lipid nanoparticles in dispersions." Acta pharmaceutica **48no**(4): 259-267.

Anand, P., A. B. Kunnumakkara, R. A. Newman and B. B. Aggarwal (2007). "Bioavailability of curcumin: problems and promises." Molecular Pharmaceutics **4**(6): 807-818.

Basnet, P., H. Hussain, I. Tho and N. Skalko-Basnet "Liposomal Delivery System Enhances Anti-Inflammatory Properties of Curcumin." Journal of Pharmaceutical Sciences **101**(2): 598-609.

Bergonzi, M. C., R. Hamdouch, F. Mazzacuva, B. Isacchi and A. R. Bilia (2014). "Optimization, characterization and in vitro evaluation of curcumin microemulsions." LWT - Food Science and Technology **59**(1): 148-155.

Bhalekar, M. R., V. Pokharkar, A. Madgulkar, N. Patil and N. Patil (2009). "Preparation and Evaluation of Miconazole Nitrate-Loaded Solid Lipid Nanoparticles for Topical Delivery." American Association of Pharmaceutical Scientists PharmSciTech **10**(1): 289-296.

Chattopadhyay, P., B. Y. Shekunov, D. Yim, D. Cipolla, B. Boyd and S. Farr (2007). "Production of solid lipid nanoparticle suspensions using supercritical fluid extraction of emulsions (SFEE) for pulmonary delivery using the AERx system." Advanced Drug Delivery Reviews **59**(6): 444-453.

Das, S., W. K. Ng, P. Kanaujia, S. Kim and R. B. Tan (2011). "Formulation design, preparation and physicochemical characterizations of solid lipid nanoparticles containing a hydrophobic drug: effects of process variables." Colloids and Surface B Biointerfaces **88**(1): 483-489.

de Jesus, M. B., A. Radaic, I. S. Zuhorn and E. de Paula (2013). "Microemulsion extrusion technique: a new method to produce lipid nanoparticles." Journal of Nanoparticle Research **15**(10): 1-15.

De Pintu Kumar, Dinda Subas C, Chakraborty Subrata and R. Soumen (2012). "Formulation and evaluation of solid lipid nanoparticles of a poorly water soluble model drug, Ibuprofen." International Research Journal of Pharmacy **3**(12): 132-137.

Devasena, T., K. N. Rajasekaran, G. Gunasekaran, P. Viswanathan and V. P. Menon (2003). "Anticarcinogenic effect of bis-1,7-(2-hydroxyphenyl)-hepta-1,6-diene-3,5-dione a curcumin analog on DMH-induced colon cancer model." Pharmacological Research **47**(2): 133-140.

Fiala, M., P. T. Liu, A. Espinosa-Jeffrey, M. J. Rosenthal, G. Bernard, J. M. Ringman, J. Sayre, L. Zhang, J. Zaghi, S. Dejbakhsh, B. Chiang, J. Hui, M. Mahanian, A. Baghaee, P. Hong and J. Cashman (2007). "Innate immunity and transcription of MGAT-III and Toll-like receptors in Alzheimer's disease patients are improved by bisdemethoxycurcumin." Proceeding of the National Academy of Sciences USA **104**(31): 12849-12854.

Freitas, C. and R. H. Mullera (1998). "Spray-drying of solid lipid nanoparticles (SLN TM)." European Journal of Pharmaceutics and Biopharmaceutics **46**(2): 145-151.

Guo, L. Y., X. F. Cai, J. J. Lee, S. S. Kang, E. M. Shin, H. Y. Zhou, J. W. Jung and Y. S. Kim (2008). "Comparison of suppressive effects of demethoxycurcumin and

bisdemethoxycurcumin on expressions of inflammatory mediators in vitro and in vivo." Archives of Pharmacal Research **31**(4): 490-496.

Hai–xia Duan, Xiang-dong Ma, Xing-Ma, Y.-W. Hu and B.-L. Chen (2011). "Antiproliferation and apoptosis induced by Bisdemethoxycurcumin in human ovarian cancer cell SKOV3." Journal of Medicinal Plants Research **5**(12): 2499-2507.

Hou, D., C. Xie, K. Huang and C. Zhu (2003). "The production and characteristics of solid lipid nanoparticles (SLNs)." Biomaterials **24**(10): 1781-1785.

Hsu, C. H., Z. Cui, R. J. Mumper and M. Jay (2003). "Preparation and characterization of novel coenzyme Q10 nanoparticles engineered from microemulsion precursors." American Association of Pharmaceutical Scientists PharmSciTech **4**(3): E32.

Huang, M. T., T. Lysz, T. Ferraro, T. F. Abidi, J. D. Laskin and A. H. Conney (1991). "Inhibitory effects of curcumin on in vitro lipoxygenase and cyclooxygenase activities in mouse epidermis." Cancer Research **51**(3): 813-819.

Huang, M. T., W. Ma, P. Yen, J. G. Xie, J. Han, K. Frenkel, D. Grunberger and A. H. Conney (1997). "Inhibitory effects of topical application of low doses of curcumin on 12-O-tetradecanoylphorbol-13-acetate-induced tumor promotion and oxidized DNA bases in mouse epidermis." Carcinogenesis **18**(1): 83-88.

Jenning, V., M. Schäfer-Korting and S. Gohla (2000). "Vitamin A-loaded solid lipid nanoparticles for topical use: drug release properties." Journal of Controlled Release **66**(2–3): 115-126.

Kim, A. N., W. K. Jeon, J. J. Lee and B. C. Kim (2010). "Up-regulation of heme oxygenase-1 expression through CaMKII-ERK1/2-Nrf2 signaling mediates the anti-inflammatory effect of bisdemethoxycurcumin in LPS-stimulated macrophages." Free Radical Biology and Medicine **49**(3): 323-331.

Lee, P. J., S. J. Woo, J. G. Jee, S. H. Sung and H. P. Kim (2015). "Bisdemethoxycurcumin Induces apoptosis in activated hepatic stellate cells via cannabinoid receptor 2." Molecules **20**(1): 1277-1292.

Lemos-Senna, E., D. Wouessidjewe, S. Lesieur and D. Duchêne (1998). "Preparation of amphiphilic cyclodextrin nanospheres using the emulsification solvent evaporation method. Influence of the surfactant on preparation and hydrophobic drug loading." International Journal of Pharmaceutics **170**(1): 119-128.

Li, Y. B., J. L. Gao, Z. F. Zhong, P. M. Hoi, S. M. Lee and Y. T. Wang (2013). "Bisdemethoxycurcumin suppresses MCF-7 cells proliferation by inducing ROS accumulation and modulating senescence-related pathways." Pharmacological Reports **65**(3): 700-709.

Lin, C.-C., H.-Y. Lin, H.-C. Chen, M.-W. Yu and M.-H. Lee (2009). "Stability and characterisation of phospholipid-based curcumin-encapsulated microemulsions." Food Chemistry **116**(4): 923-928.

Luo, C., Z. Du, X. Wei, G. Chen and Z. Fu (2015). "Bisdemethoxycurcumin attenuates gastric adenocarcinoma growth by inducing mitochondrial dysfunction." Oncology Letters **9**(1): 270-274.

Mahattanadul, S., T. Nakamura, P. Panichayupakaranant, N. Phdoongsombut, K. Tungsinmunkong and P. Bouking (2009). "Comparative antiulcer effect of bisdemethoxycurcumin and curcumin in a gastric ulcer model system." Phytomedicine **16**(4): 342-351.

Manjunath, K., J. S. Reddy and V. Venkateswarlu (2005). "Solid lipid nanoparticles as drug delivery systems." Methods Find Exp Clin Pharmacol **27**(2): 127-144.

Martins, S., B. Sarmento, D. C. Ferreira and E. B. Souto (2007). "Lipid-based colloidal carriers for peptide and protein delivery – liposomes versus lipid nanoparticles." International Journal of Nanomedicine **2**(4): 595-607.

Maru, A. D., R. K. Surawase and P. V. Bodhe (2012). "Studies on Physico-Chemical Properties of Rice Bran Wax and its Comparison with Carnauba Wax." International Journal of Pharmaceutical and Phytopharmacological Research.

Müller, R. H., K. Mäder and S. Gohla (2000). "Solid lipid nanoparticles (SLN) for controlled drug delivery – a review of the state of the art." European Journal of Pharmaceutics and Biopharmaceutics **50**(1): 161-177.

Onoue, S., H. Takahashi, Y. Kawabata, Y. Seto, J. Hatanaka, B. Timmermann and S. Yamada (2010). "Formulation design and photochemical studies on nanocrystal solid dispersion of curcumin with improved oral bioavailability." Journal of Pharmaceutical Sciences **99**(4): 1871-1881.

Pandey and Anushree (2014). "Role of Surfactants as Penetration Enhancer in Transdermal Drug Delivery System." Journal of Molecular Pharmaceutics & Organic Process Research **02**(02).

Pragna Shelat, Vinod K. Mandowara, Deepak G. Gupta and S. Patel (2015). "Formulation of curcuminoid loaded solid lipid nanoparticles in order to improve oral bioavailability." International Journal of Pharmacy and Pharmaceutical Sciences **7**(6): 278-282.

Ramsewak, R. S., D. L. DeWitt and M. G. Nair (2000). "Cytotoxicity, antioxidant and anti-inflammatory activities of curcumins I-III from Curcuma longa." Phytomedicine **7**(4): 303-308.

Rawia M. Khalila, Ahmed Abd El-Baryb, Mahfoz A. Kassema, M. M. Ghorabc and M. Basha (2013). "Influence of formulation parameters on the physicochemical properties of meloxicam-loaded solid lipid nanoparticles." Egyptian Pharmaceutical Journal **12**(1): 63-72.

Souto, E. B., C. Anselmi, M. Centini and R. H. Muller (2005). "Preparation and characterization of n-dodecyl-ferulate-loaded solid lipid nanoparticles (SLN)." International Journal of Pharmaceutics **295**(1-2): 261-268.

Sun, J., C. Bi, H. M. Chan, S. Sun, Q. Zhang and Y. Zheng (2013). "Curcumin-loaded solid lipid nanoparticles have prolonged in vitro antitumour activity, cellular uptake and improved in vivo bioavailability." Colloids and Surfaces B: Biointerfaces **111**: 367-375.

Swarnlata Saraf and G. Jeswani (2014). "Topical Delivery of Curcuma longa Extract Loaded Nanosized Ethosomes to Combat Facial Wrinkles Research Article." Journal of Pharmaceutics & Drug Delivery Research **03**(01).

Tikekar, R. V., Y. Pan and N. Nitin (2013). "Fate of curcumin encapsulated in silica nanoparticle stabilized Pickering emulsion during storage and simulated digestion." Food Research International **51**(1): 370-377.

Tiyaboonchai, W., W. Tungpradit and P. Plianbangchang (2007). "Formulation and characterization of curcuminoids loaded solid lipid nanoparticles." International Journal of Pharmaceutics **337**(1–2): 299-306.

U.G., B. (2013). "Rice bran wax-a novel excipient for pharmaceutical topical dosage forms." International Journal of Bioassays; Vol 2, No 05 (2013).

UG, B. (2013). "Rice Bran Wax-A Novel Excipient For Pharmaceutical Topical Dosage Forms." International Journal of Bioassays **2**(5): 828-832.

Üner, M. and G. Yener (2007). "Importance of solid lipid nanoparticles (SLN) in various administration routes and future perspectives." International Journal of Nanomedicine **2**(3): 289-300.

Vaghasiya, H., A. Kumar and K. Sawant (2013). "Development of solid lipid nanoparticles based controlled release system for topical delivery of terbinafine hydrochloride." European Journal of Pharmaceutical Sciences **49**(2): 311-322.

Wang, X., Y. Jiang, Y.-W. Wang, M.-T. Huang, C.-T. Ho and Q. Huang (2008). "Enhancing anti-inflammation activity of curcumin through O/W nanoemulsions." Food Chemistry **108**(2): 419-424.

Westesen, K., H. Bunjes and M. H. J. Koch (1997). "Physicochemical characterization of lipid nanoparticles and evaluation of their drug loading capacity and sustained release potential." Journal of Controlled Release **48**(2–3): 223-236.

Wissing, S. A., O. Kayser and R. H. Muller (2004). "Solid lipid nanoparticles for parenteral drug delivery." Adv Drug Deliv Rev **56**(9): 1257-1272.

Zhao, Y. Z., C. T. Lu, Y. Zhang, J. Xiao, Y. P. Zhao, J. L. Tian, Y. Y. Xu, Z. G. Feng and C. Y. Xu (2013). "Selection of high efficient transdermal lipid vesicle for curcumin skin delivery." International Journal of Pharmaceutics **454**(1): 302-309.

APPENDIX

APPENDIX A

Molecular structure and physical properties of some materials

Properties of some materials used in this study

1. Cetyl palmitate

   Synonyms: hexadecyl hexadecanoate, palmityl palmitate, hexadecyl ester

   Molecular formula: $C_{32}H_{64}O_2$

   Molecular weight: 480.84 g/mol

   HLB value: 10

   Melting point: 54°C

   Chemical structure

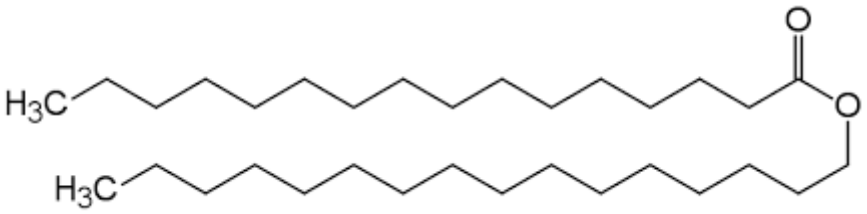

2. Glyceryl behenate

   Synonyms: 2,3-dihydroxypropyl docosanoate, Compritol ATO 888

   Molecular formula: $C_{25}H_{50}O_4$

   Molecular weight: 414.66 g/mol

   HLB value: 2

   Melting point: 69-74°C

   Chemical structure

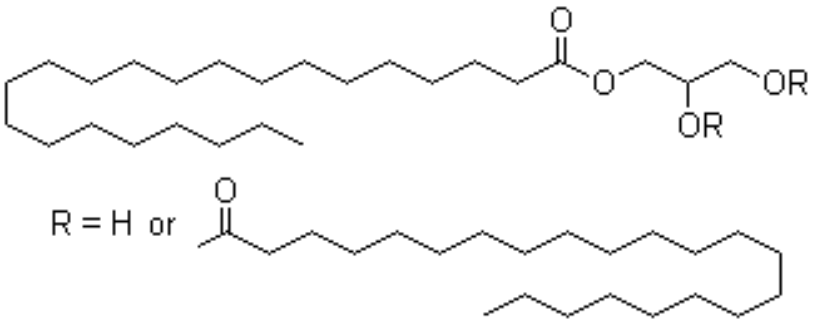

3. Rice bran wax

Solubility: Insoluble in water, soluble in ether, ethanol and isopropyl alcohol

HLB: 10

Melting point: 77-80.5°C

Specific gravity: 0.912

Moisture content: 0.074 %w/w

Saponification value: 80.88

Acid value: 2.848

Ester value: 78.04

Hydroxyl value: 19.62

Iodine value: 10

Chemical structure

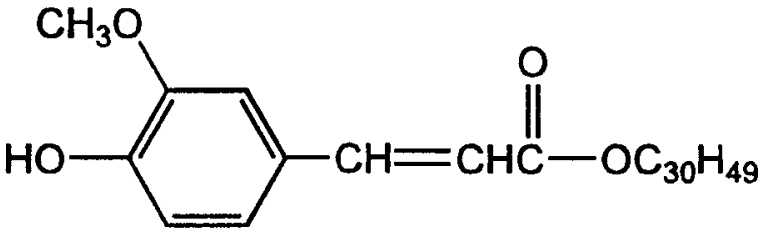

4. Tween 80

Synonyms: polysorbate 80, polyoxyethylene sorbitan (20) monooleate, polyoxyethylenesorbitan monooleate, PEG (80) sorbitan monooleate

Molecular formula: $C_{32}H_{60}O_{10}$

Molecular weight: 604.81 g/mol

HLB value: 15

Chemical structure

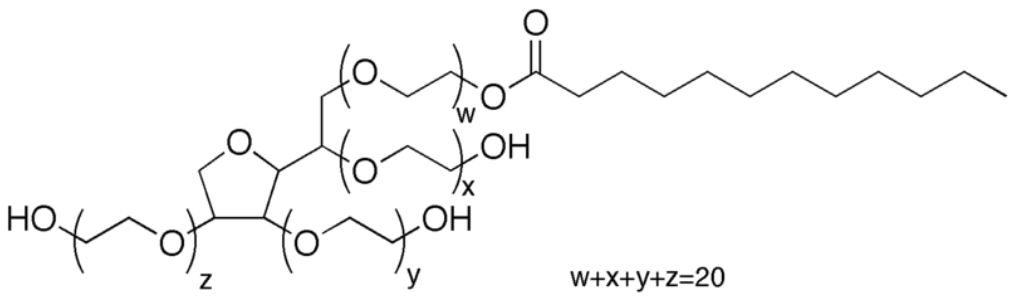

APPENDIX B

Particle size analysis

Particle size analysis of blank SLN

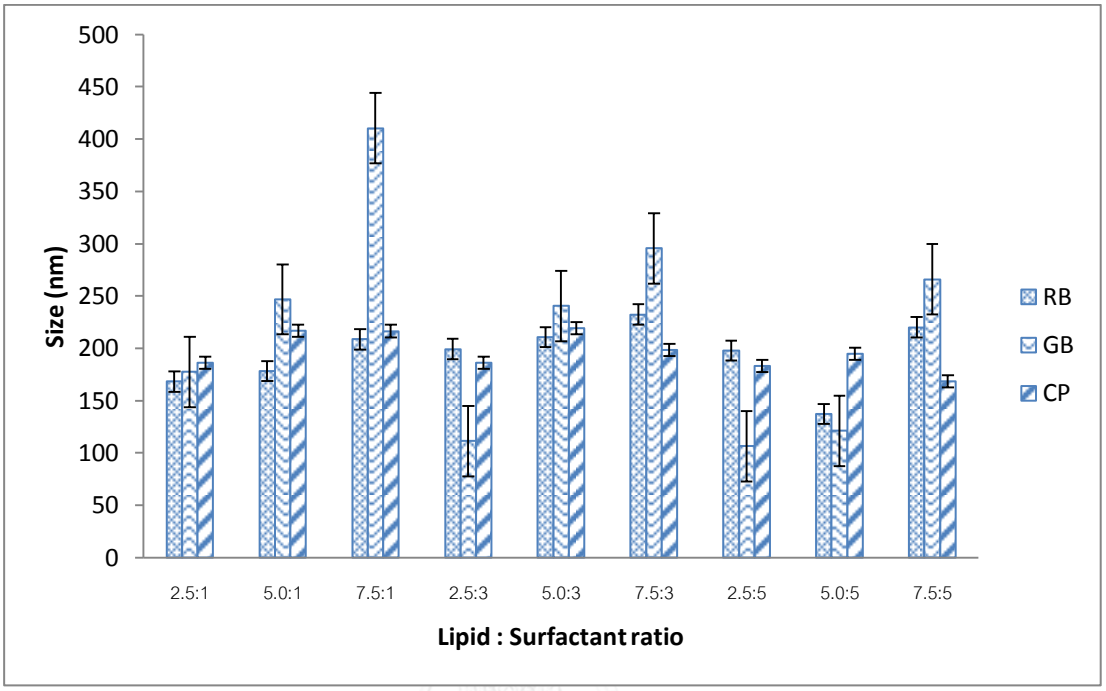

Comparison of particle size of freshly prepared blank-SLN formulations (RB = Rice bran wax, GB = Glyceryl behenate, CP = Cetyl palmitate)

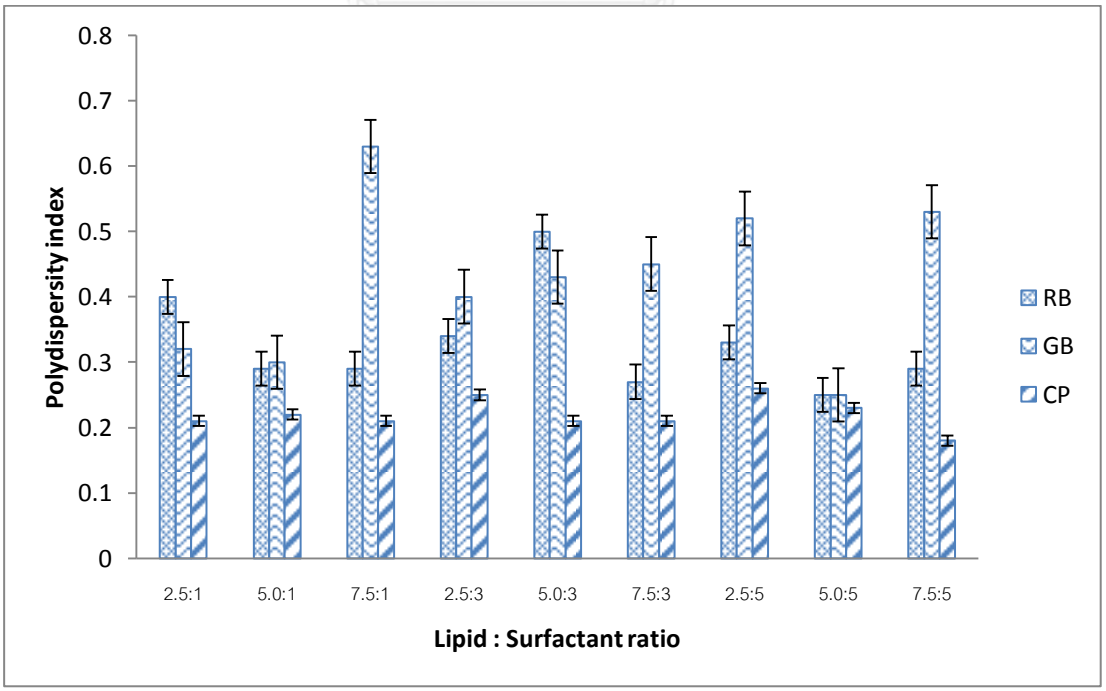

Comparison of polydispersity index of freshly prepared blank-SLN formulations (RB = Rice bran wax, GB = Glyceryl behenate, CP = Cetyl palmitate)

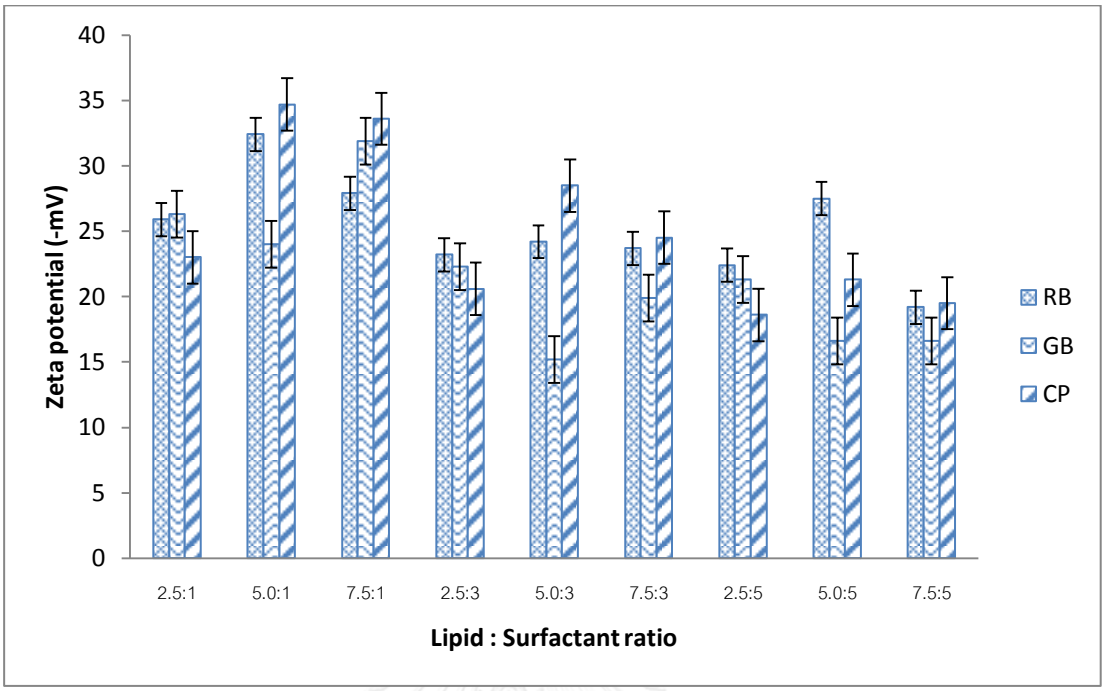

Comparison of zeta potential of freshly prepared blank-SLN formulations (RB = Rice bran wax, GB = Glyceryl behenate, CP = Cetyl palmitate)

Particle size analysis of CUR loaded SLN

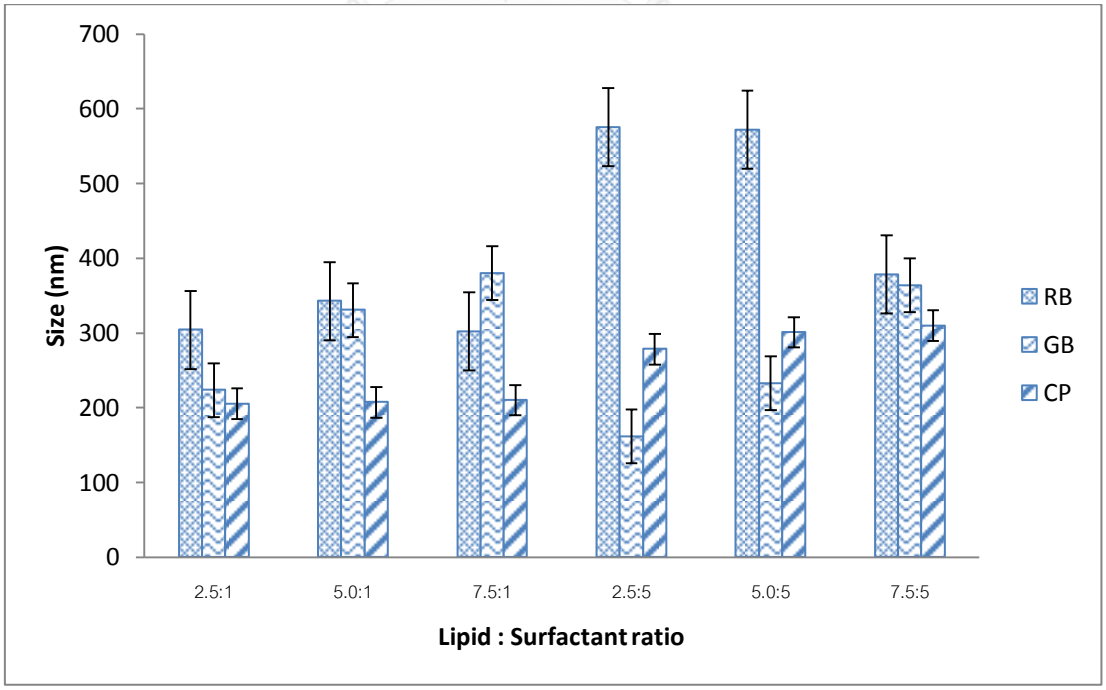

Particle size of freshly prepared C-SLN formulations (RB = Rice bran wax, GB = Glyceryl behenate, CP = Cetyl palmitate)

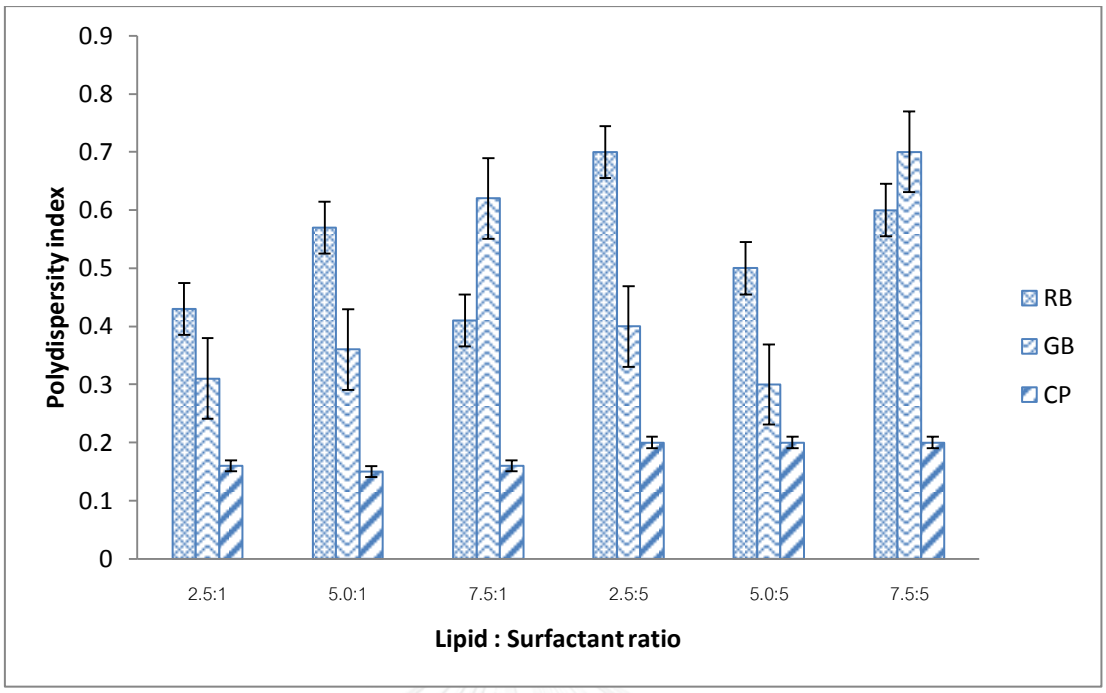

Polydispersity index of freshly prepared C-SLN formulations (RB = Rice bran wax, GB = Glyceryl behenate, CP = Cetyl palmitate)

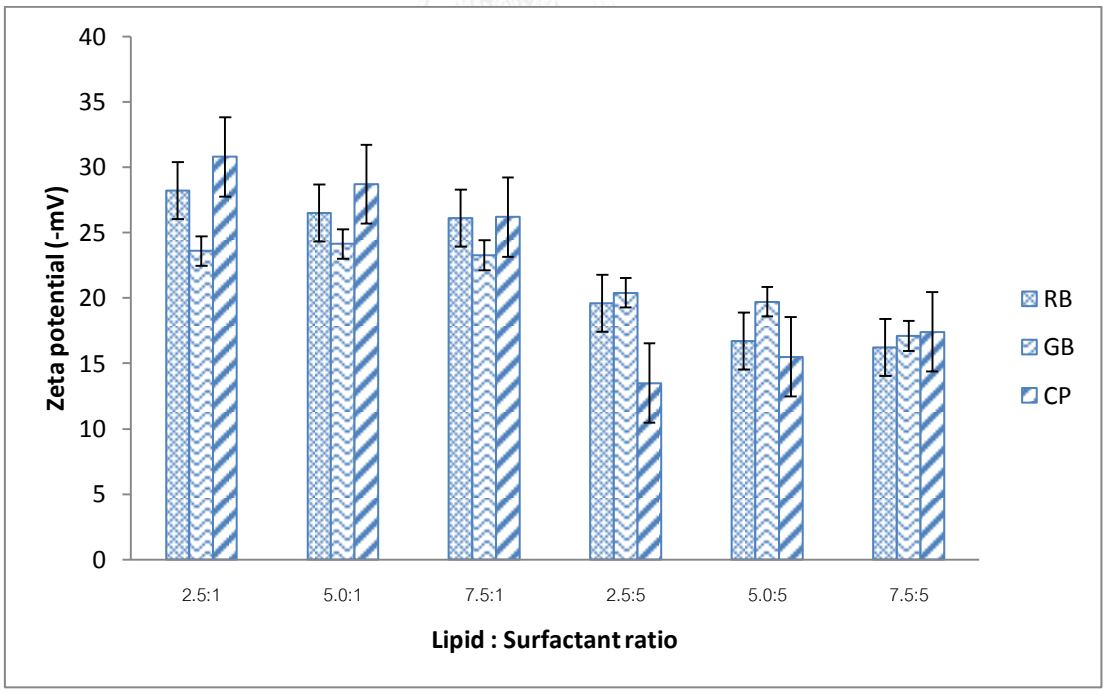

Zeta potential of freshly prepared C-SLN formulations (RB = Rice bran wax, GB = Glyceryl behenate, CP = Cetyl palmitate)

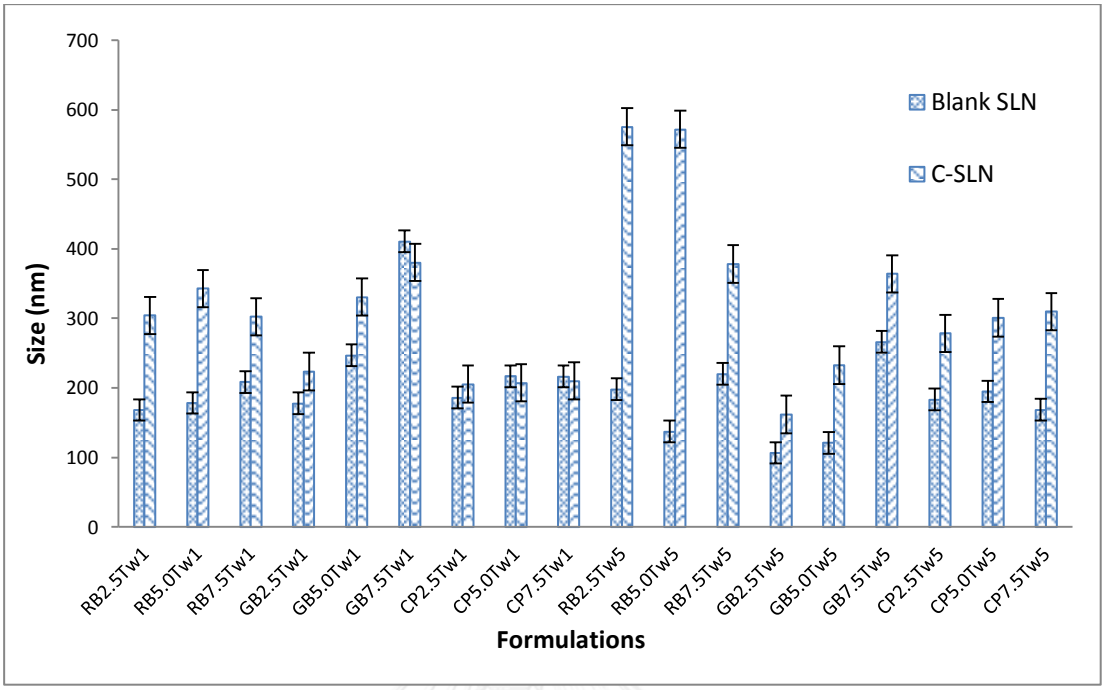

Comparison of size of Blank SLN and C-SLN

Particle size analysis of BDMC loaded SLN

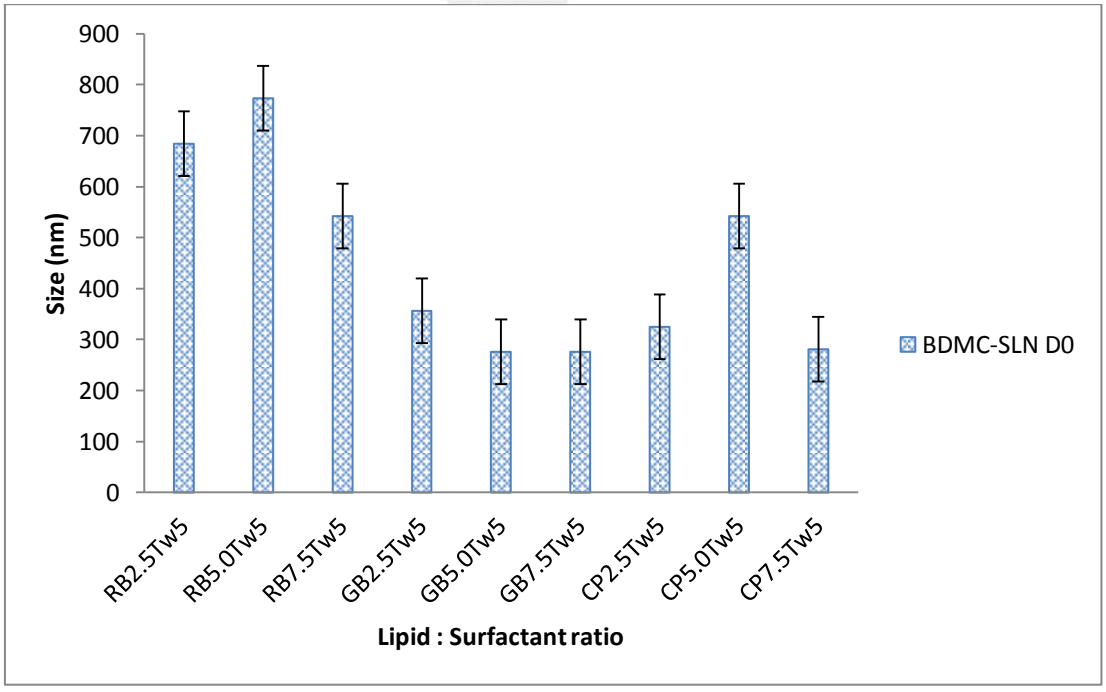

Particle size of freshly prepared BDMC-SLN formulations

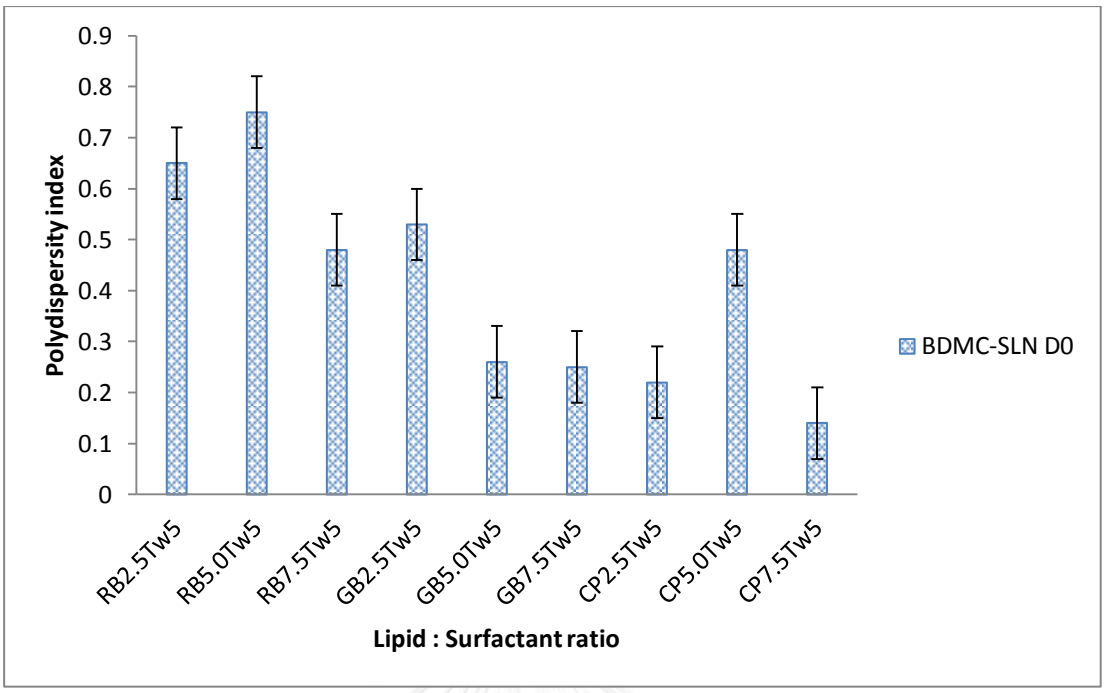

Polydispersity index of freshly prepared BDMC-SLN formulations

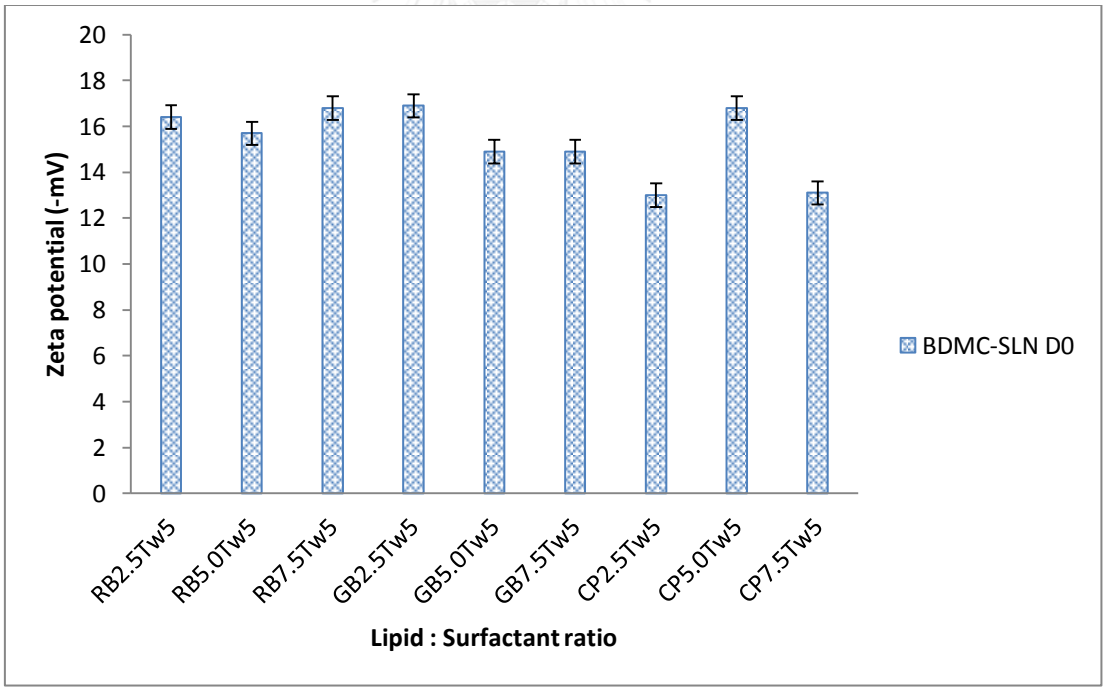

Zeta potential of freshly prepared BDMC-SLN formulations

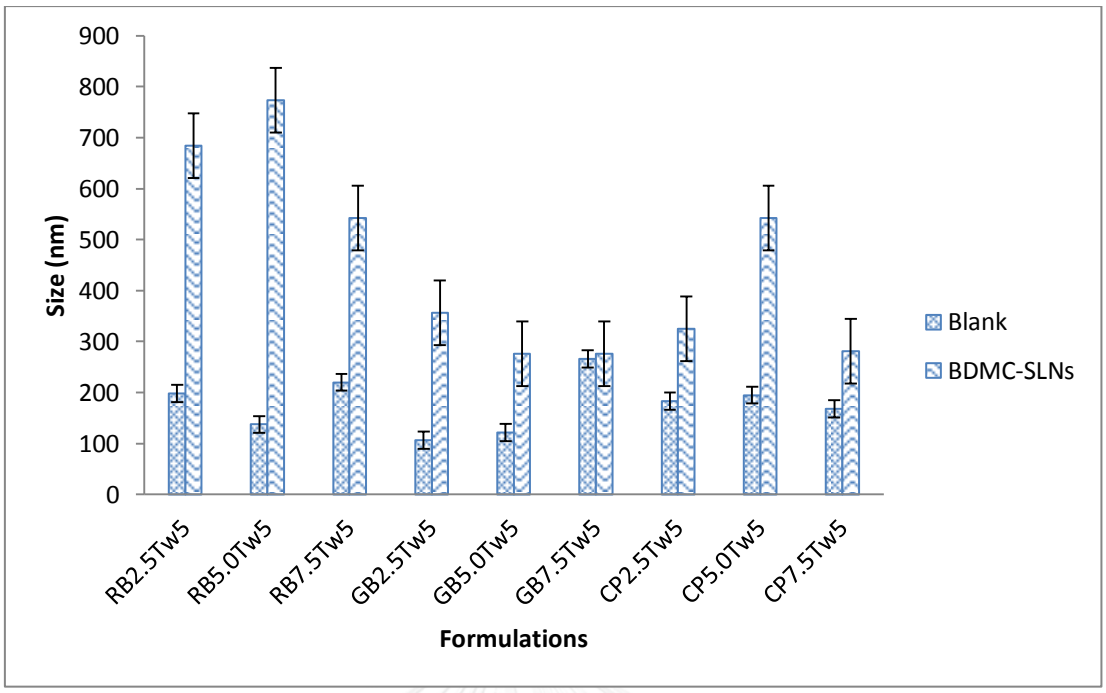

Comparison of size of Blank SLN and BDMC-SLN

APPENDIX C

DSC Thermograms

DSC thermograms of the Raw material

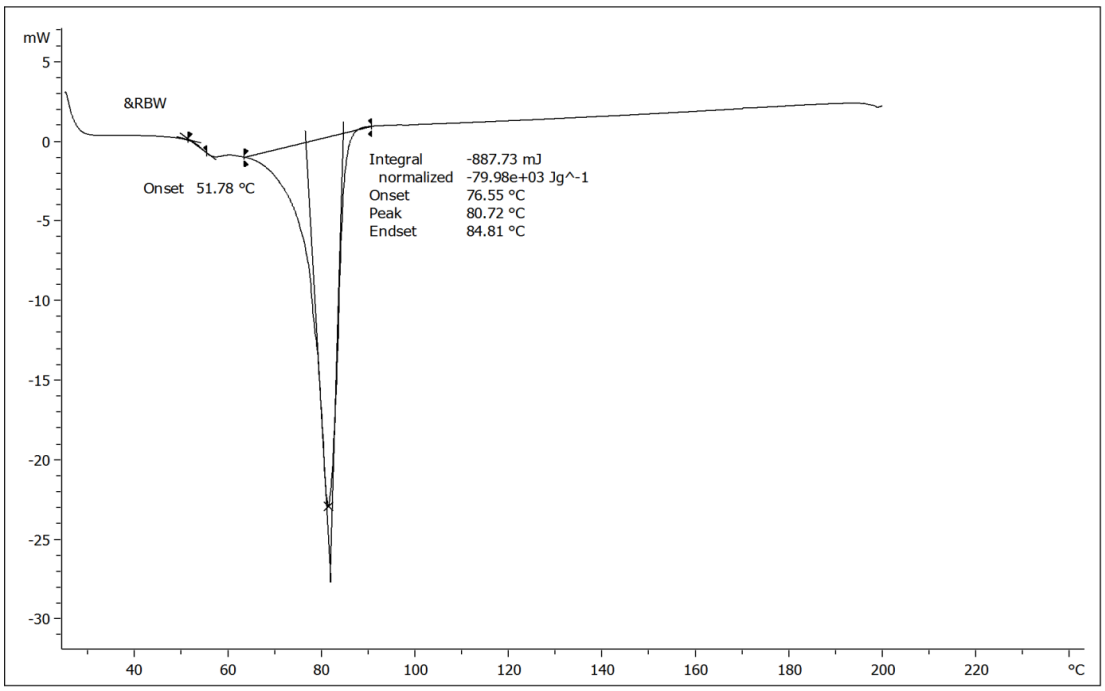

DSC thermograms of the Raw material: Rice bran wax

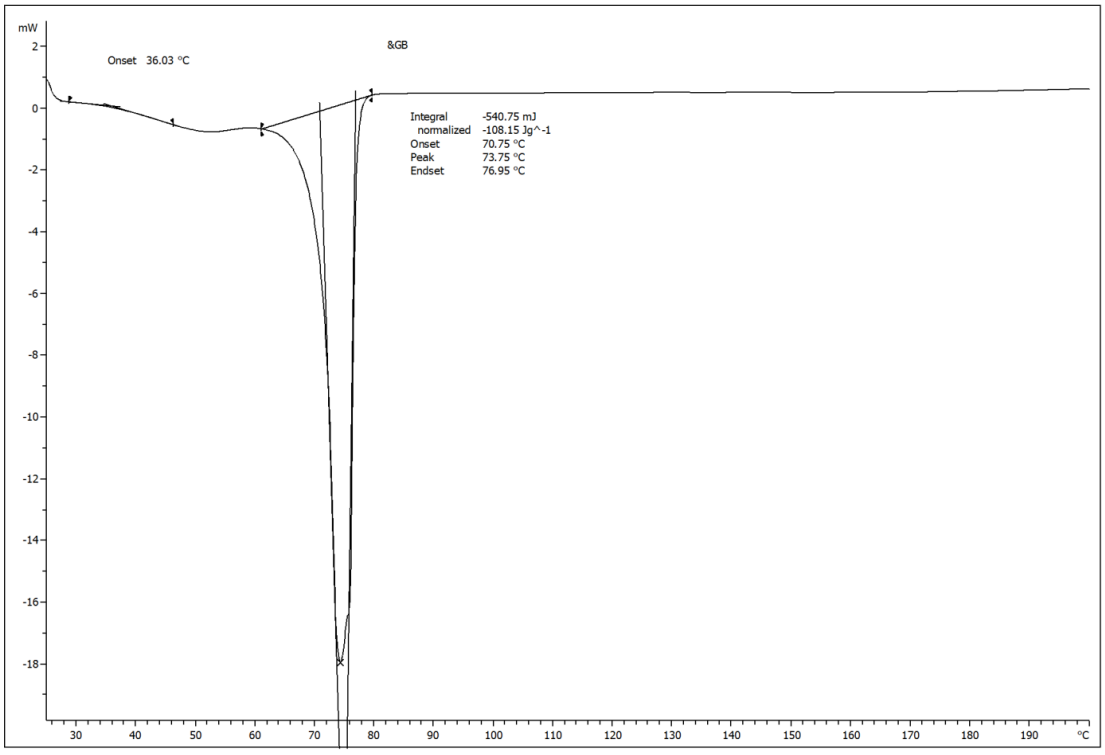

DSC thermograms of the Raw material: Glyceryl behenate

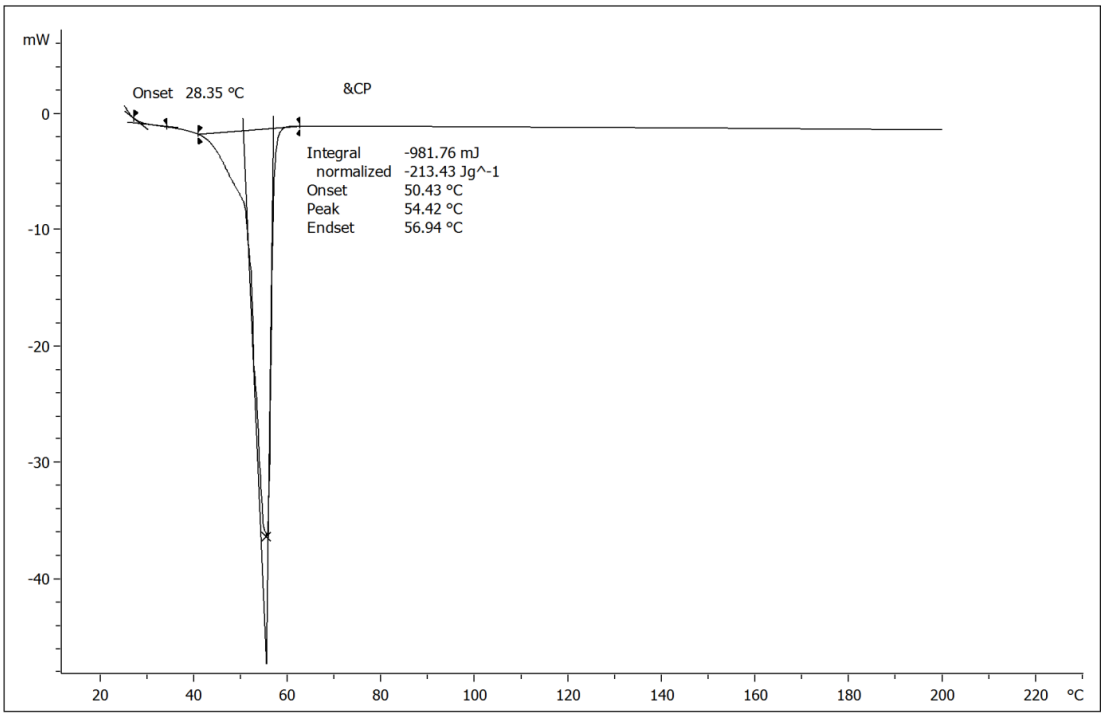

DSC thermograms of the Raw material: Cetyl palmitate

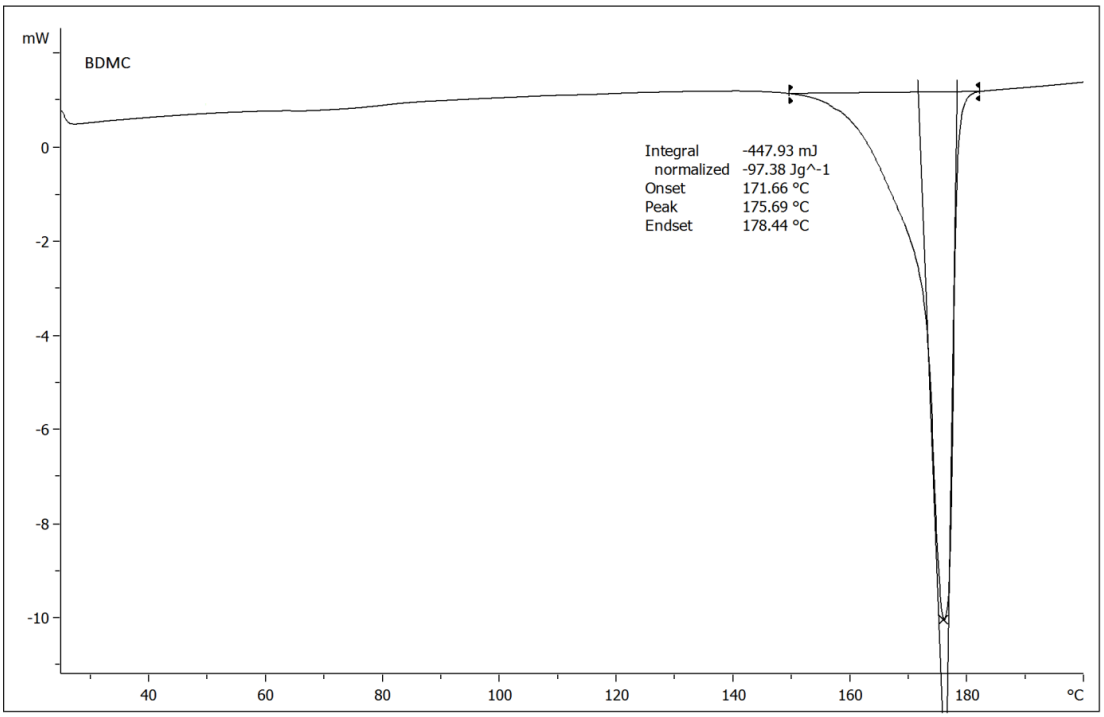

DSC thermograms of the Raw material: Bisdemethoxycurcumin (D)

DSC thermograms of the Physical mixture of bulk lipid and drug

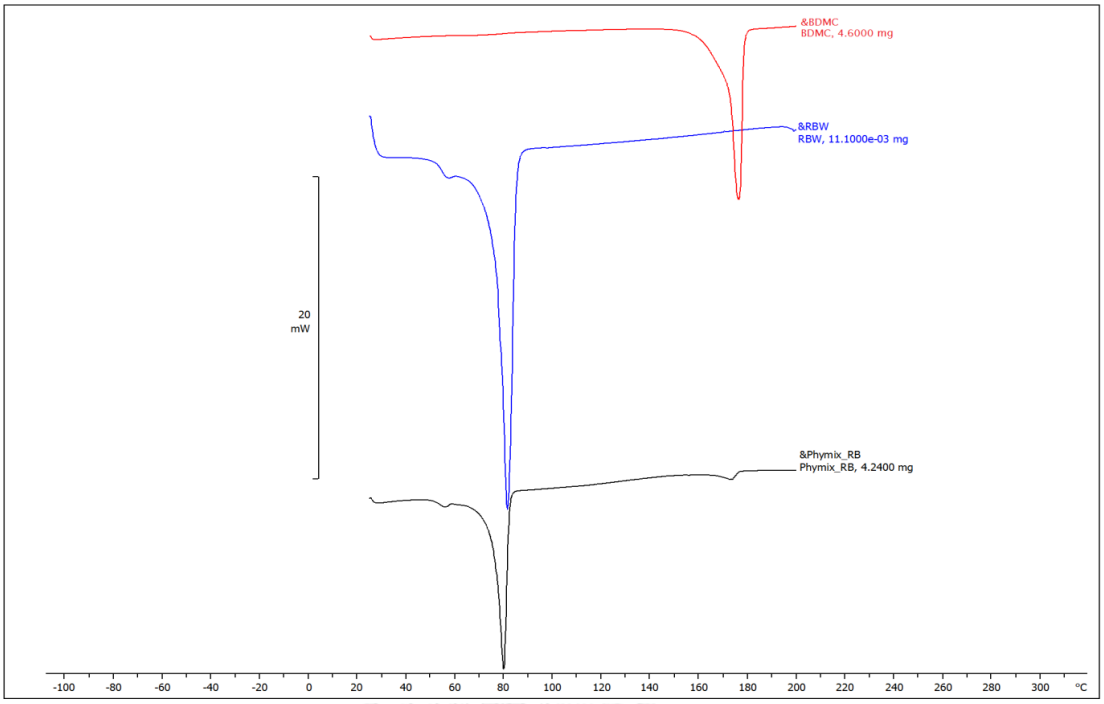

DSC thermograms of the Physical mixture of bulk lipid and drug (Rice bran wax: bisdemethoxycurcumin)

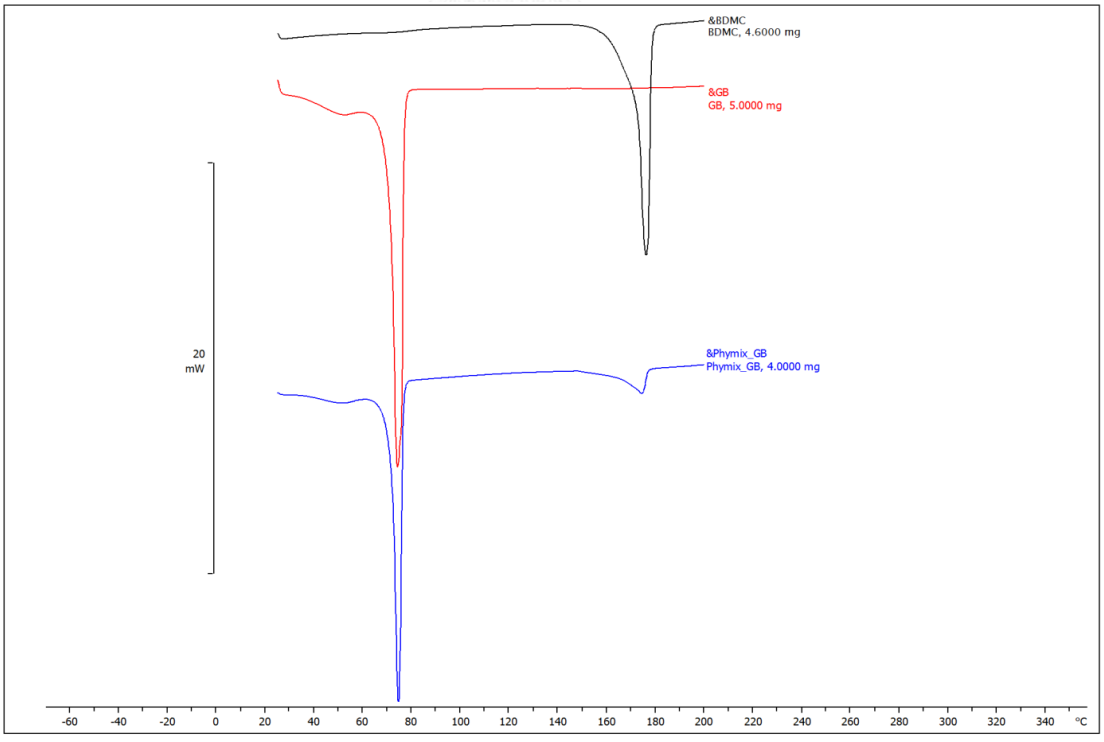

DSC thermograms of the Physical mixture of bulk lipid and drug (glyceryl behenate : bisdemethoxycurcumin)

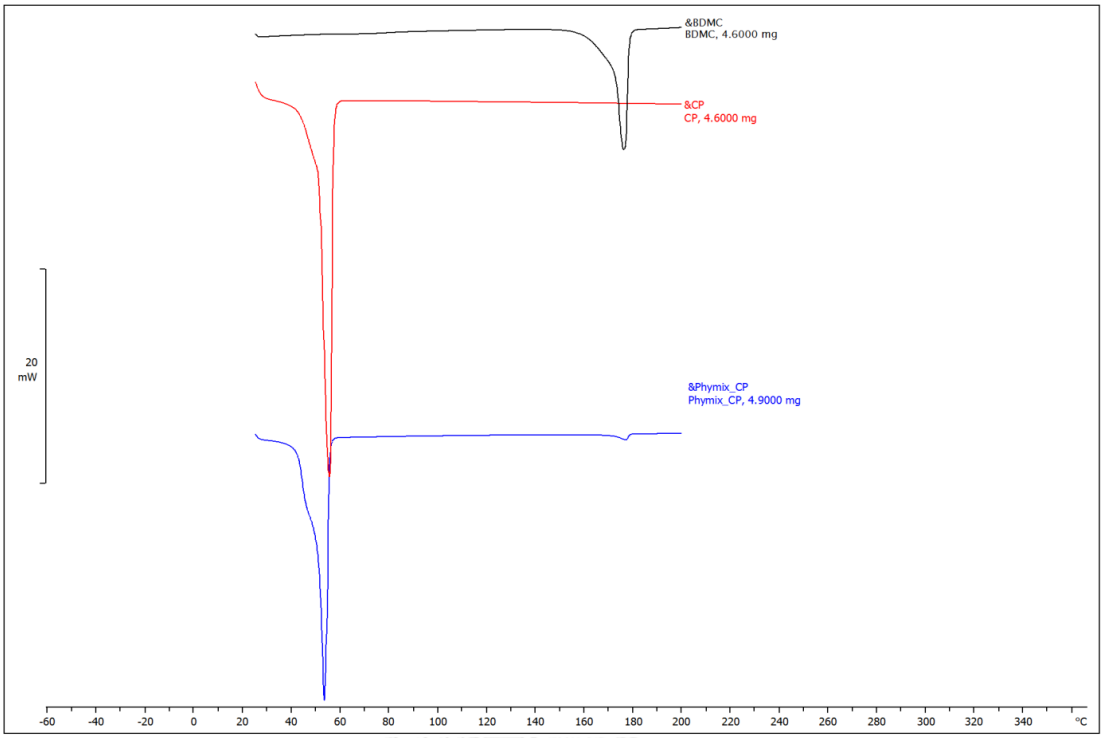

DSC thermograms of the Physical mixture of bulk lipid and drug (cetyl palmitate : bisdemethoxycurcumin)

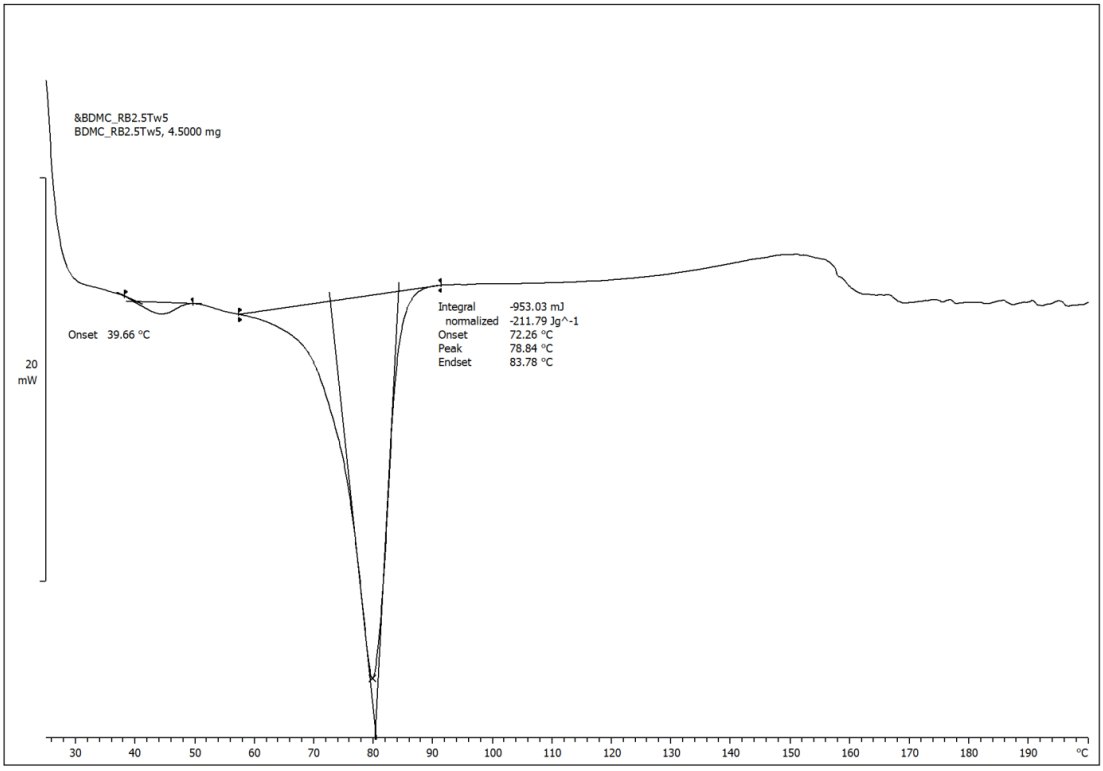

DSC thermogram of the loaded solid lipid nanoparticles: RB2.5Tw5-BDMC

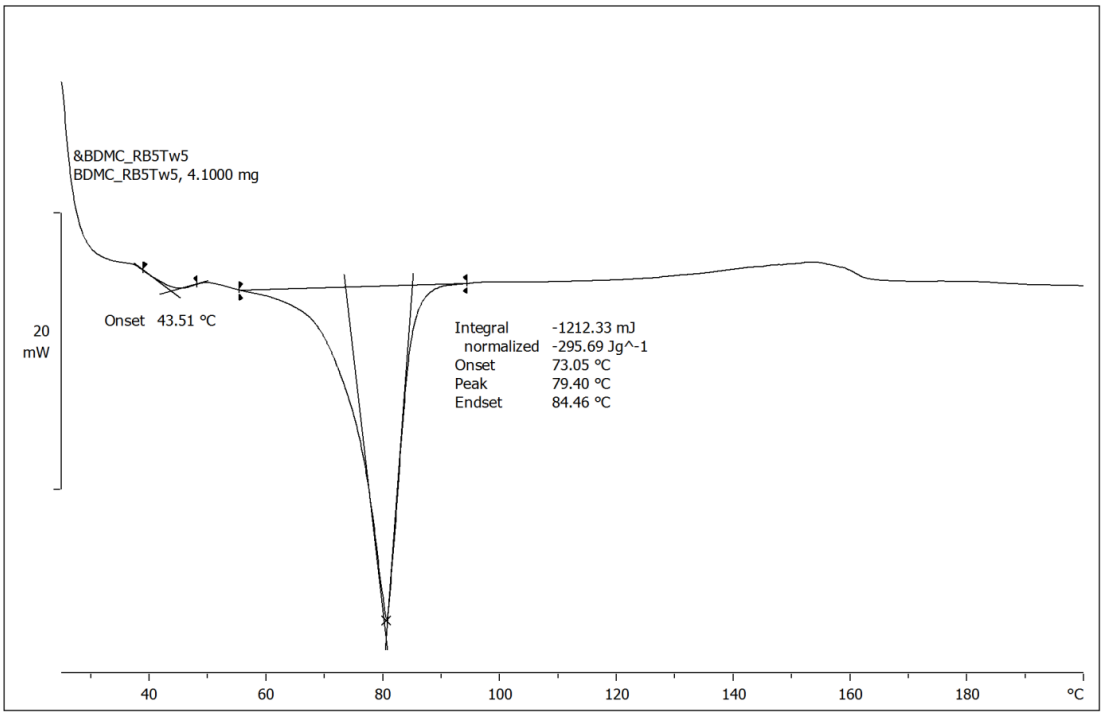

DSC thermogram of the loaded solid lipid nanoparticles: RB5.0Tw5-BDMC

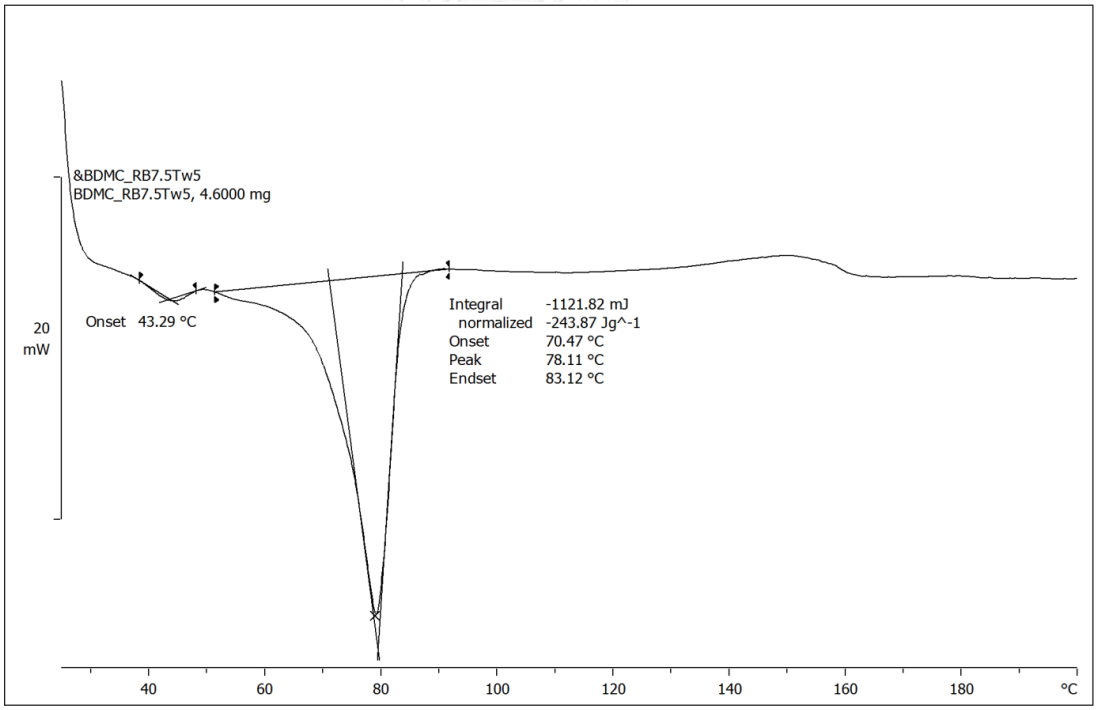

DSC thermogram of the loaded solid lipid nanoparticles: RB7.5Tw5-BDMC

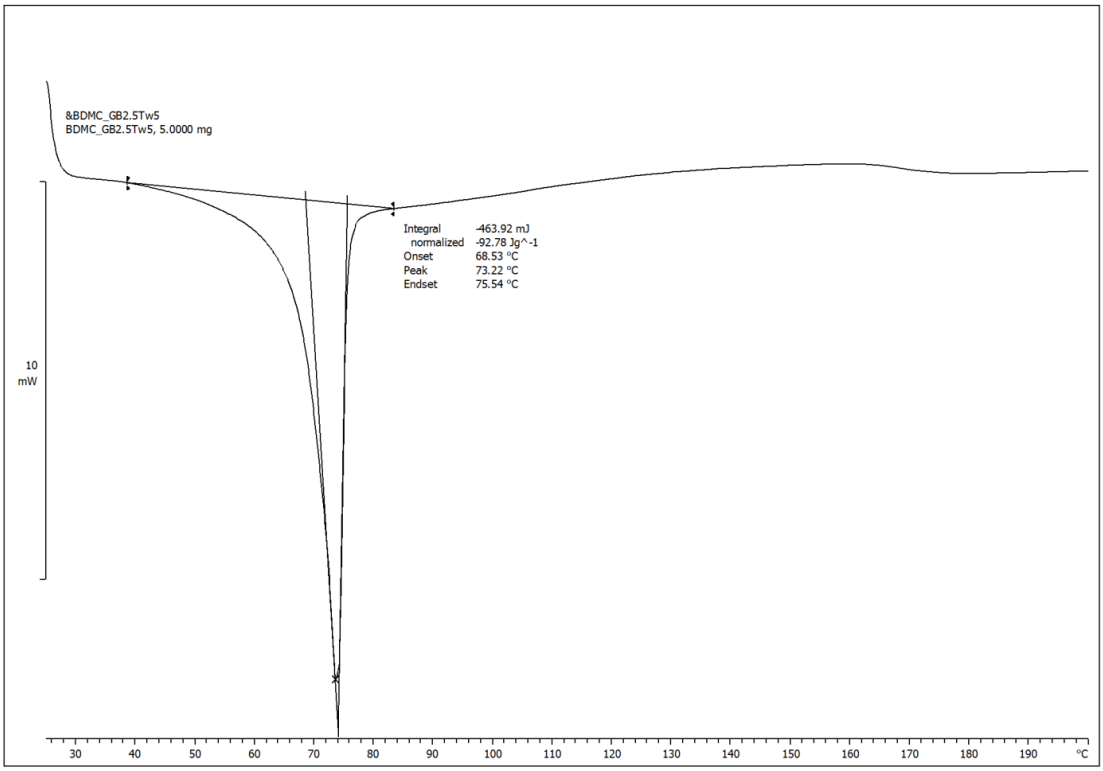

DSC thermogram of the loaded solid lipid nanoparticles: GB2.5Tw5-BDMC

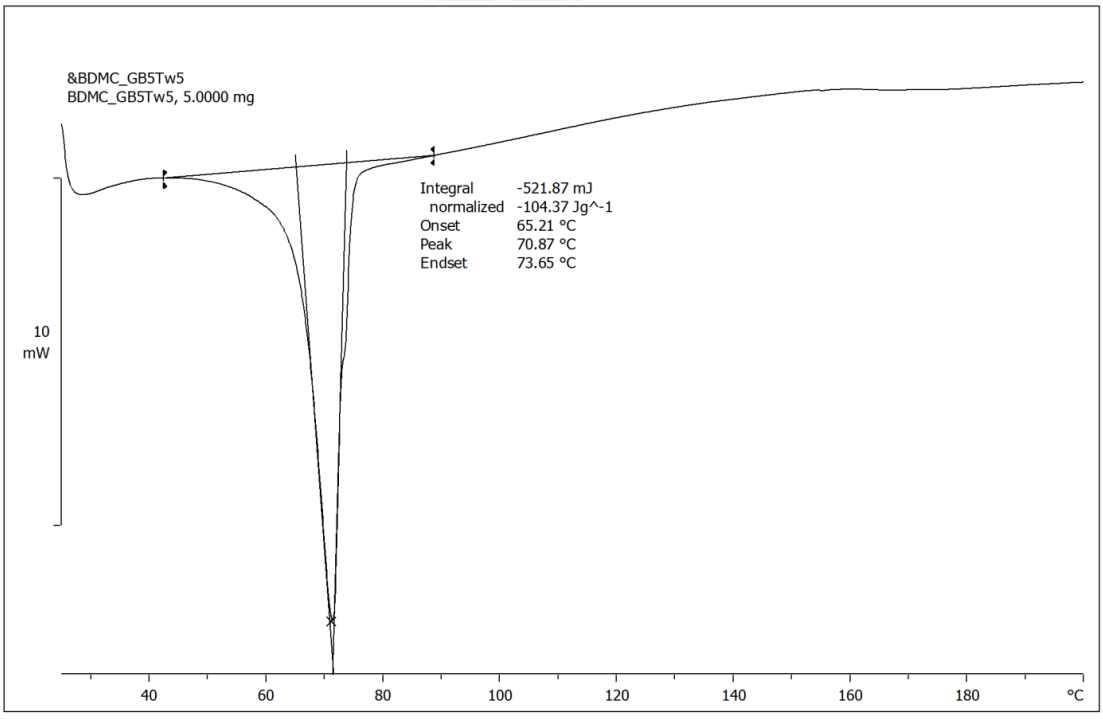

DSC thermogram of the loaded solid lipid nanoparticles: GB5.0Tw5-BDMC

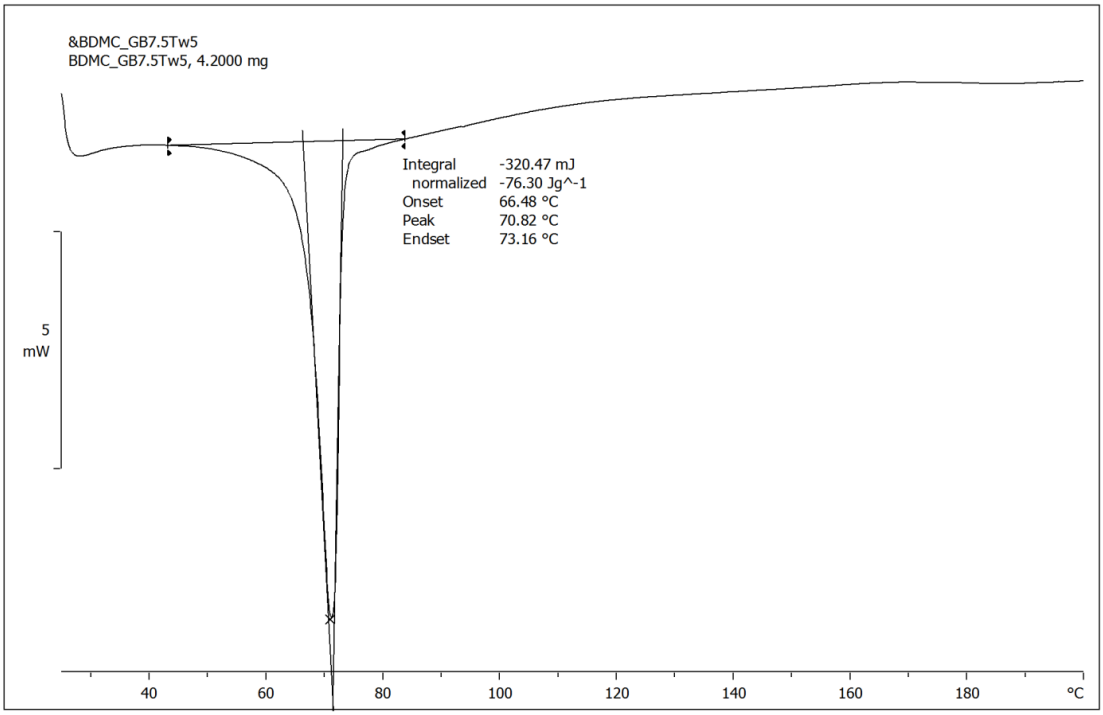

DSC thermogram of the loaded solid lipid nanoparticles: GB7.5Tw5-BDMC

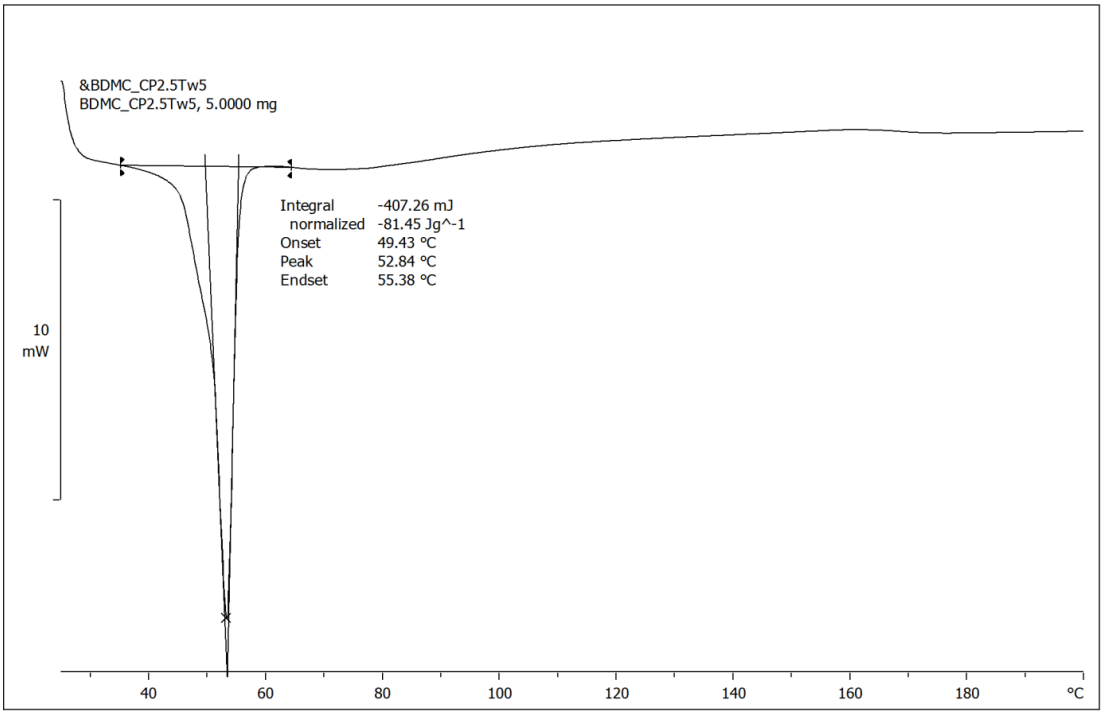

DSC thermogram of the loaded solid lipid nanoparticles: CP2.5Tw5-BDMC

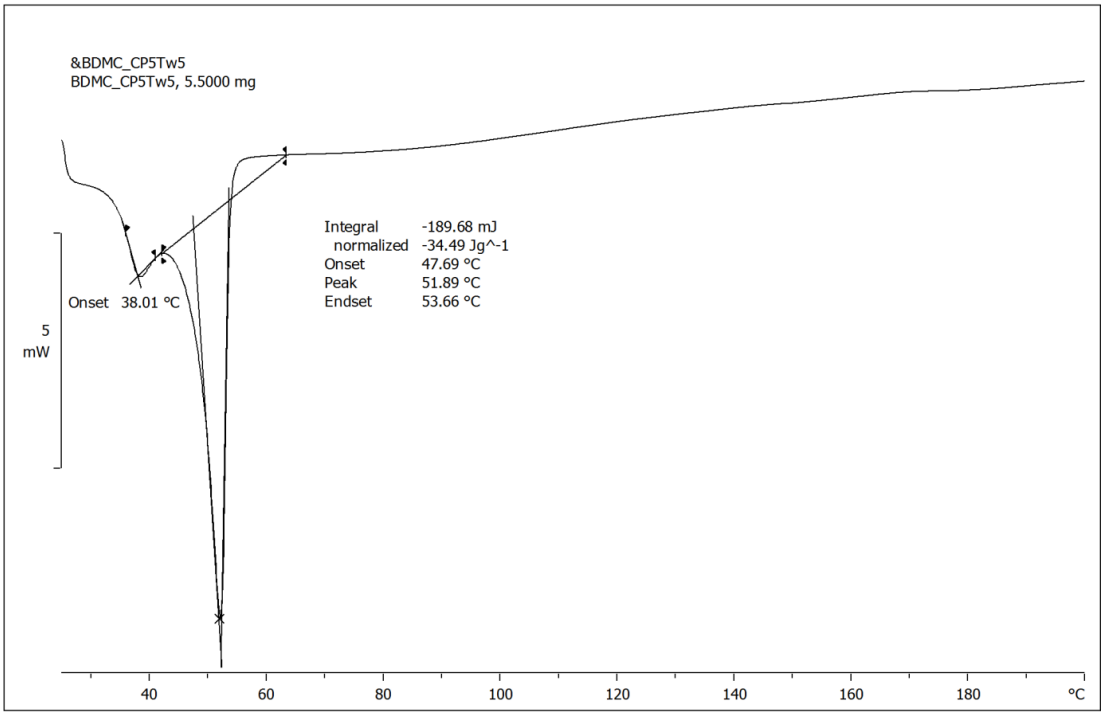

DSC thermogram of the loaded solid lipid nanoparticles: CP5.0Tw5-BDMC

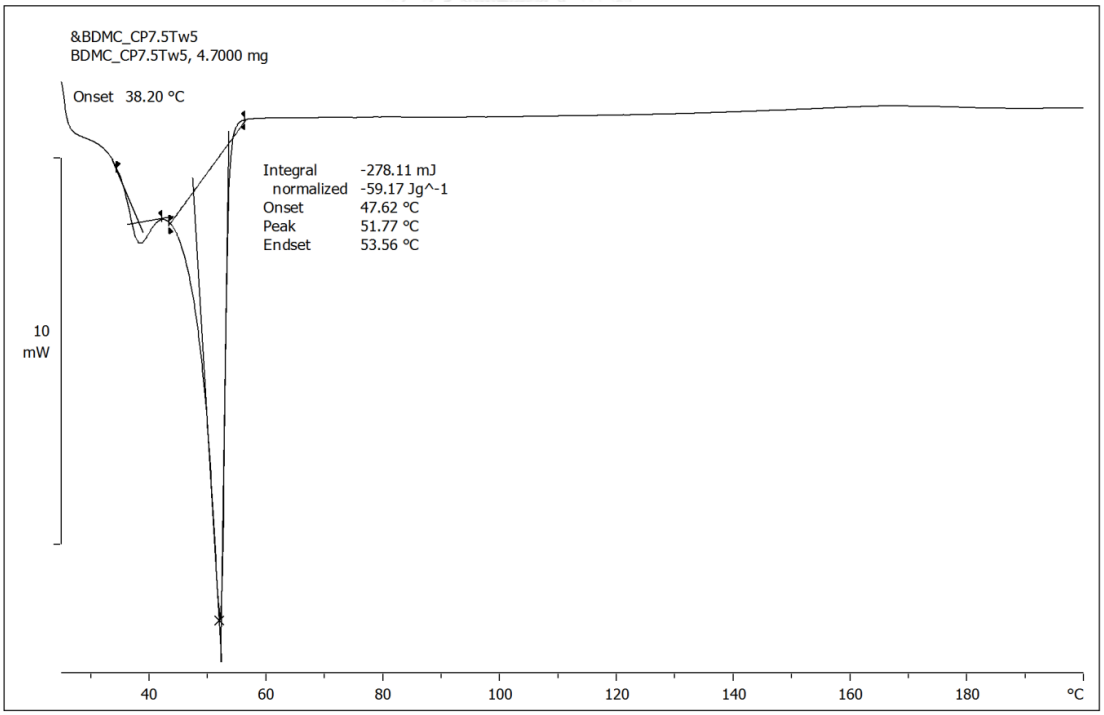

DSC thermogram of the loaded solid lipid nanoparticles: CP7.5Tw5-BDMC

APPENDIX D

Physical stability

Physical stability of blank SLN

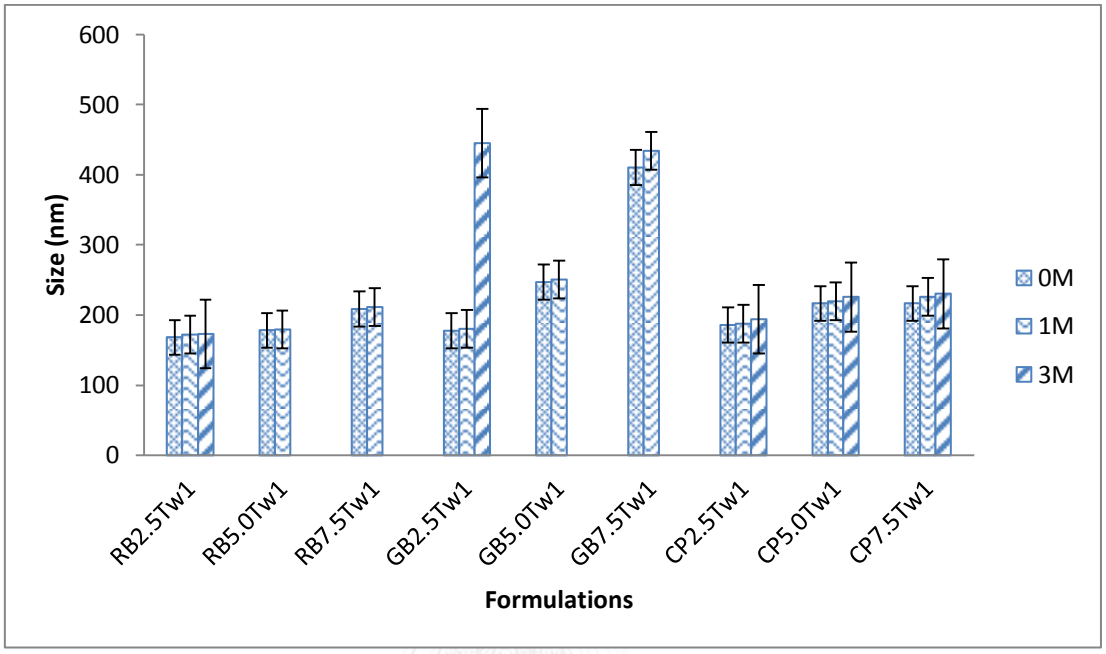

Comparison of particle size of blank-SLN formulations during storage at ambient room temperature for 3 months. (At Surfactant 1% w/w)

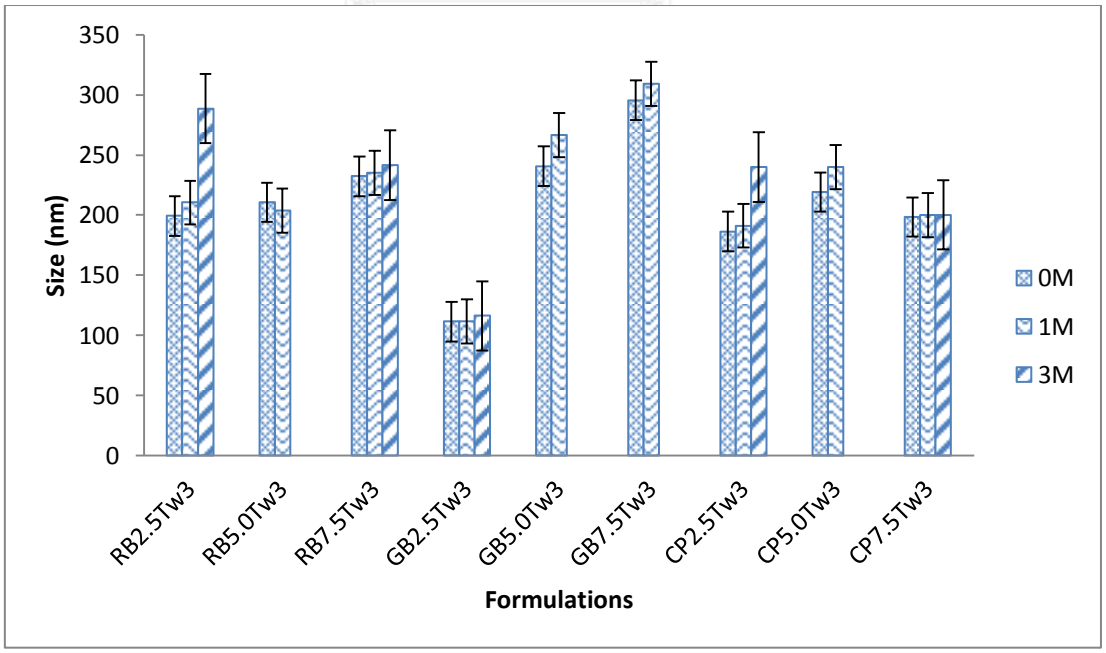

Comparison of particle size of blank-SLN formulations during storage at ambient room temperature for 3 months. (At Surfactant 3% w/w)

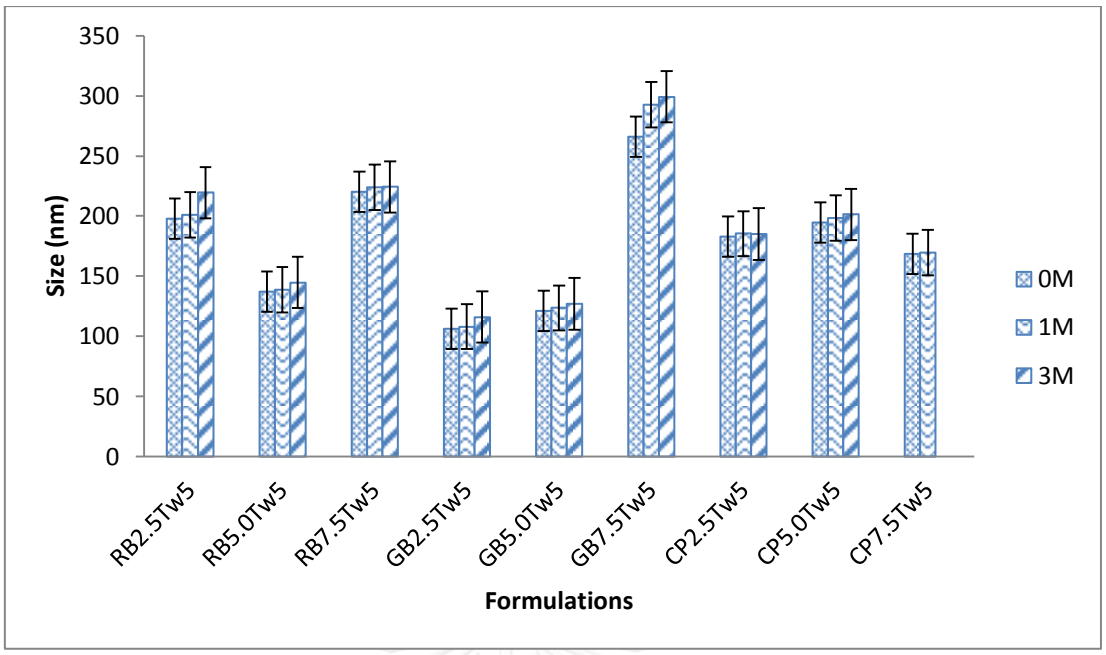

Comparison of particle size of blank-SLN formulations during storage at ambient room temperature for 3 months. (At Surfactant 5% w/w)

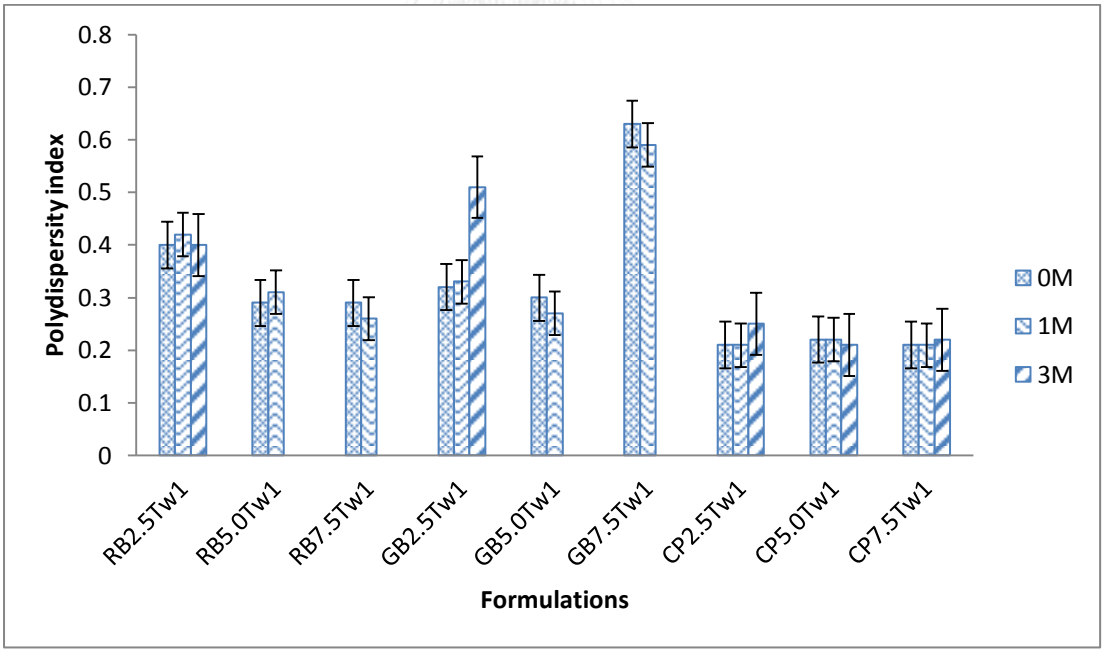

Comparison of polydispersity index of blank-SLN formulations during storage at ambient room temperature for 3 months. (At Surfactant 1% w/w)

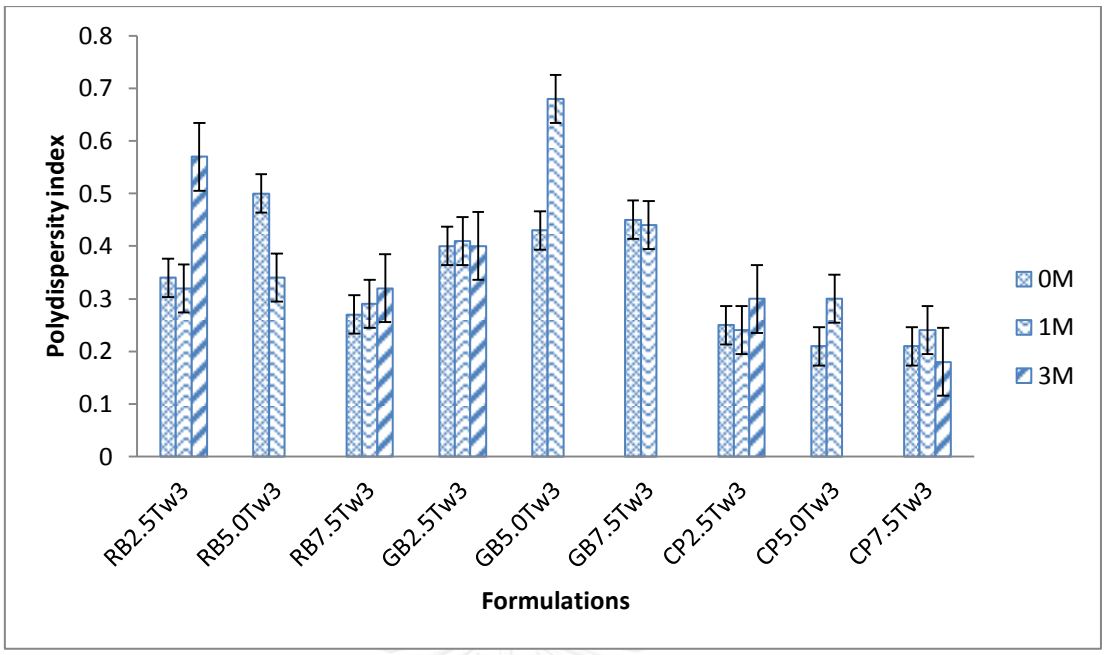

Comparison of polydispersity index of blank-SLN formulations during storage at ambient room temperature for 3 months. (At Surfactant 3% w/w)

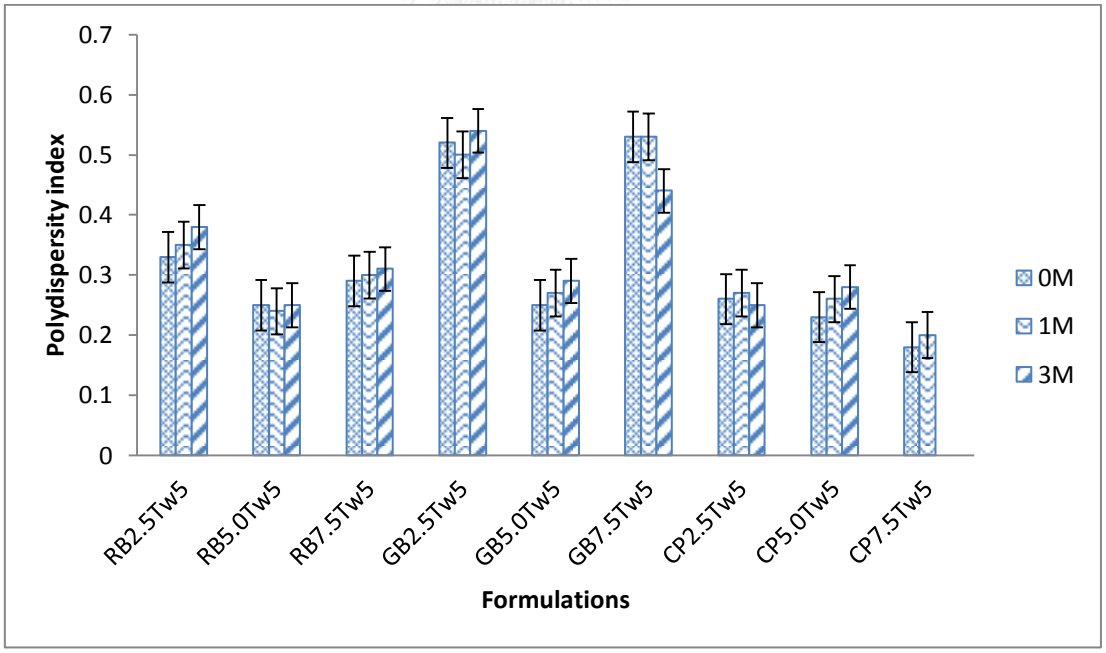

Comparison of polydispersity index of blank-SLN formulations during storage at ambient room temperature for 3 months. (At Surfactant 5% w/w)

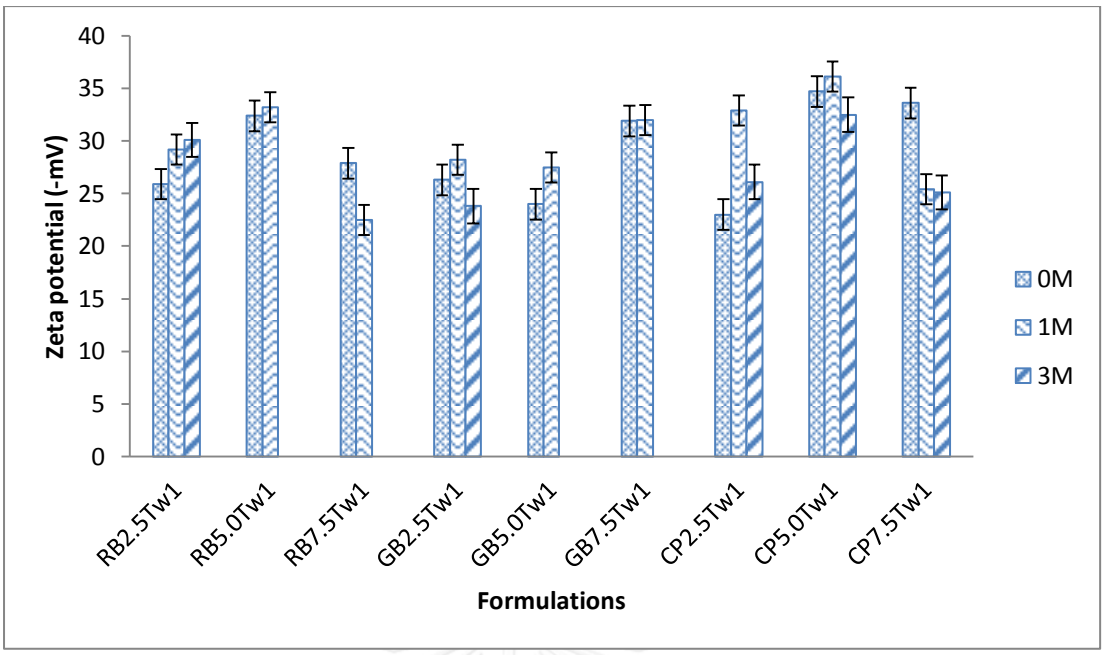

Comparison of zeta potential of blank-SLN formulations during storage at ambient room temperature for 3 months. (At Surfactant 1% w/w)

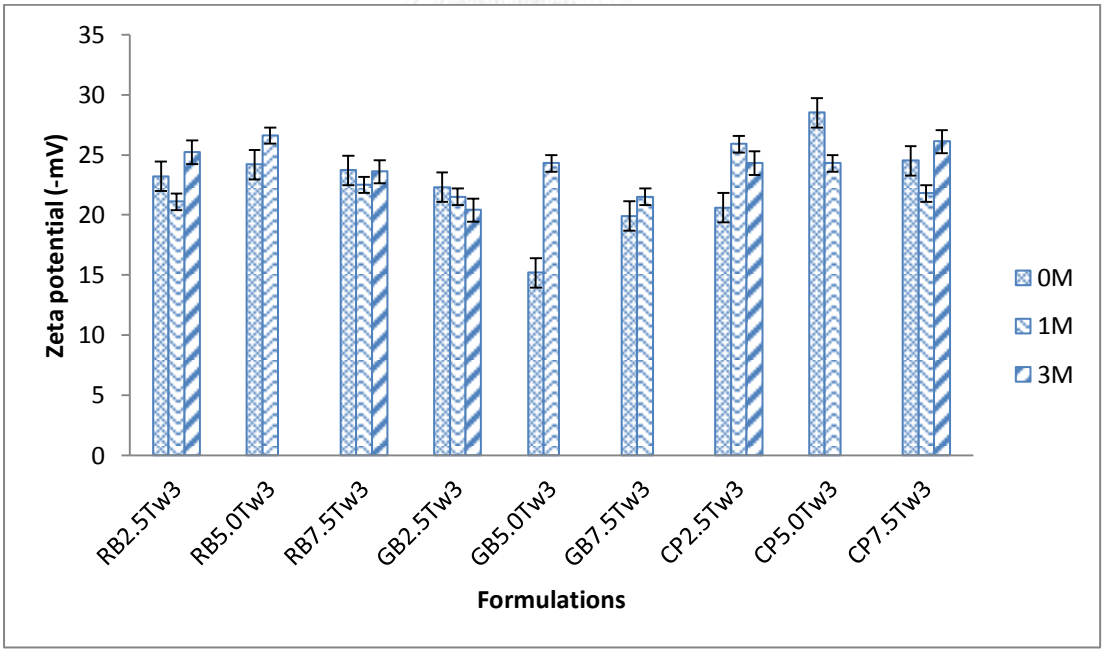

Comparison of zeta potential of blank-SLN formulations during storage at ambient room temperature for 3 months. (At Surfactant 3% w/w)

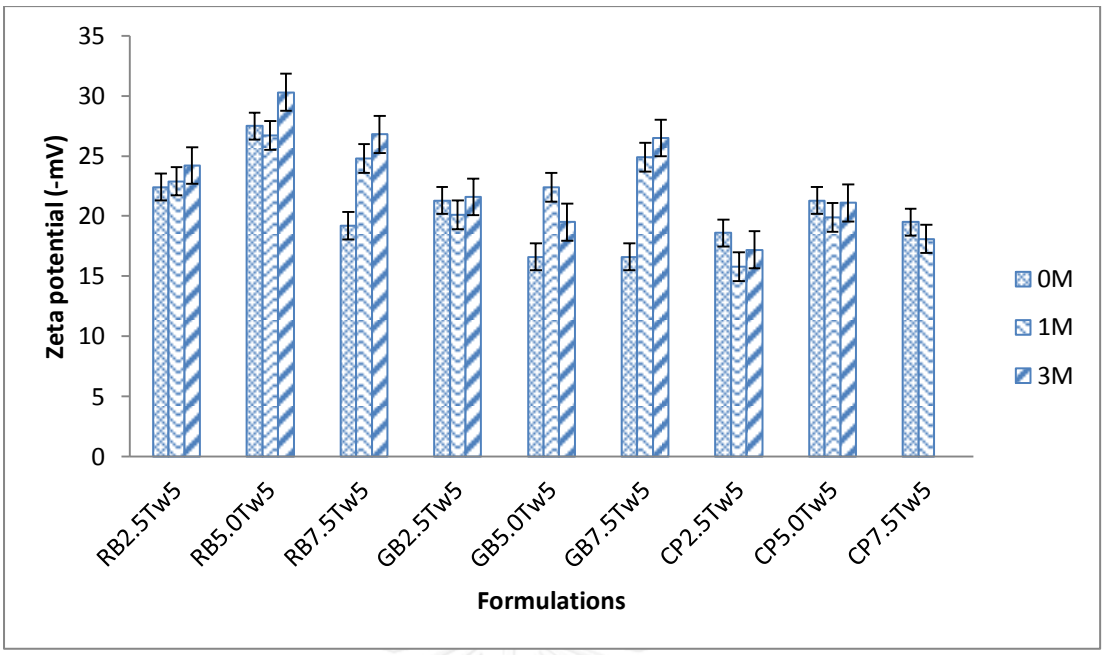

Comparison of zeta potential of blank-SLN formulations during storage at ambient room temperature for 3 months. (At Surfactant 5% w/w)

Physical stability of Curcuminoid loaded SLN

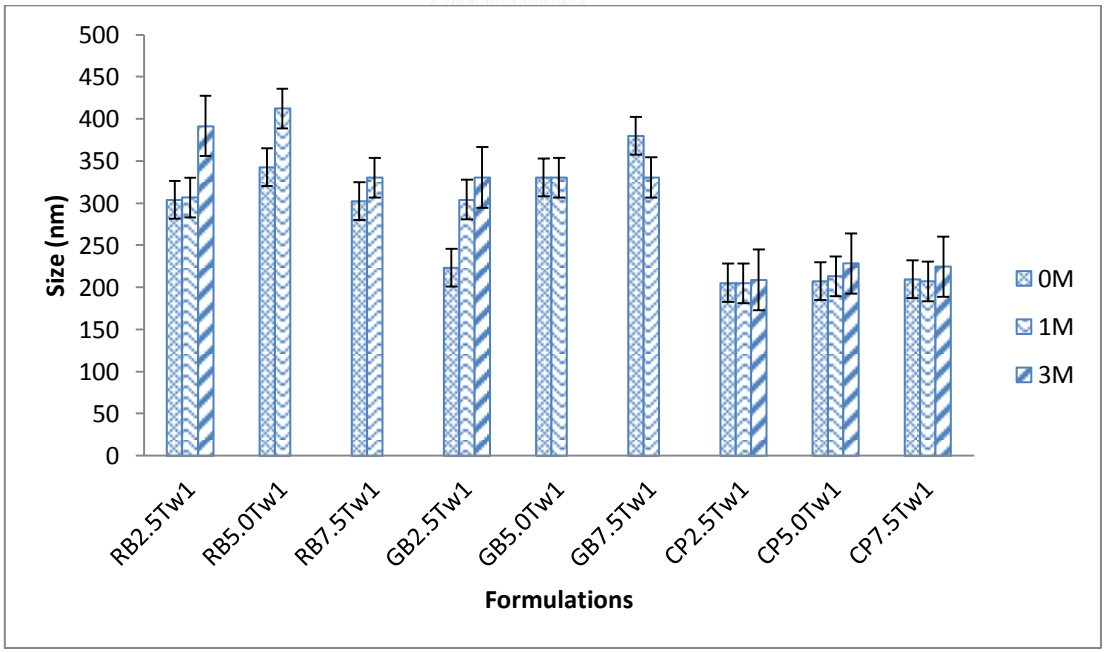

Comparison of particle size of C-SLN formulations during storage at ambient room temperature for 3 months. (At Surfactant 1% w/w)

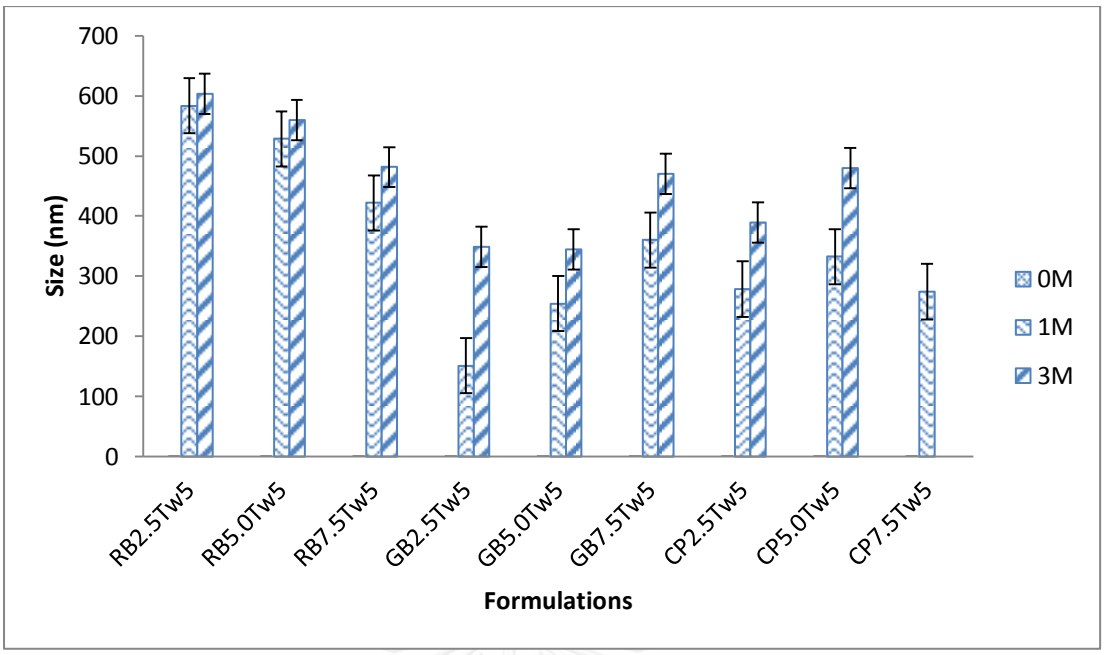

Comparison of particle size of C-SLN formulations during storage at ambient room temperature for 3 months. (At Surfactant 5% w/w)

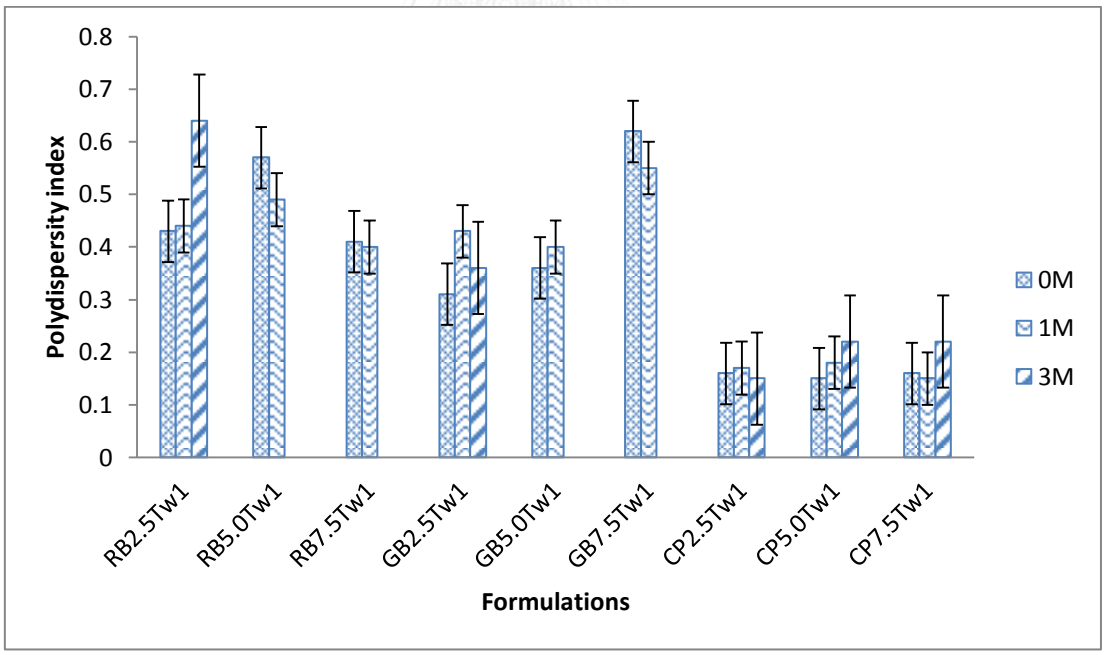

Comparison of polydispersity index of C-SLN formulations during storage at ambient room temperature for 3 months. (At Surfactant 1% w/w)

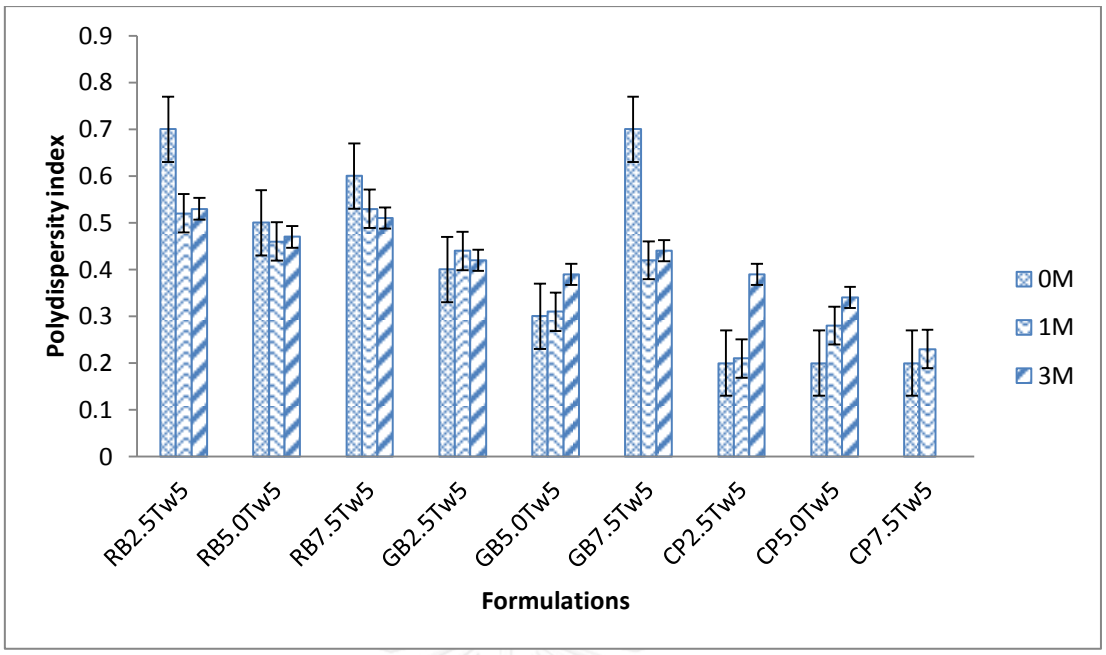

Comparison of polydispersity index of C-SLN formulations during storage at ambient room temperature for 3 months. (At Surfactant 5% w/w)

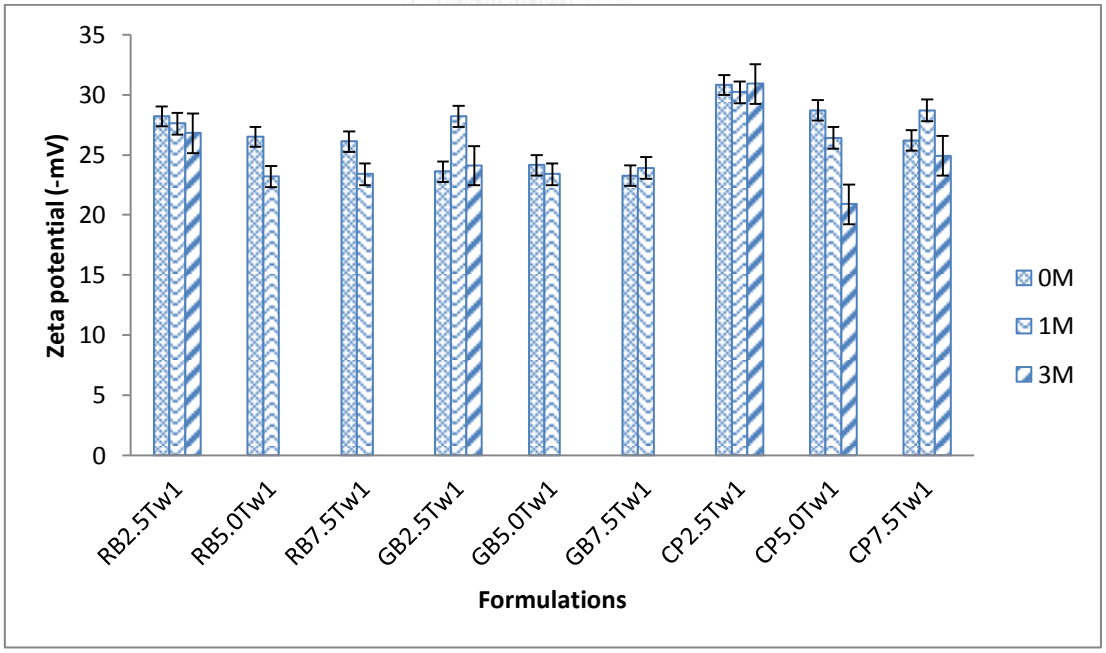

Comparison of zeta potential of C-SLN formulations during storage at ambient room temperature for 3 months. (At Surfactant 1% w/w)

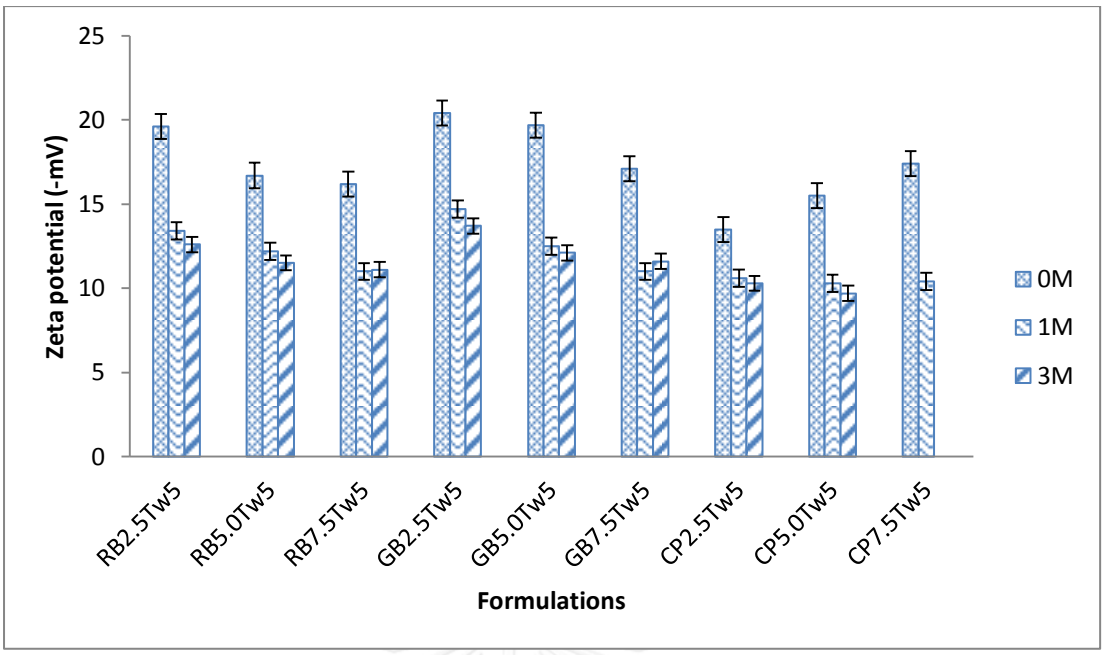

Comparison of zeta potential of C-SLN formulations during storage at ambient room temperature for 3 months. (At Surfactant 5% w/w)

Physical stability of BDMC loaded SLN

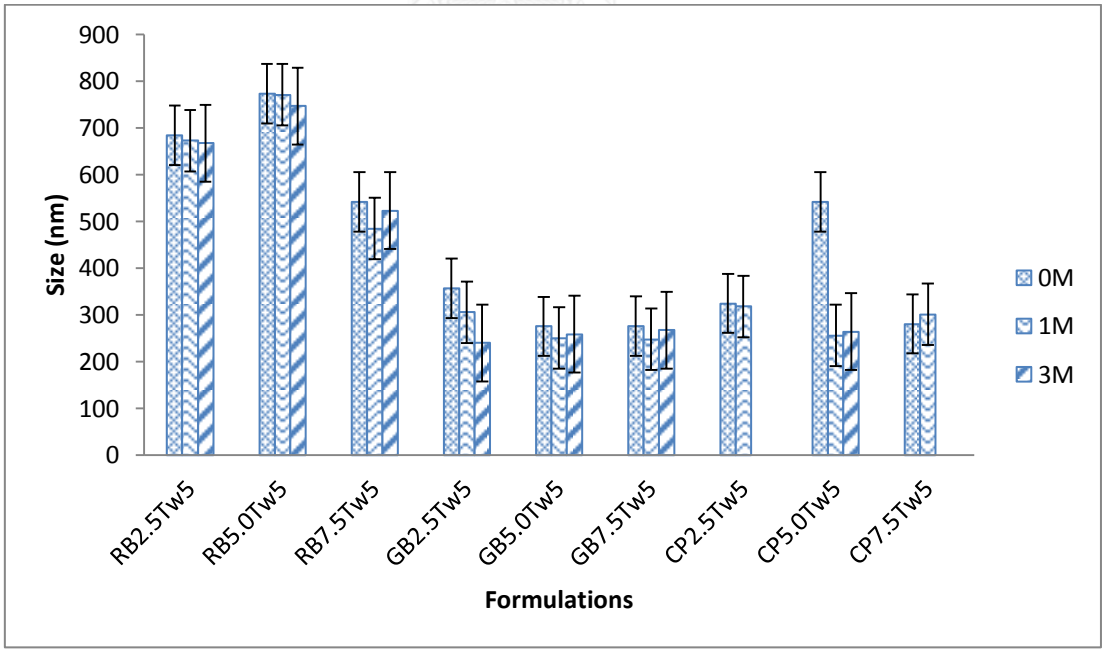

Comparison of particle size of BDMC-SLN formulations during storage at ambient room temperature for 3 months.

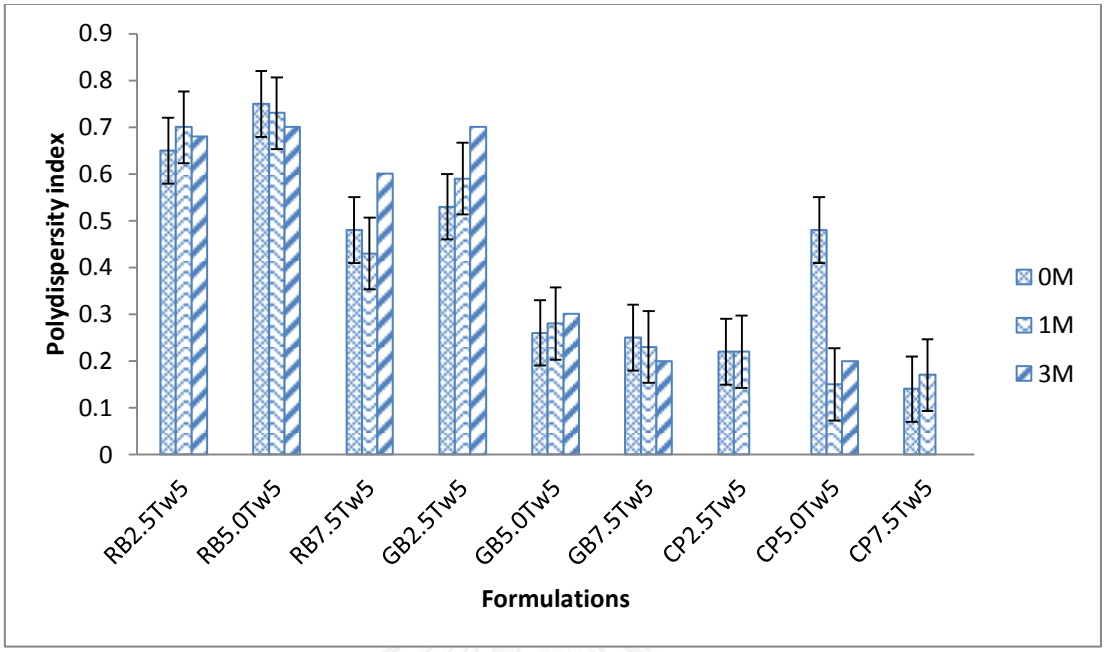

Comparison of polydispersity index of BDMC-SLN formulations during storage at ambient room temperature for 3 months.

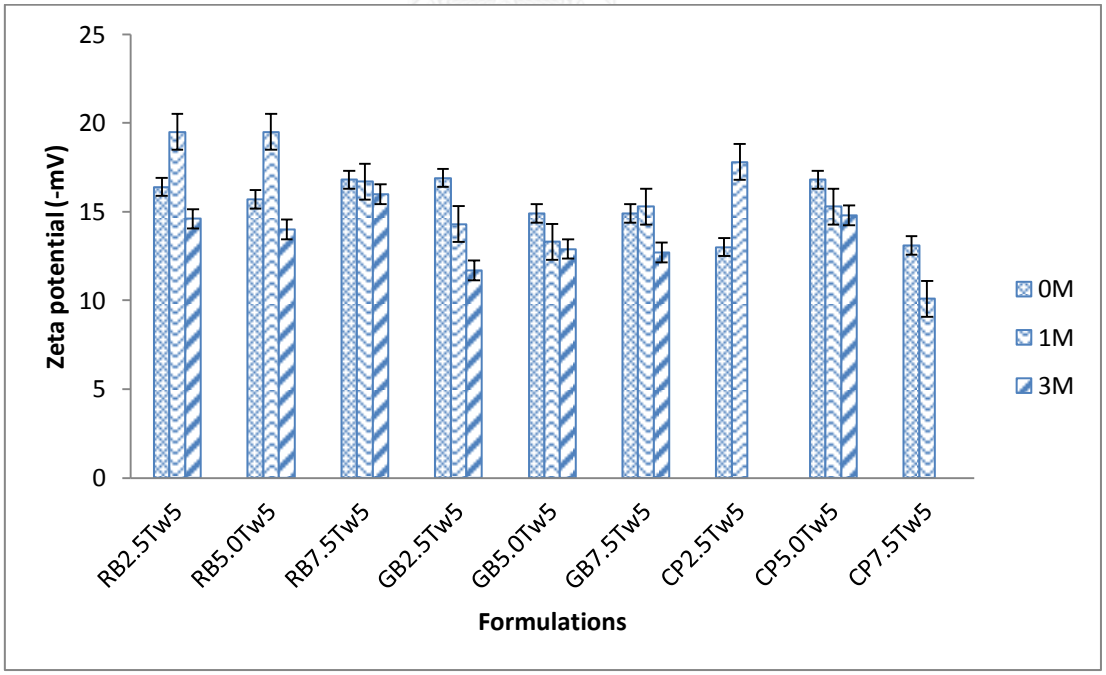

Comparison of zeta potential of BDMC-SLN formulations during storage at ambient room temperature for 3 months.

APPENDIX E

Statistics

One-way analysis of variance of blank-SLN lipid type on size

ANOVA

Size (nm)

	Sum of Squares	df	Mean Square	F	Sig.
Between Groups	481.296	2	240.648	213.804	.000
Within Groups	6.753	6	1.126		
Total	488.049	8			

Multiple comparison of blank-SLN lipid type on size

Multiple Comparisons

Dependent Variable: Size (nm)

Tukey HSD

(I) Lipid		Mean Difference (I-J)	Std. Error	Sig.	95% Confidence Interval	
					Lower Bound	Upper Bound
RB	GB	-9.5333*	.8662	.000	-12.191	-6.875
	CP	-17.9000*	.8662	.000	-20.558	-15.242
GB	RB	9.5333*	.8662	.000	6.875	12.191
	CP	-8.3667*	.8662	.000	-11.025	-5.709
CP	RB	17.9000*	.8662	.000	15.242	20.558
	GB	8.3667*	.8662	.000	5.709	11.025

*. The mean difference is significant at the 0.05 level.

One-way analysis of variance of blank-SLN lipid amount on size

ANOVA

Size (nm)

	Sum of Squares	df	Mean Square	F	Sig.
Between Groups	2665.762	2	1332.881	352.821	.000
Within Groups	22.667	6	3.778		
Total	2688.429	8			

Multiple comparison of blank-SLN lipid amount on size

Multiple Comparisons

Dependent Variable: Size (nm)

Tukey HSD

(I) Lipid Percent		Mean Difference (I-J)	Std. Error	Sig.	95% Confidence Interval	
					Lower Bound	Upper Bound
2.5	5.0	-10.2333*	1.5870	.002	-15.103	-5.364
	7.5	-40.5333*	1.5870	.000	-45.403	-35.664
5.0	2.5	10.2333*	1.5870	.002	5.364	15.103
	7.5	-30.3000*	1.5870	.000	-35.169	-25.431
7.5	2.5	40.5333*	1.5870	.000	35.664	45.403
	5.0	30.3000*	1.5870	.000	25.431	35.169

One-way analysis of variance of blank-SLN surfactant concentration on size

ANOVA

Size (nm)

	Sum of Squares	df	Mean Square	F	Sig.
Between Groups	1859.102	2	929.551	75.335	.000
Within Groups	74.033	6	12.339		
Total	1933.136	8			

Multiple comparison of blank-SLN surfactant concentration on size

Multiple Comparisons

Dependent Variable: Size (nm)

Tukey HSD

(I) Tween Percent		Mean Difference (I-J)	Std. Error	Sig.	95% Confidence Interval	
					Lower Bound	Upper Bound
1	3	-31.1333*	2.8681	.000	-39.933	-22.333
	5	-29.8000*	2.8681	.000	-38.600	-21.000
3	1	31.1333*	2.8681	.000	22.333	39.933
	5	1.3333	2.8681	.890	-7.467	10.133
5	1	29.8000*	2.8681	.000	21.000	38.600
	3	-1.3333	2.8681	.890	-10.133	7.467

*. The mean difference is significant at the 0.05 level.

One-way analysis of variance of C-SLN lipid type on size

ANOVA

Size (nm)

	Sum of Squares	df	Mean Square	F	Sig.
Between Groups	63869.556	2	31934.778	1017.427	.000
Within Groups	188.327	6	31.388		
Total	64057.882	8			

Multiple comparison of C-SLN lipid type on size

Multiple Comparisons

Dependent Variable: Size (nm)

Tukey HSD

(I) Lipid		Mean Difference (I-J)	Std. Error	Sig.	95% Confidence Interval	
					Lower Bound	Upper Bound
RB	GB	167.6667*	4.5744	.000	153.631	181.702
	CP	188.0000*	4.5744	.000	173.964	202.036
GB	RB	-167.6667*	4.5744	.000	-181.702	-153.631
	CP	20.3333*	4.5744	.010	6.298	34.369
CP	RB	-188.0000*	4.5744	.000	-202.036	-173.964
	GB	-20.3333*	4.5744	.010	-34.369	-6.298

*. The mean difference is significant at the 0.05 level.

One-way analysis of variance of C-SLN lipid amount on size

ANOVA

Size (nm)

	Sum of Squares	df	Mean Square	F	Sig.
Between Groups	12015.727	2	6007.863	153.711	.000
Within Groups	234.513	6	39.086		
Total	12250.240	8			

Multiple comparison of C-SLN lipid amount on size

Multiple Comparisons

Dependent Variable: Size (nm)

Tukey HSD

(I) Lipid Percent		Mean Difference (I-J)	Std. Error	Sig.	95% Confidence Interval	
					Lower Bound	Upper Bound
2.5	5.0	48.9333*	5.1046	.000	33.271	64.596
	7.5	89.3667*	5.1046	.000	73.704	105.029
5.0	2.5	-48.9333*	5.1046	.000	-64.596	-33.271
	7.5	40.4333*	5.1046	.001	24.771	56.096
7.5	2.5	-89.3667*	5.1046	.000	-105.029	-73.704
	5.0	-40.4333*	5.1046	.001	-56.096	-24.771

*. The mean difference is significant at the 0.05 level.

One-way analysis of variance of C-SLN lipid type on entrapment efficiency

ANOVA

Entrapment Efficiency

	Sum of Squares	df	Mean Square	F	Sig.
Between Groups	1111.993	2	555.996	415.515	.000
Within Groups	8.029	6	1.338		
Total	1120.021	8			

Multiple comparison of C-SLN lipid type on entrapment efficiency

Multiple Comparisons

Dependent Variable: Entrapment Efficiency

Tukey HSD

(I) Lipid		Mean Difference (I-J)	Std. Error	Sig.	95% Confidence Interval	
					Lower Bound	Upper Bound
RB	GB	14.01667*	.94449	.000	11.1187	16.9146
	CP	27.22333*	.94449	.000	24.3254	30.1213
GB	RB	-14.01667*	.94449	.000	-16.9146	-11.1187
	CP	13.20667*	.94449	.000	10.3087	16.1046
CP	RB	-27.22333*	.94449	.000	-30.1213	-24.3254
	GB	-13.20667*	.94449	.000	-16.1046	-10.3087

*. The mean difference is significant at the 0.05 level.

One-way analysis of variance of C-SLN lipid amount on entrapment efficiency

ANOVA

Entrapment Efficiency

	Sum of Squares	df	Mean Square	F	Sig.
Between Groups	137.898	2	68.949	86.062	.000
Within Groups	4.807	6	.801		
Total	142.705	8			

Multiple comparison of C-SLN lipid amount on entrapment efficiency

Multiple Comparisons

Dependent Variable: Entrapment Efficiency

Tukey HSD

(I) Lipid Percent		Mean Difference (I-J)	Std. Error	Sig.	95% Confidence Interval	
					Lower Bound	Upper Bound
2.5	5.0	-3.67333*	.73082	.006	-5.9157	-1.4310
	7.5	-9.50667*	.73082	.000	-11.7490	-7.2643
5.0	2.5	3.67333*	.73082	.006	1.4310	5.9157
	7.5	-5.83333*	.73082	.001	-8.0757	-3.5910
7.5	2.5	9.50667*	.73082	.000	7.2643	11.7490
	5.0	5.83333*	.73082	.001	3.5910	8.0757

*. The mean difference is significant at the 0.05 level.

One-way analysis of variance of BDMC-SLN lipid type on size

ANOVA

Size (nm)

	Sum of Squares	df	Mean Square	F	Sig.
Between Groups	237697.342	2	118848.671	1503.885	.000
Within Groups	474.167	6	79.028		
Total	238171.509	8			

Multiple comparison of BDMC-SLN lipid type on size

Multiple Comparisons

Dependent Variable: Size (nm)

Tukey HSD

(I) Lipid		Mean Difference (I-J)	Std. Error	Sig.	95% Confidence Interval	
					Lower Bound	Upper Bound
RB	GB	327.6667*	7.2585	.000	305.396	349.938
	CP	359.6000*	7.2585	.000	337.329	381.871
GB	RB	-327.6667*	7.2585	.000	-349.938	-305.396
	CP	31.9333*	7.2585	.011	9.662	54.204
CP	RB	-359.6000*	7.2585	.000	-381.871	-337.329
	GB	-31.9333*	7.2585	.011	-54.204	-9.662

*. The mean difference is significant at the 0.05 level.

One-way analysis of variance of BDMC-SLN lipid amount on size

ANOVA

Size (nm)

	Sum of Squares	df	Mean Square	F	Sig.
Between Groups	81734.060	2	40867.030	94.099	.000
Within Groups	2605.780	6	434.297		
Total	84339.840	8			

Multiple comparison of BDMC-SLN lipid amount on size

Multiple Comparisons

Dependent Variable: Size (nm)

Tukey HSD

(I) Lipid Percent		Mean Difference (I-J)	Std. Error	Sig.	95% Confidence Interval	
					Lower Bound	Upper Bound
2.5	5.0	-89.1000*	17.0156	.005	-141.309	-36.891
	7.5	142.3000*	17.0156	.000	90.091	194.509
5.0	2.5	89.1000*	17.0156	.005	36.891	141.309
	7.5	231.4000*	17.0156	.000	179.191	283.609
7.5	2.5	-142.3000*	17.0156	.000	-194.509	-90.091
	5.0	-231.4000*	17.0156	.000	-283.609	-179.191

*. The mean difference is significant at the 0.05 level.

One-way analysis of variance of BDMC-SLN lipid type on entrapment efficiency

ANOVA

Entrapment Efficiency

	Sum of Squares	df	Mean Square	F	Sig.
Between Groups	180.779	2	90.389	84.072	.000
Within Groups	6.451	6	1.075		
Total	187.230	8			

Multiple comparison of BDMC-SLN lipid type on entrapment efficiency

Multiple Comparisons

Dependent Variable: Entrapment Efficiency

Tukey HSD

(I) Lipid		Mean Difference (I-J)	Std. Error	Sig.	95% Confidence Interval	
					Lower Bound	Upper Bound
RB	GB	9.75667*	.84662	.000	7.1590	12.3543
	CP	.52000	.84662	.818	-2.0777	3.1177
GB	RB	-9.75667*	.84662	.000	-12.3543	-7.1590
	CP	-9.23667*	.84662	.000	-11.8343	-6.6390
CP	RB	-.52000	.84662	.818	-3.1177	2.0777
	GB	9.23667*	.84662	.000	6.6390	11.8343

*. The mean difference is significant at the 0.05 level.

One-way analysis of variance of BDMC-SLN lipid amount on entrapment efficiency

ANOVA

Entrapment Efficiency

	Sum of Squares	df	Mean Square	F	Sig.
Between Groups	157.171	2	78.585	163.307	.000
Within Groups	2.887	6	.481		
Total	160.058	8			

Multiple comparison of BDMC-SLN lipid amount on entrapment efficiency

Multiple Comparisons

Dependent Variable: Entrapment Efficiency

Tukey HSD

(I) Lipid Percent		Mean Difference (I-J)	Std. Error	Sig.	95% Confidence Interval	
					Lower Bound	Upper Bound
2.5	5.0	-9.98333*	.56640	.000	-11.7212	-8.2455
	7.5	-6.95000*	.56640	.000	-8.6879	-5.2121
5.0	2.5	9.98333*	.56640	.000	8.2455	11.7212
	7.5	3.03333*	.56640	.004	1.2955	4.7712
7.5	2.5	6.95000*	.56640	.000	5.2121	8.6879
	5.0	-3.03333*	.56640	.004	-4.7712	-1.2955

*. The mean difference is significant at the 0.05 level.

VITA

Ms. Pinnisa Tangkhajornchaisak was born on July, 25th, 1989 in Bangkok, Thailand. She had graduated in Pharmaceutical Sciences from Rangsit University since 2011. She decided to further her study in Department of Pharmaceutics and Industrial Pharmacy of master degree in Chulalongkorn University in 2012.